Galactic Cosmic Ray Anisotropy in IceCube

Paolo Desiati

IceCube Research Center & Department of Astronomy
University of Wisconsin - Madison

<desiati@icecube.wisc.edu>

NuSky 2011, ICTP - Trieste
June 20th, 2011

cosmic rays spectrum

- spectral structure & mass composition hold information on
    - **origin** of cosmic rays and
    - **propagation** from *sources* to Earth
- **anisotropy** in arrival distribution
    - spectral structure
    - origin & propagation

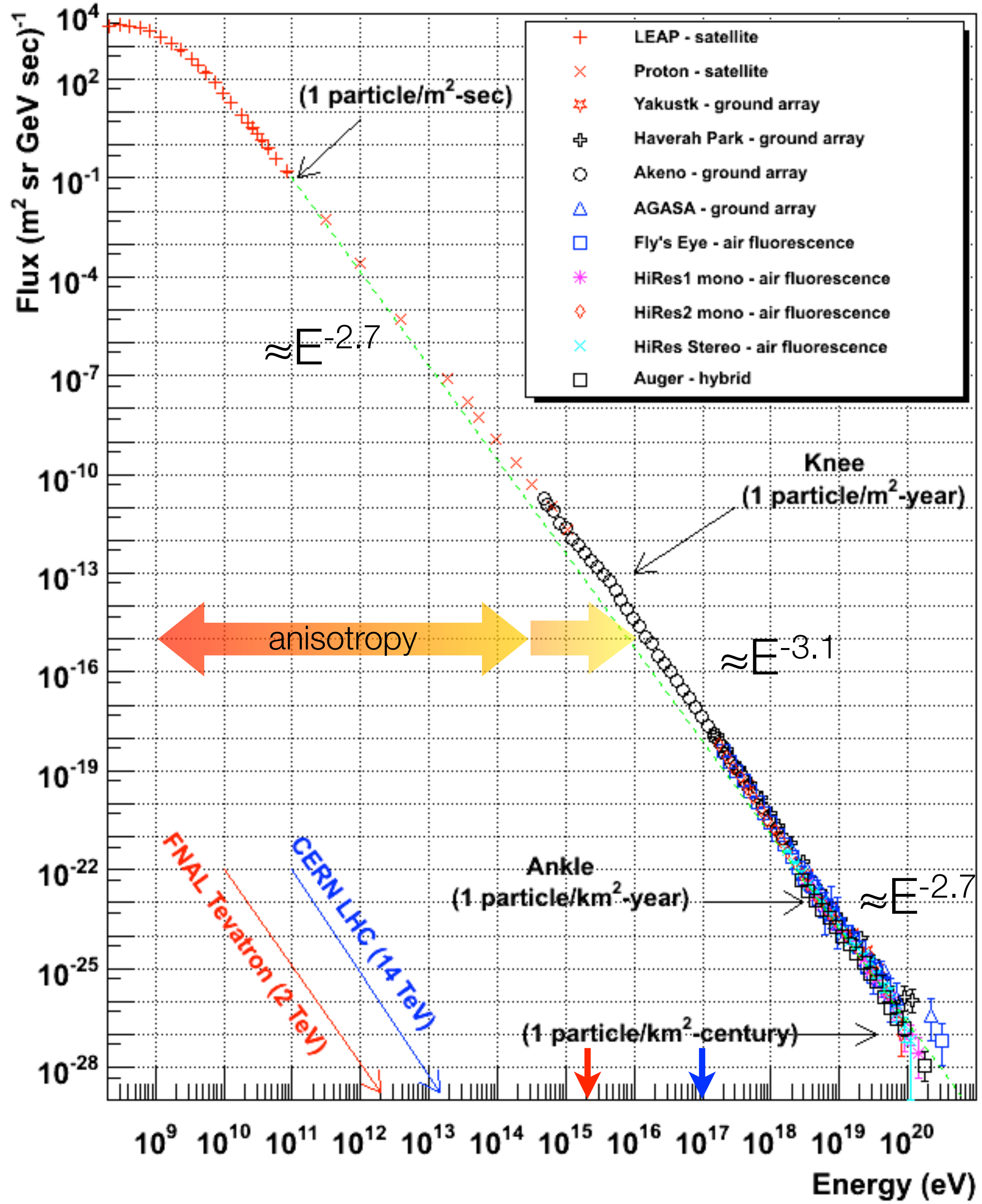

cosmic ray anisotropy vs energy

J.L. Zhang et al., 31st ICRC Łódź - Poland, 2009

ARGO-YBJ

- data from 2008
- 365 days livetime
- $6.5 \cdot 10^{10}$ events
- median CR energy ~ 1.1 TeV

Amenomori et al., Science Vol. 314, pp. 439, 2006

Tibet-III

- data from 1997 to 2005
- 1874 days livetime
- $3.7 \cdot 10^{10}$ events
- angular resolution ~ 0.9°
- modal CR energy ~ 3 TeV

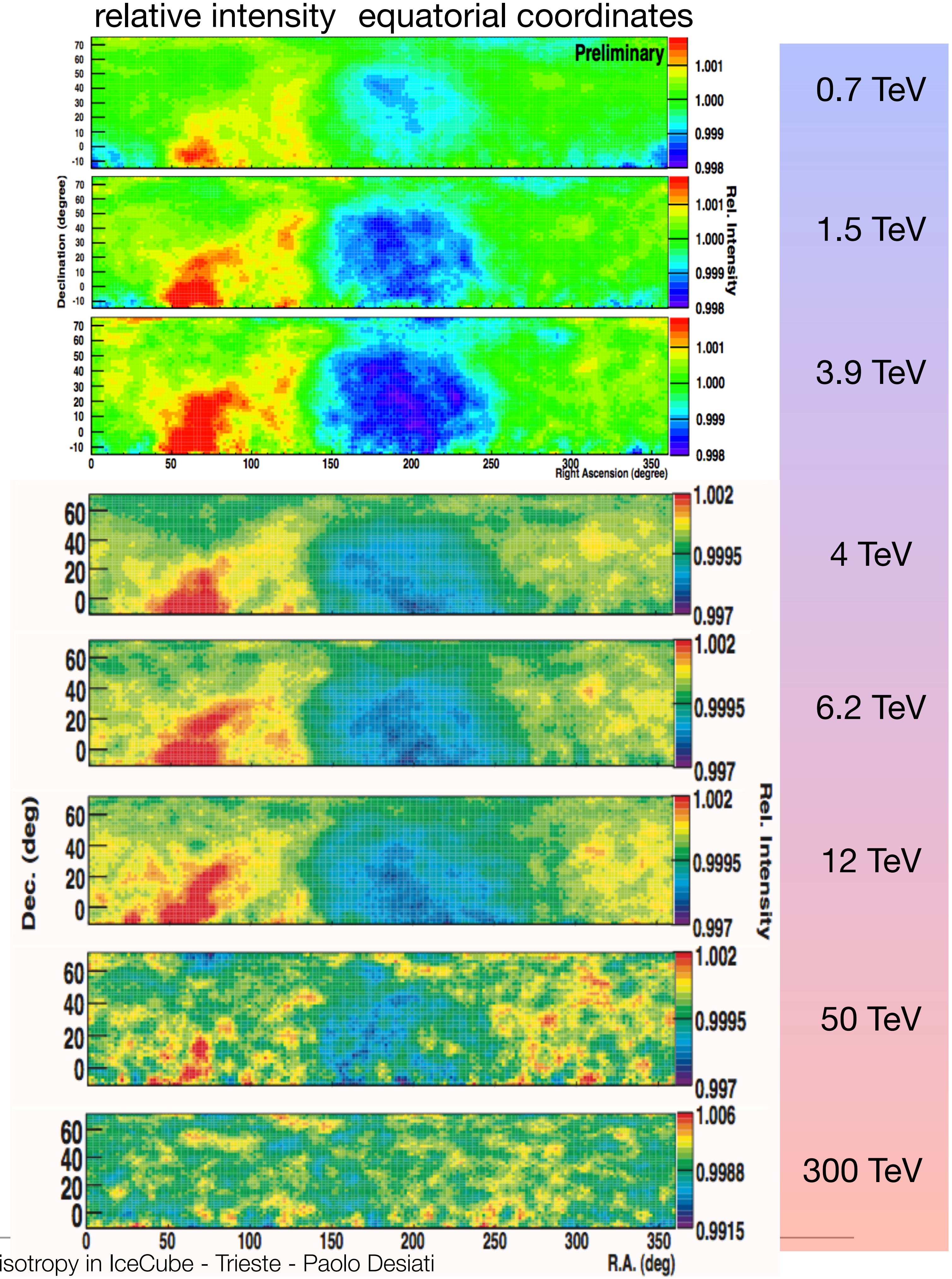

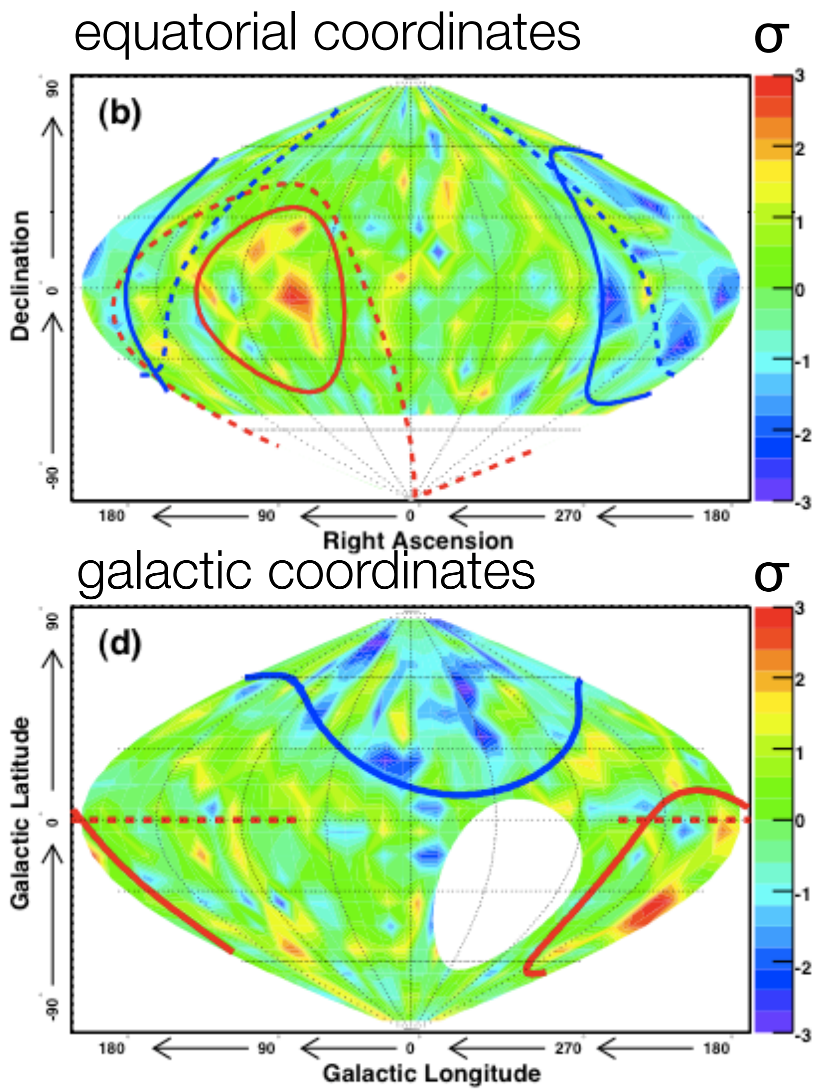

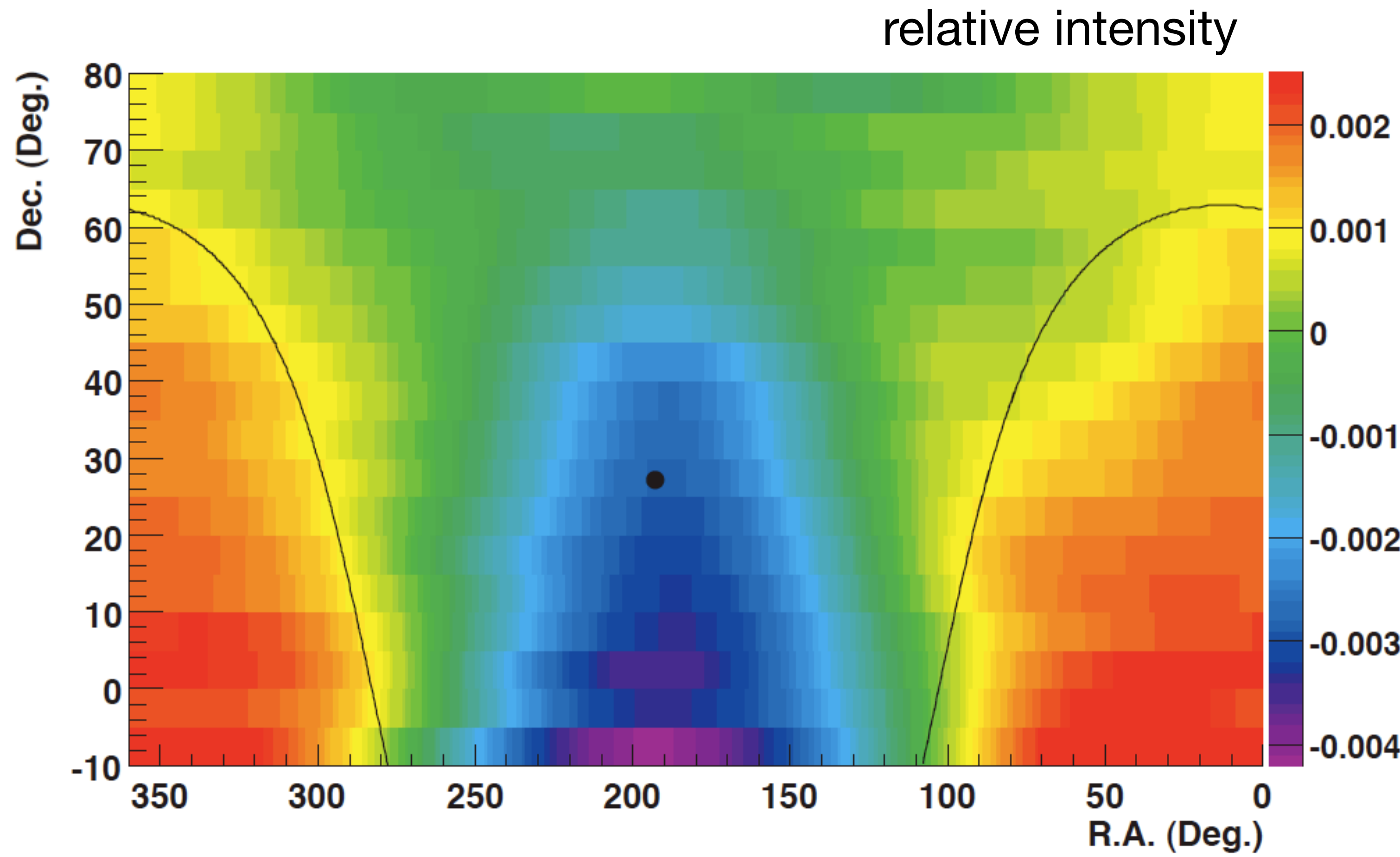

Super-Kamiokande

Guillian et al., Phys Rev D, Vol 75, 063002 (2007)

- data from 1996 to 2001
- 1662 days livetime
- $2.1 \cdot 10^8$ events
- angular resolution < 2°
- median CR energy ~ 10 TeV

Milagro

Abdo et al., ApJ, Vol 698-2, pag 2121 (2009)

- data from 2000 to 2007
- $9.5 \cdot 10^{10}$ events
- angular resolution < 1°
- median CR energy ~ 6 TeV

cosmic ray anisotropy vs energy

relative intensity equatorial coordinates

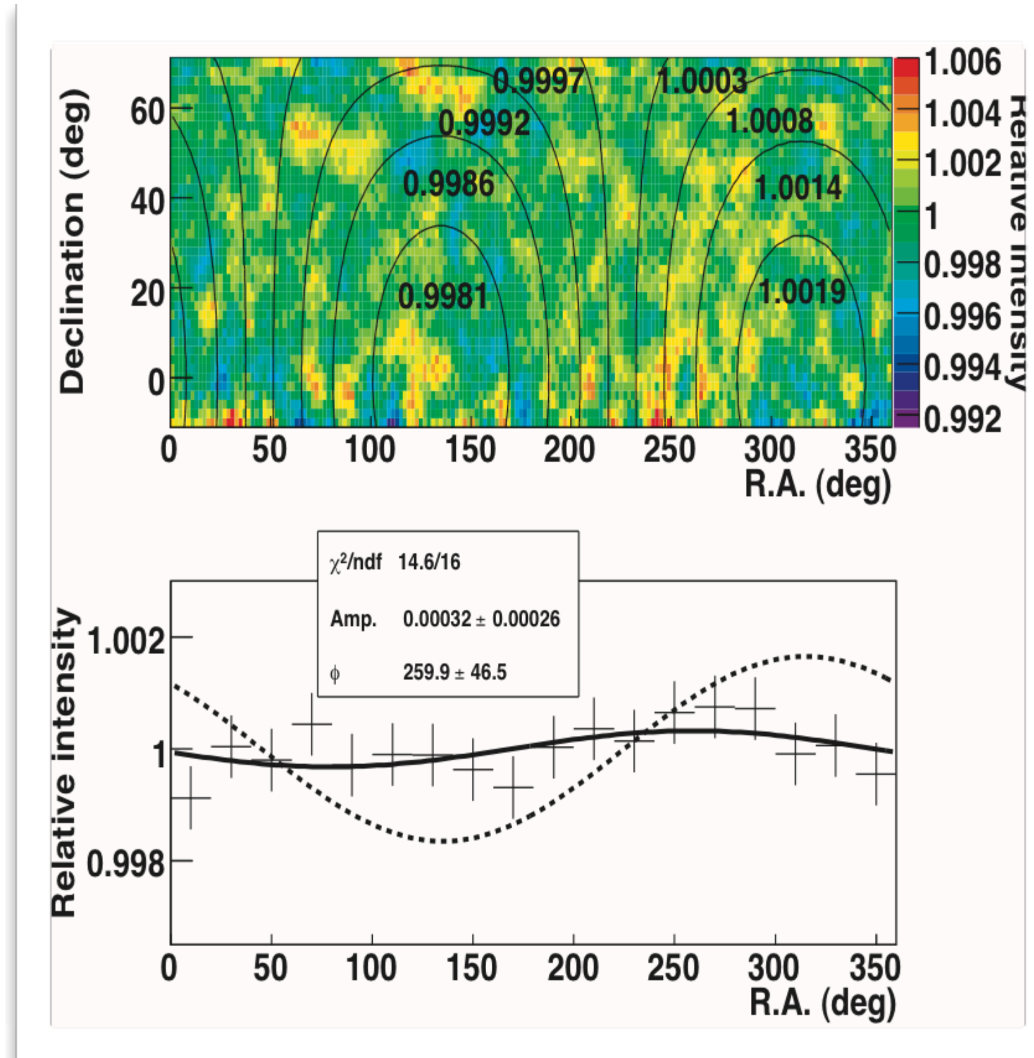

300 TeV

Tibet-III

Amenomori et al., Science Vol. 314, pp. 439, 2006

relative intensity

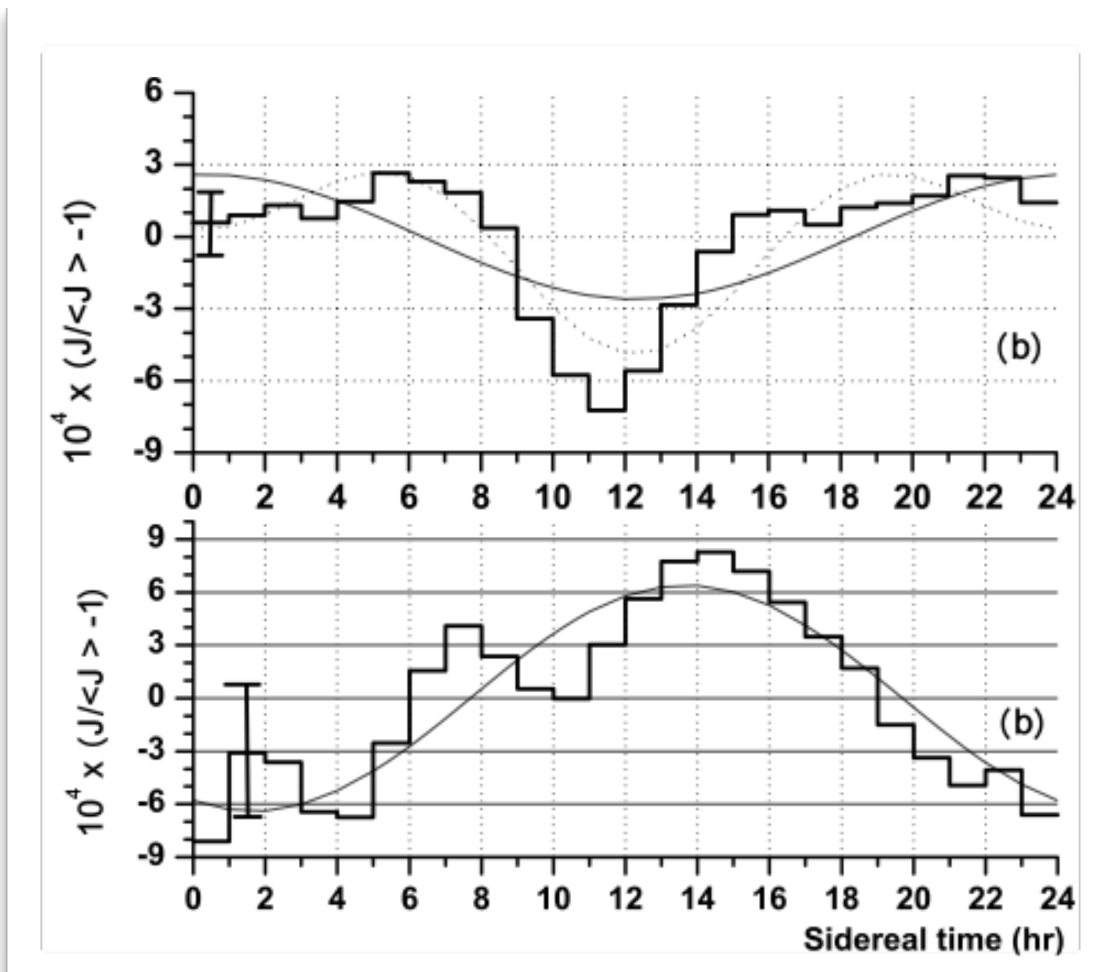

110 TeV

370 TeV

EAS-TOP

Aglietta et al., ApJ 692, L130, 2009

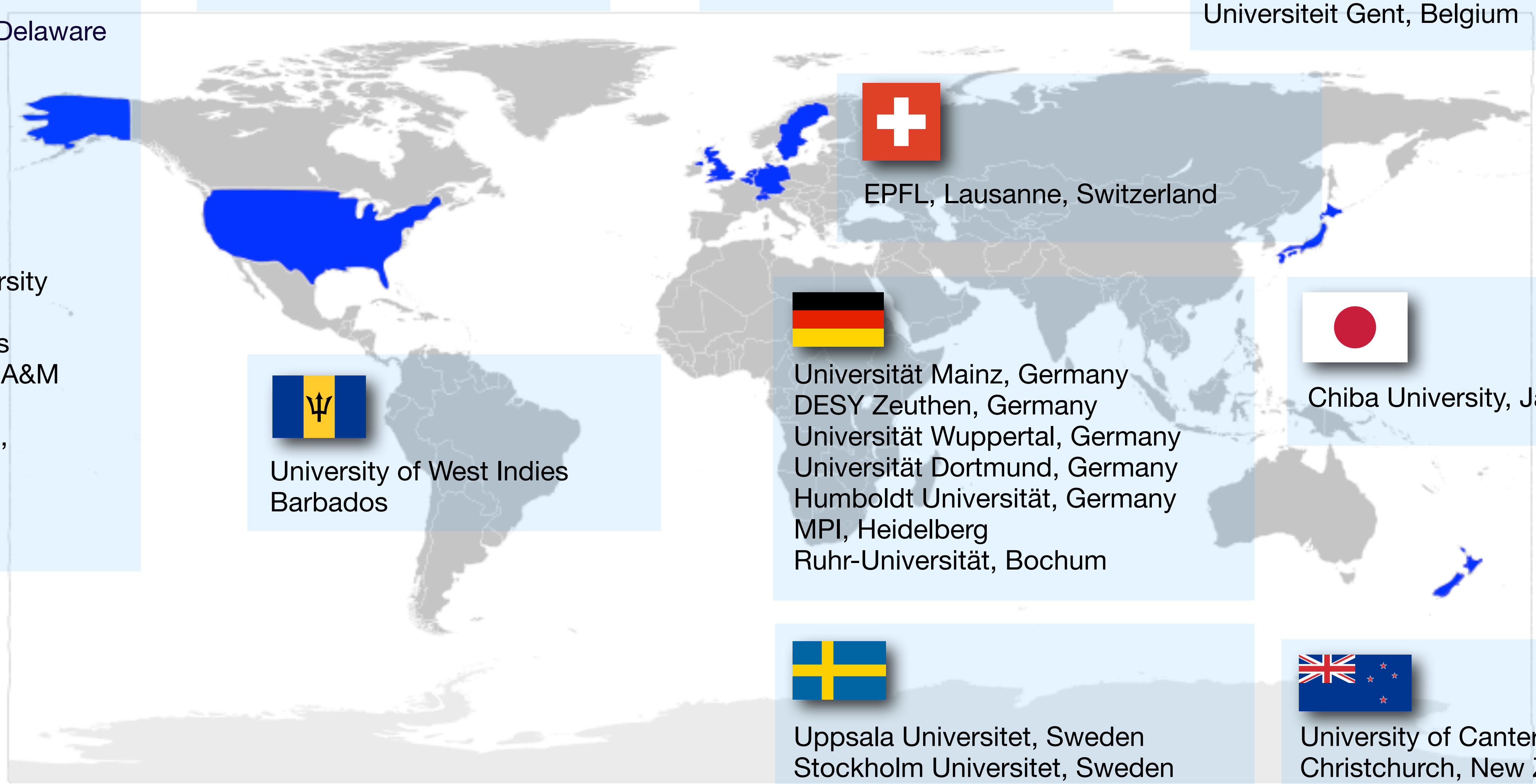

Bartol Inst, Univ of Delaware
Penn State
UW-Madison
UW-River Falls
LBNL, Berkeley
UC Berkeley
UC Irvine
Univ. of Alabama
Clark-Atlanta University
Univ. of Maryland
University of Kansas
Southern Univ. and A&M College
University of Alaska, Anchorage
Georgia Tech
Ohio State

University of Alberta, Canada

Utrecht University, Netherlands

Université Libre de Bruxelles, Belgium
Vrije Universiteit Brussel, Belgium
Université de Mons-Hainaut, Belgium
Universiteit Gent, Belgium

EPFL, Lausanne, Switzerland

University of West Indies Barbados

Universität Mainz, Germany
DESY Zeuthen, Germany
Universität Wuppertal, Germany
Universität Dortmund, Germany
Humboldt Universität, Germany
MPI, Heidelberg
Ruhr-Universität, Bochum

Chiba University, Japan

Uppsala Universitet, Sweden
Stockholm Universitet, Sweden
Kalmar Universitet, Sweden

University of Canterbury, Christchurch, New Zealand

Madison, WI - May 2011

IceCube Collaboration

10 countries
36 institutions
~260 collaborators

IceCube Observatory

- 86 strings
- 5160 DOMs
- 17 m vertical spacing
- 125 m between strings

Digital Optical Module - DOM

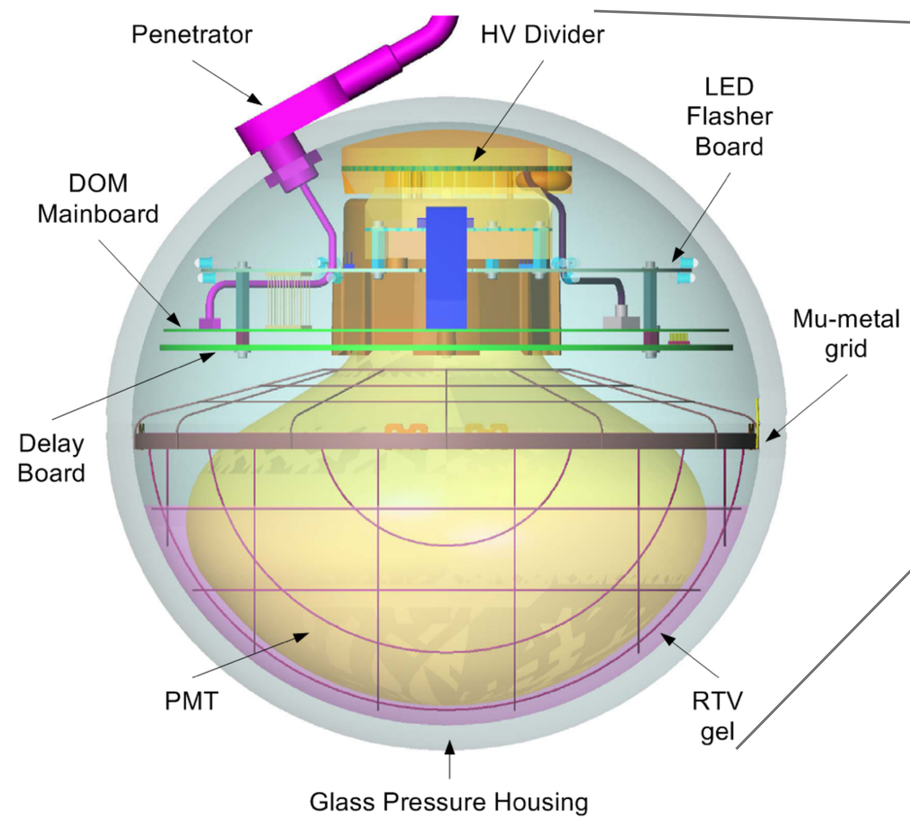

IceCube

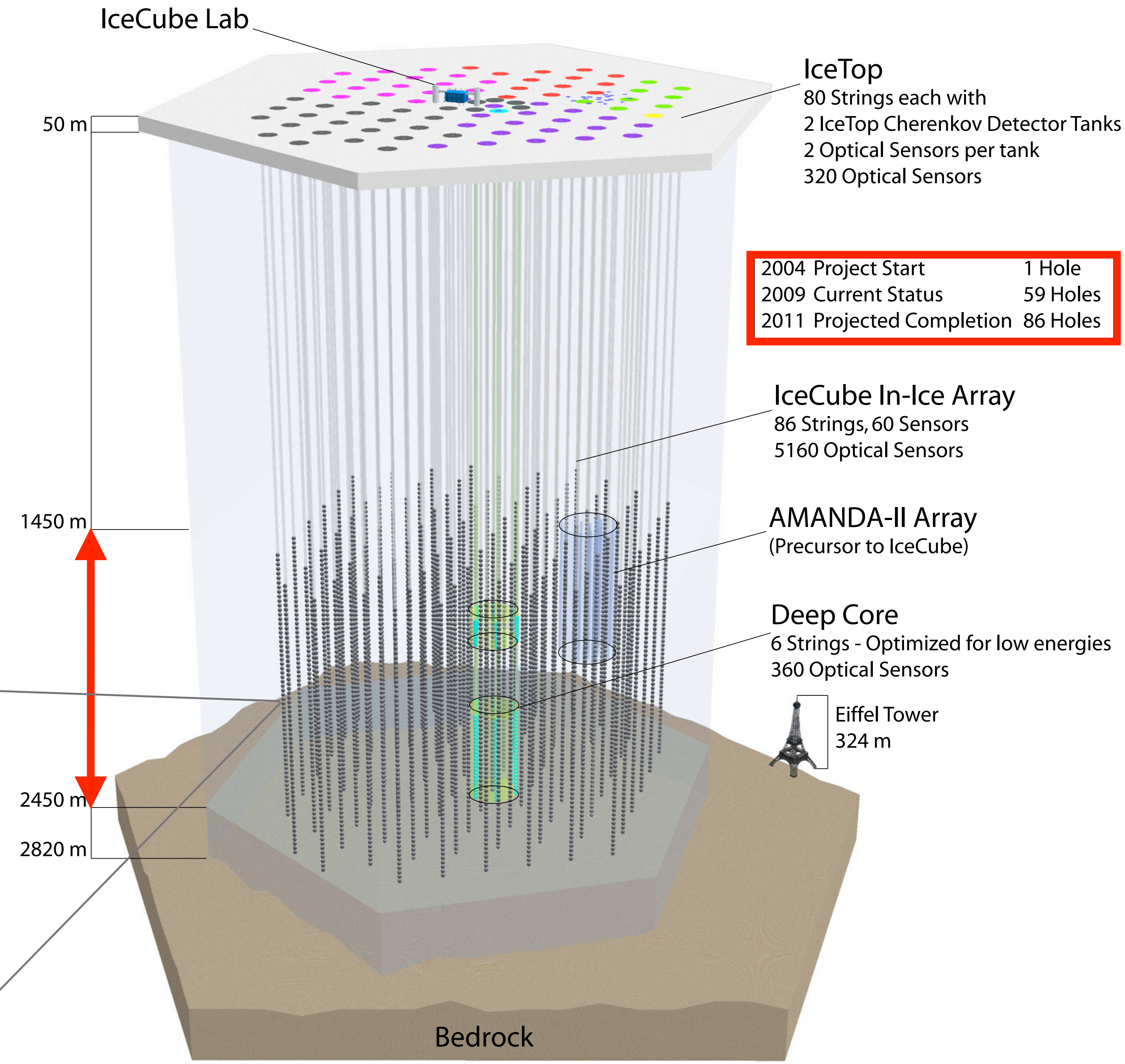

IceCube configurations

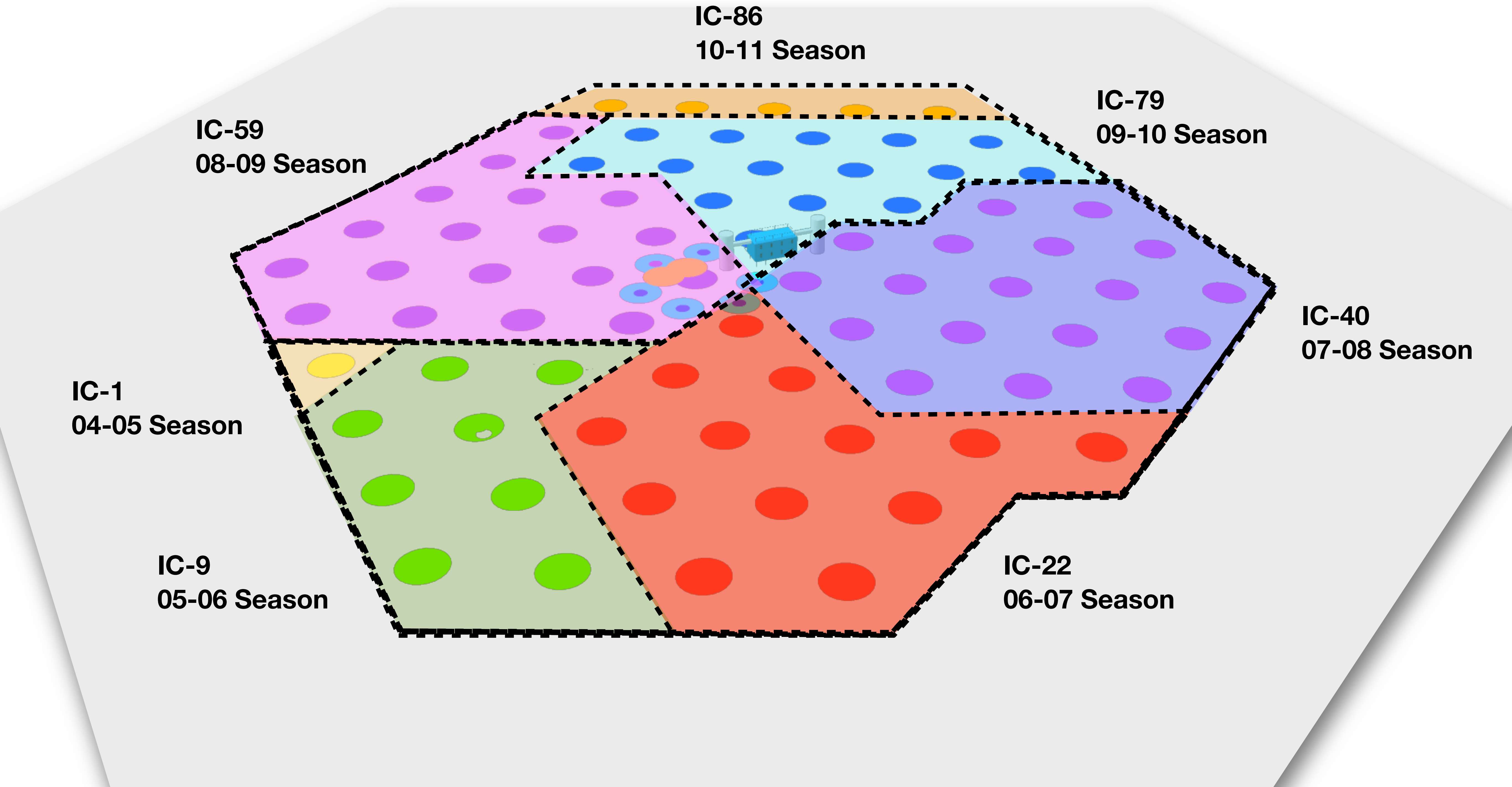

growing IceCube & temperature correlations

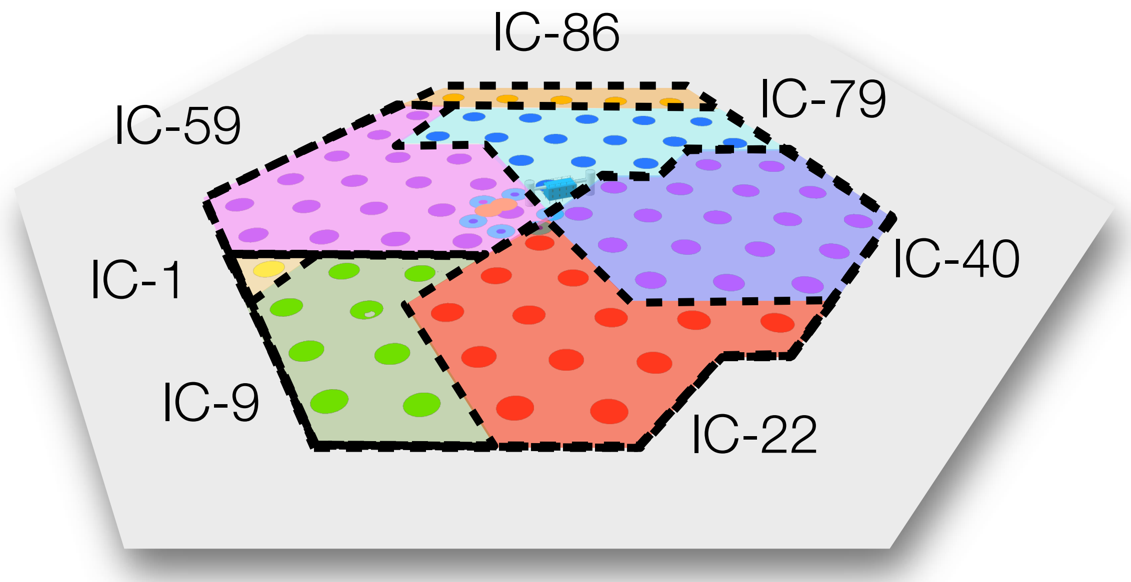

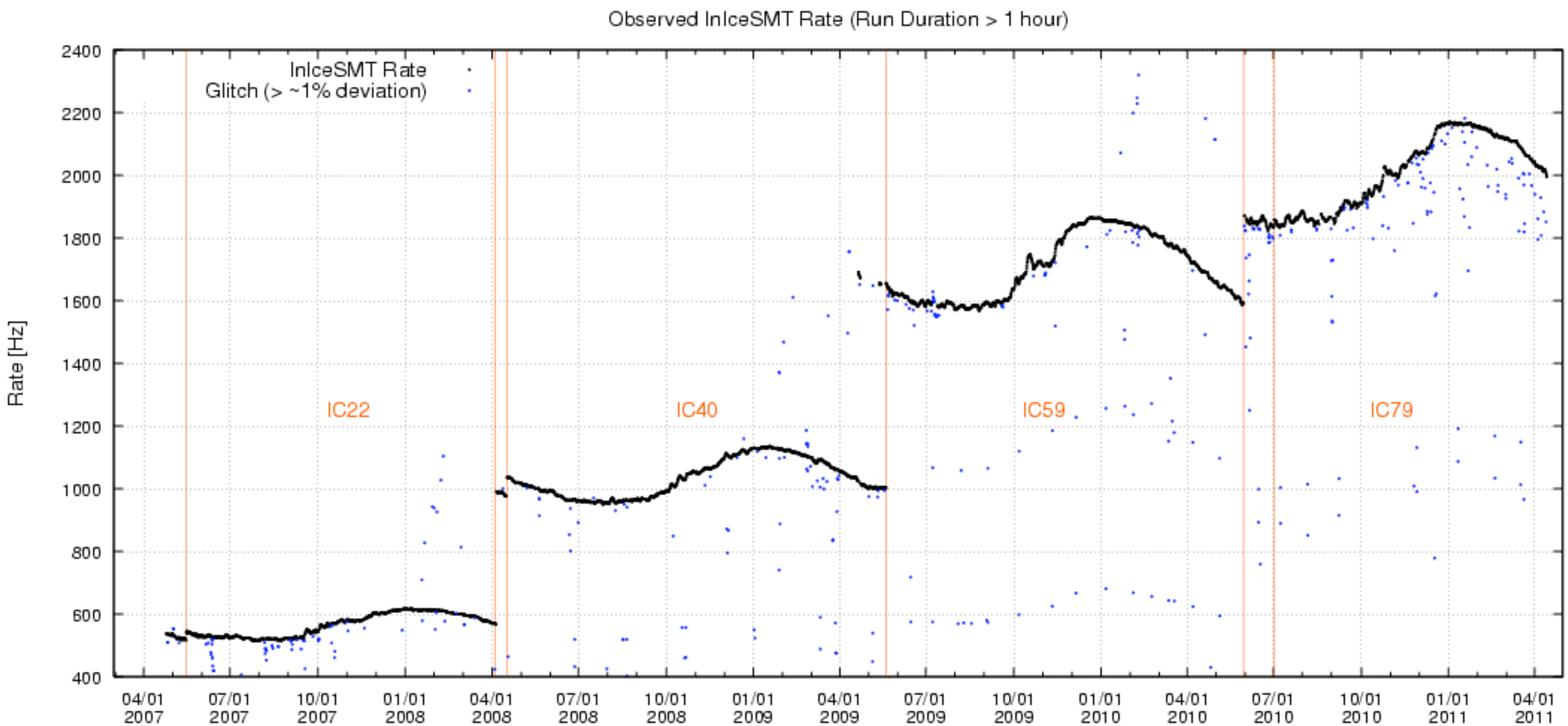

detection technique

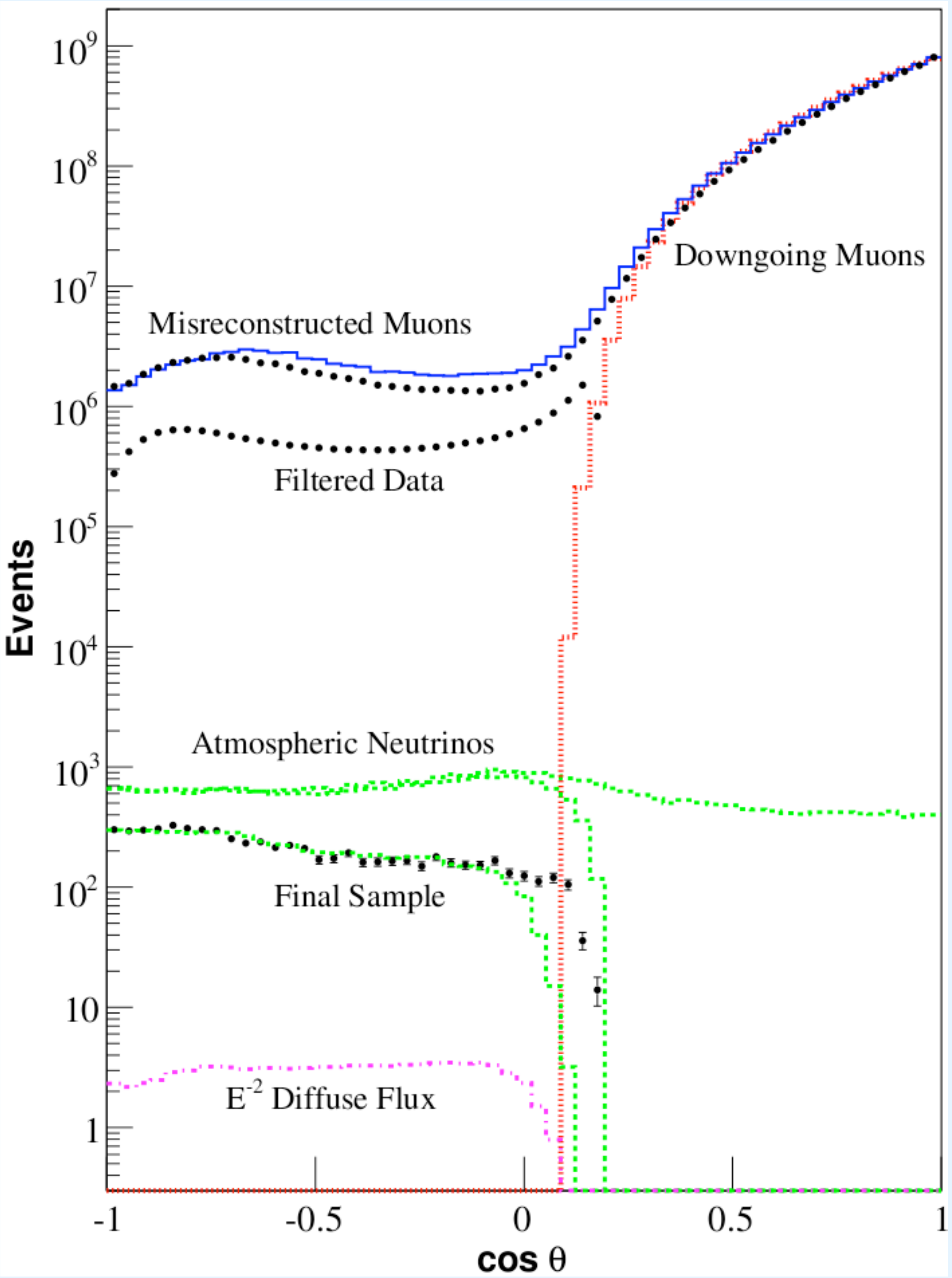

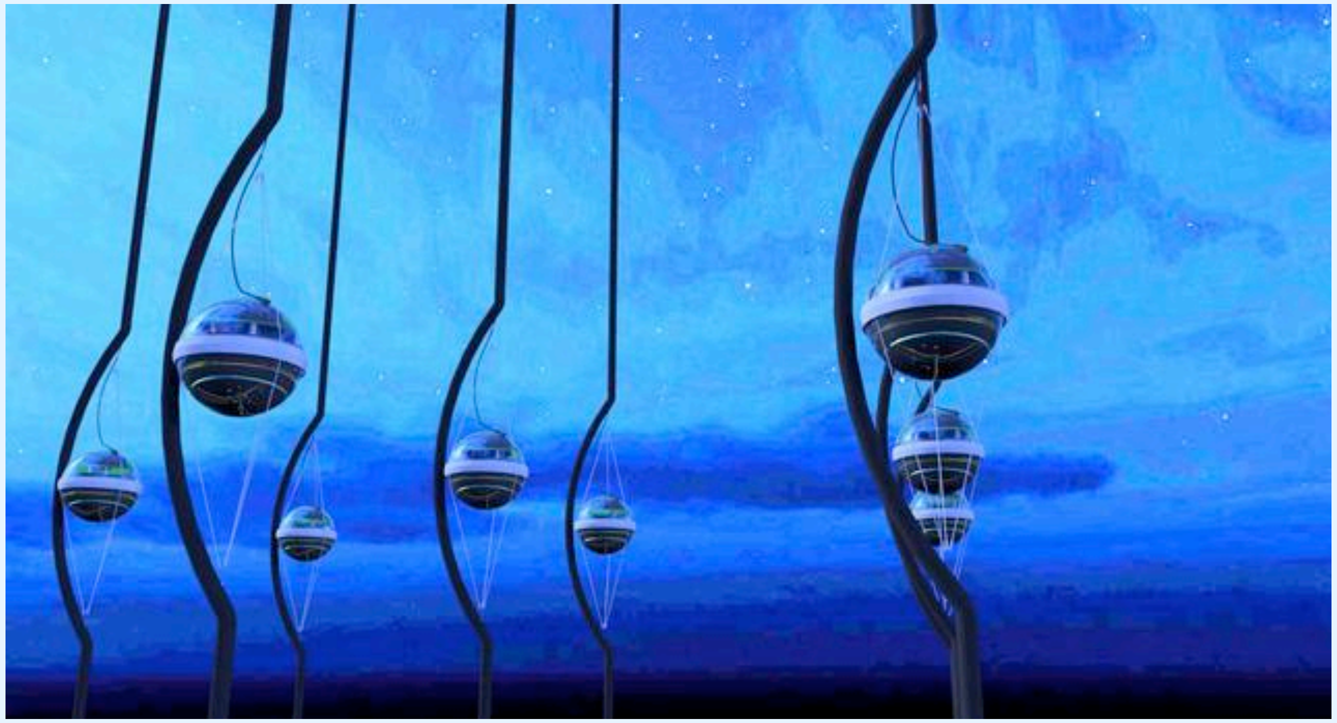

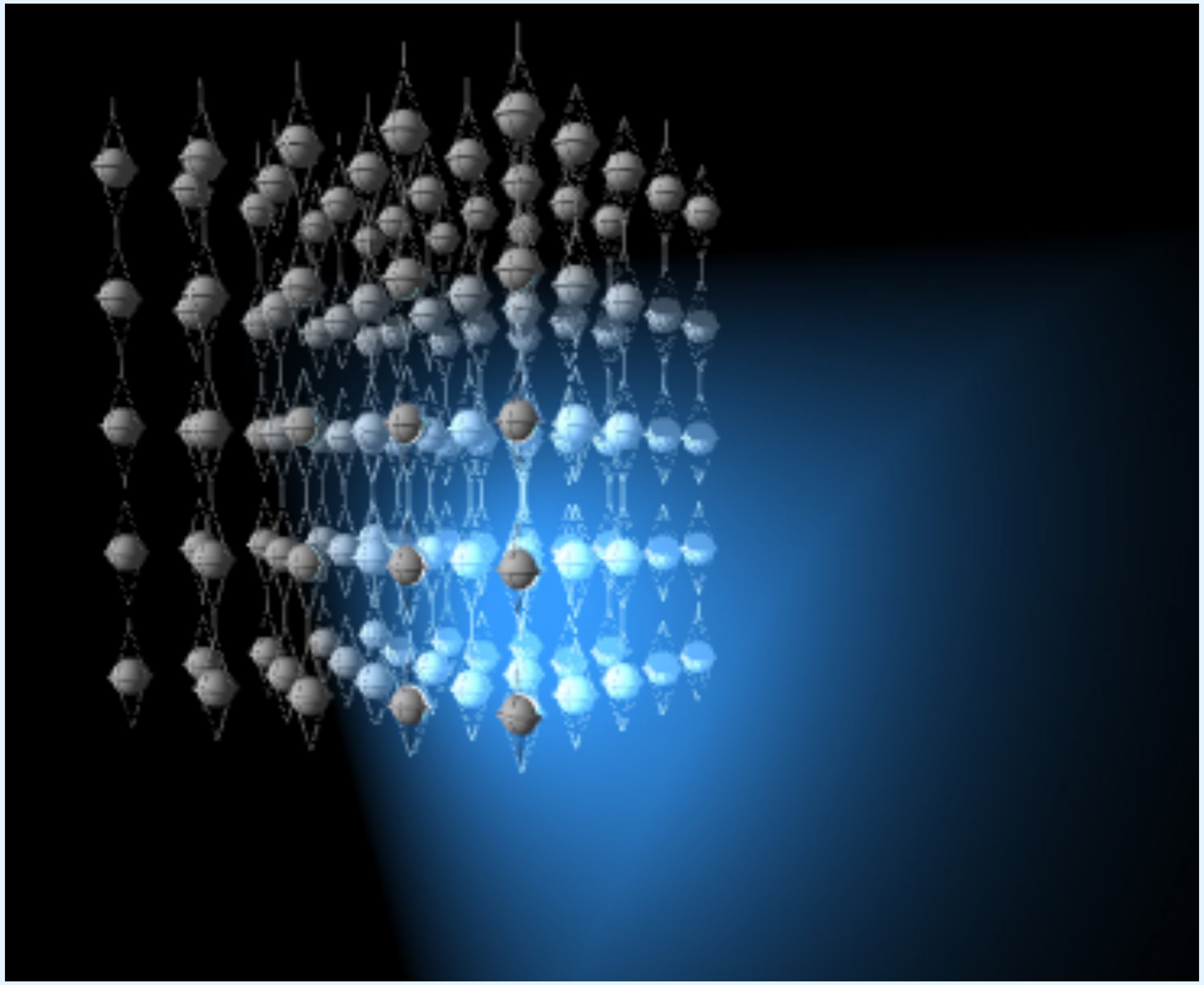

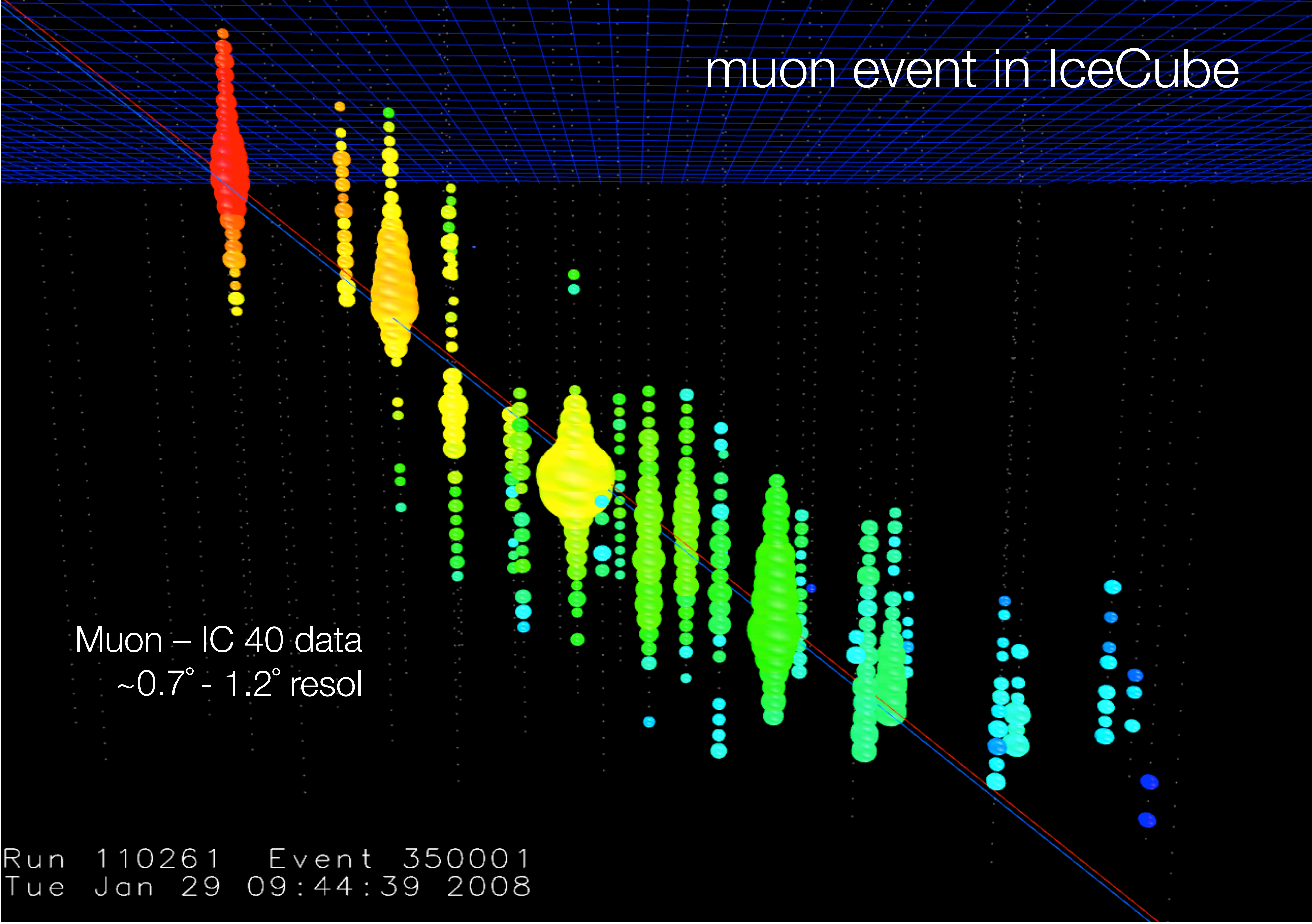
muon event in IceCube
Muon – IC 40 data
~0.7° - 1.2° resol
Run 110261 Event 350001
Tue Jan 29 09:44:39 2008

IceCube muon (bundles) data

detector	trigger rate (Hz)	actual time (d)	livetime (d)	number of events (*)
IceCube-22	500	300	226	5.4×10^9
IceCube-40	1,100	358	324	19×10^9
IceCube-59	1,700	367	334.5	34×10^9
IceCube-79	2,000	365	337	40×10^9
IceCube-86	2,500	365	365	50×10^9

(*) number of events with LLH reconstruction from online-filter collected by DST

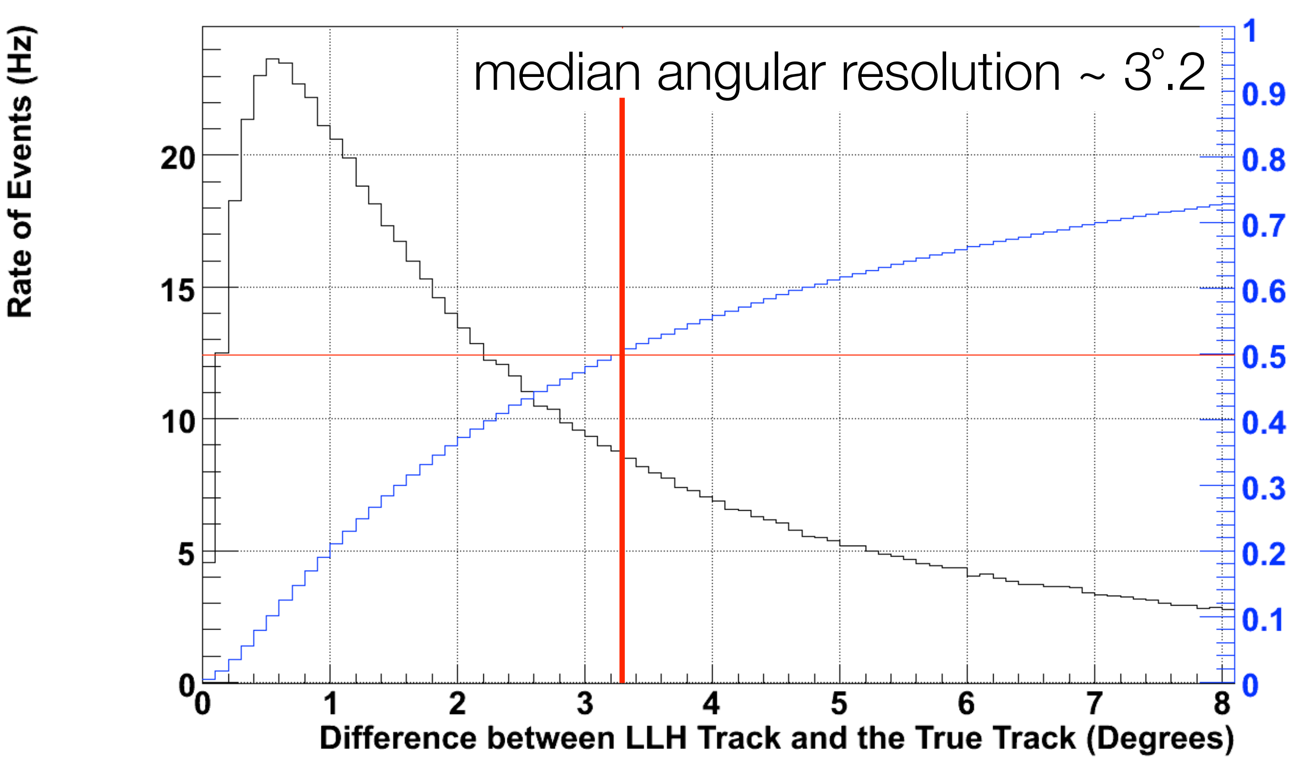

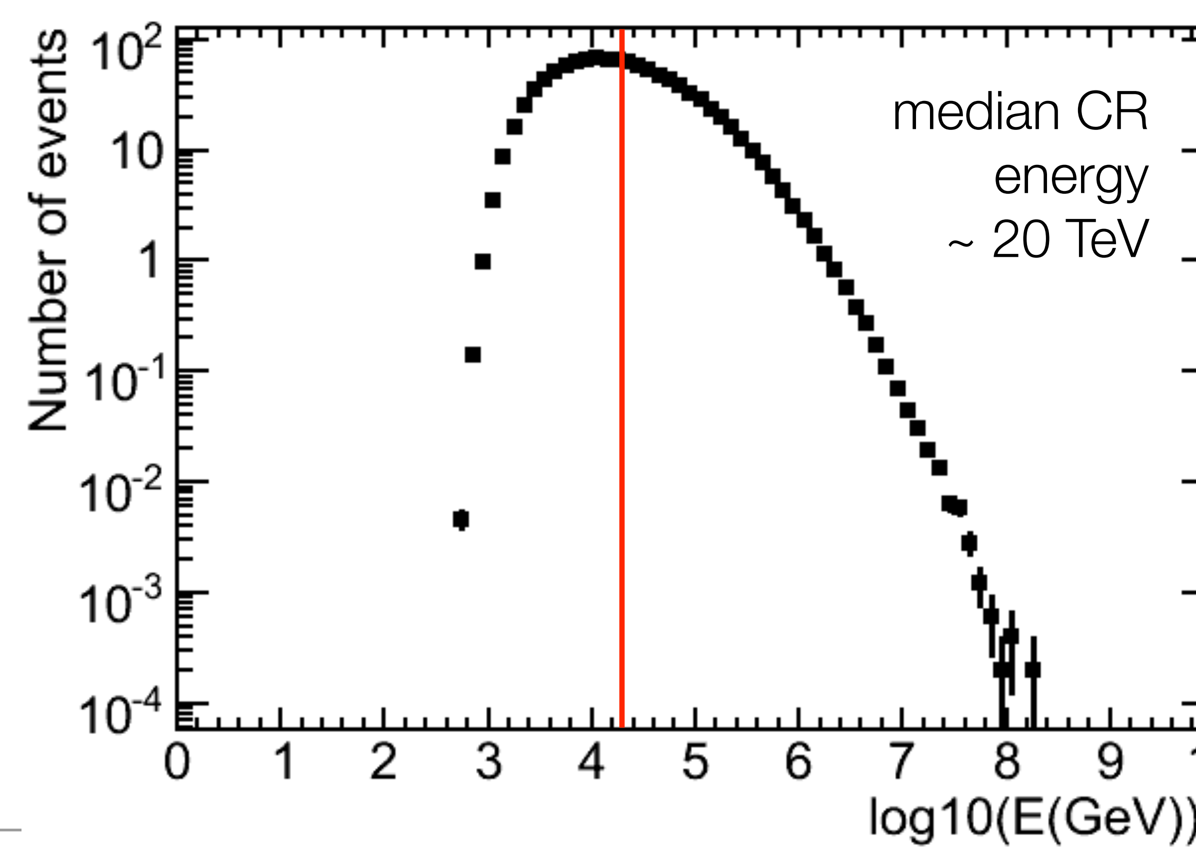

cosmic ray anisotropy in IceCube

time

relative intensity

equatorial coordinates

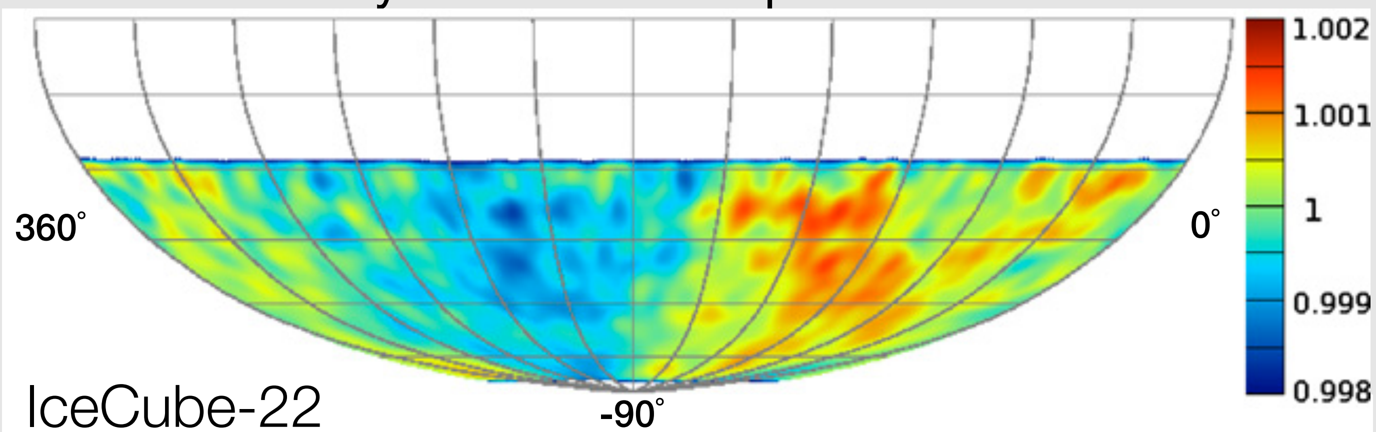

$$I_i = \frac{N_i(\alpha,\delta)}{\langle N_i(\delta)\rangle_\alpha}$$

20 TeV

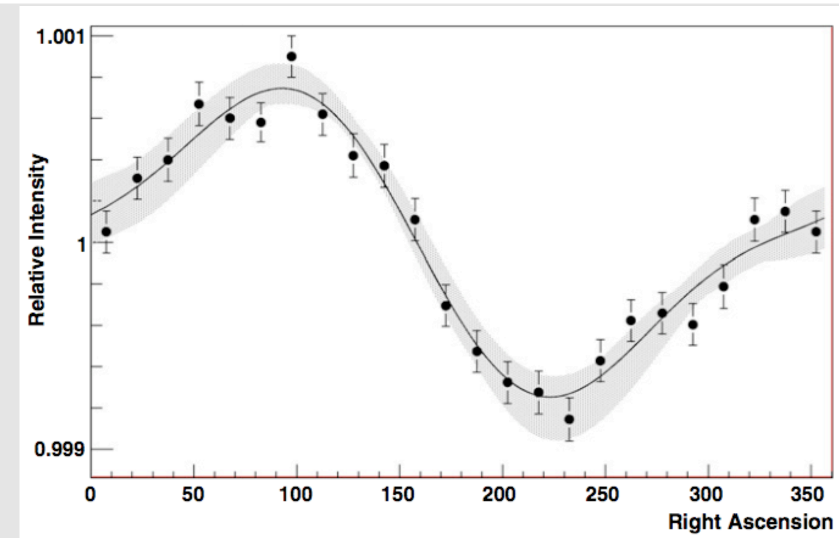

Abbasi et al., ApJ, **718**, L194, 2010

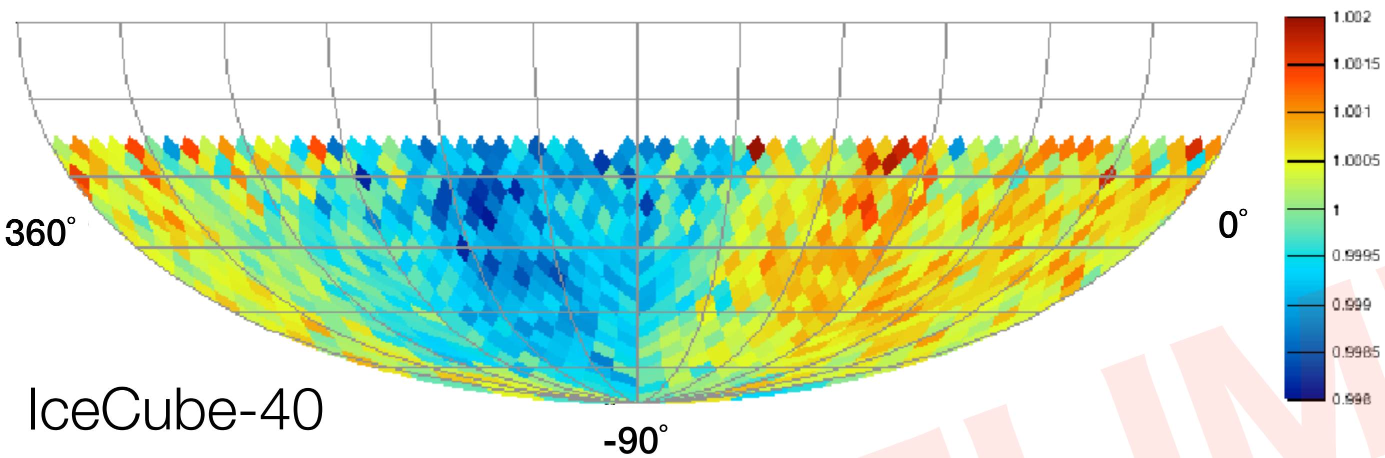

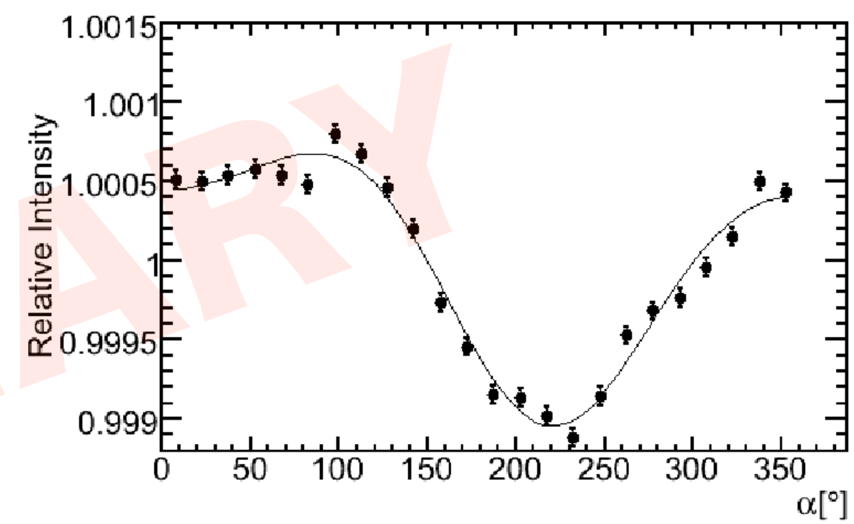

PRELIMINARY

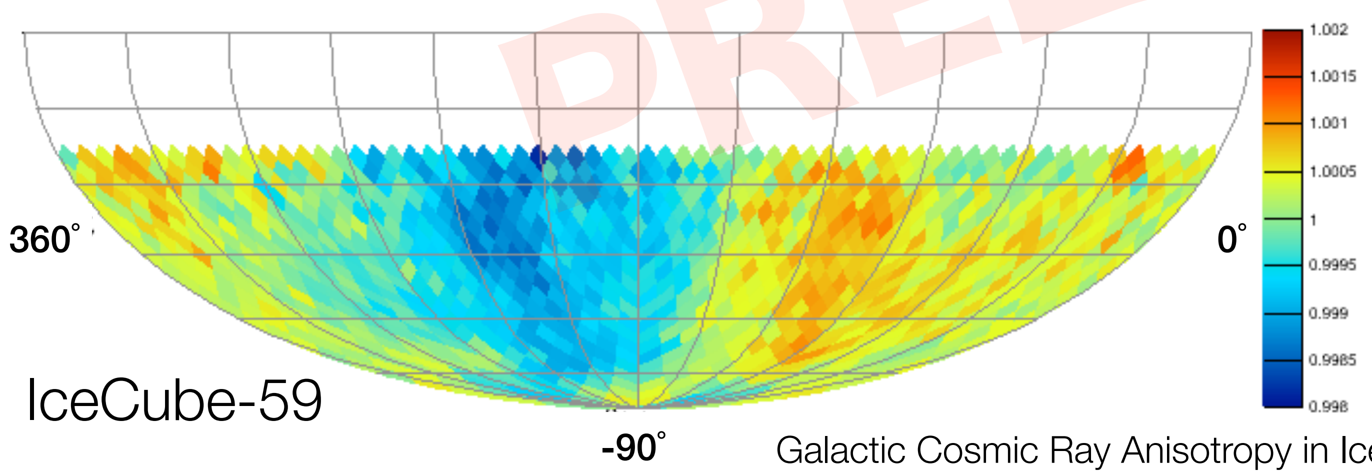

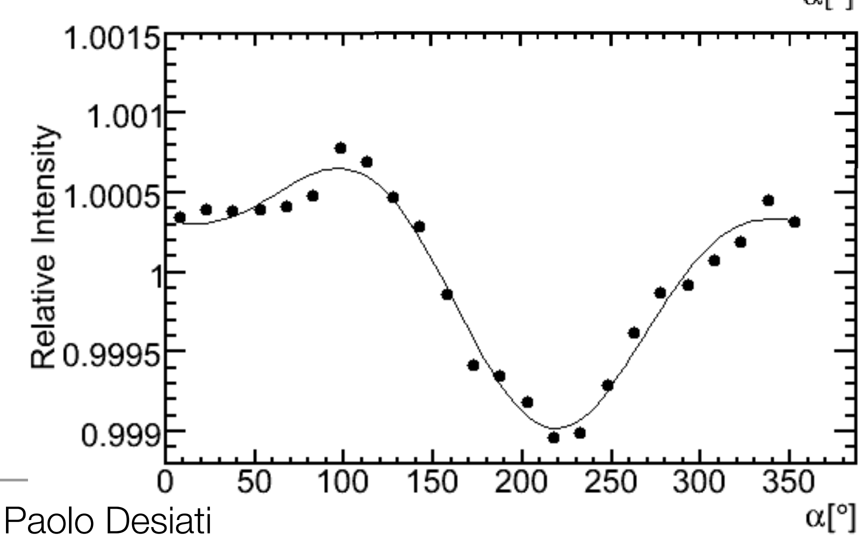

cosmic ray anisotropy in arrival direction

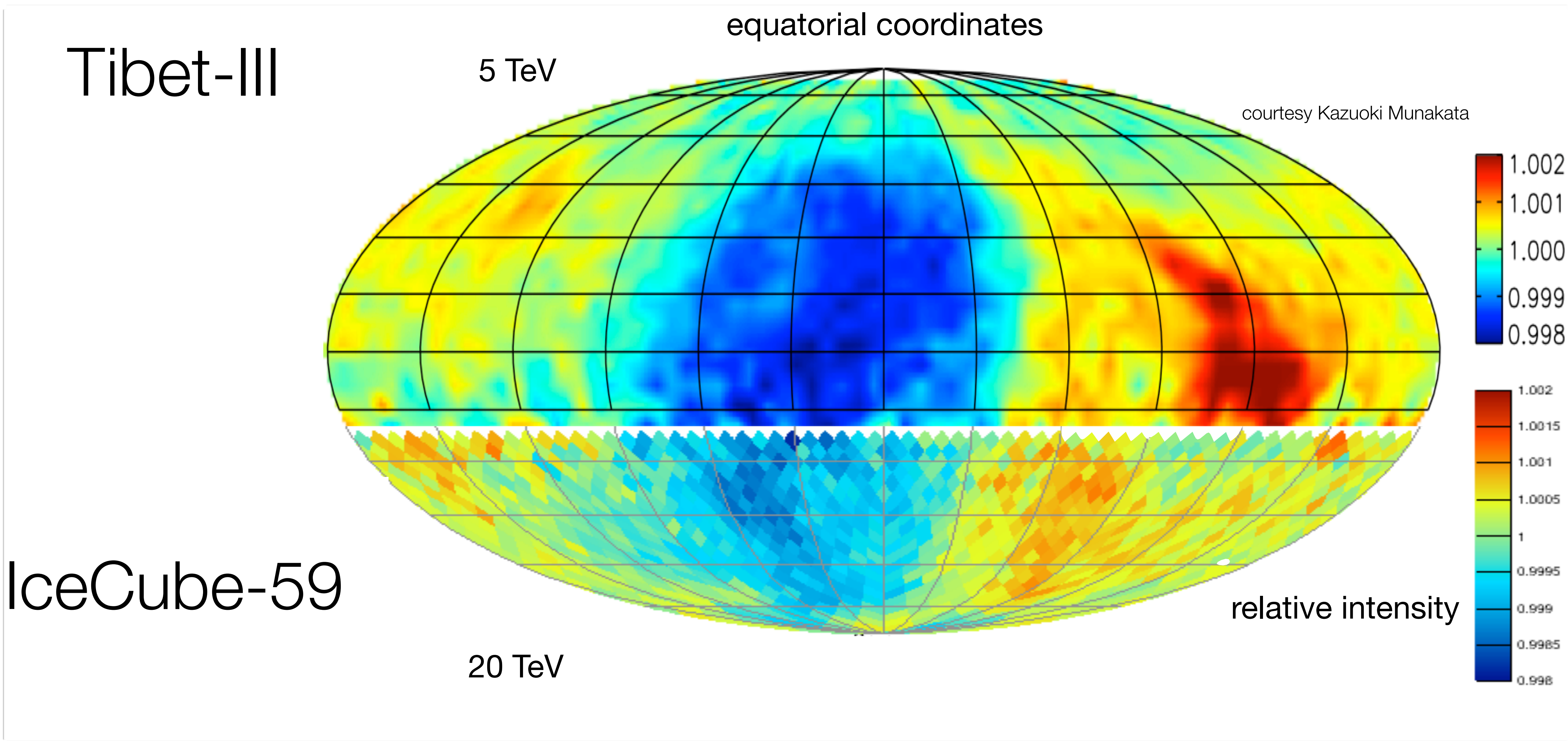

cosmic ray anisotropy in arrival direction

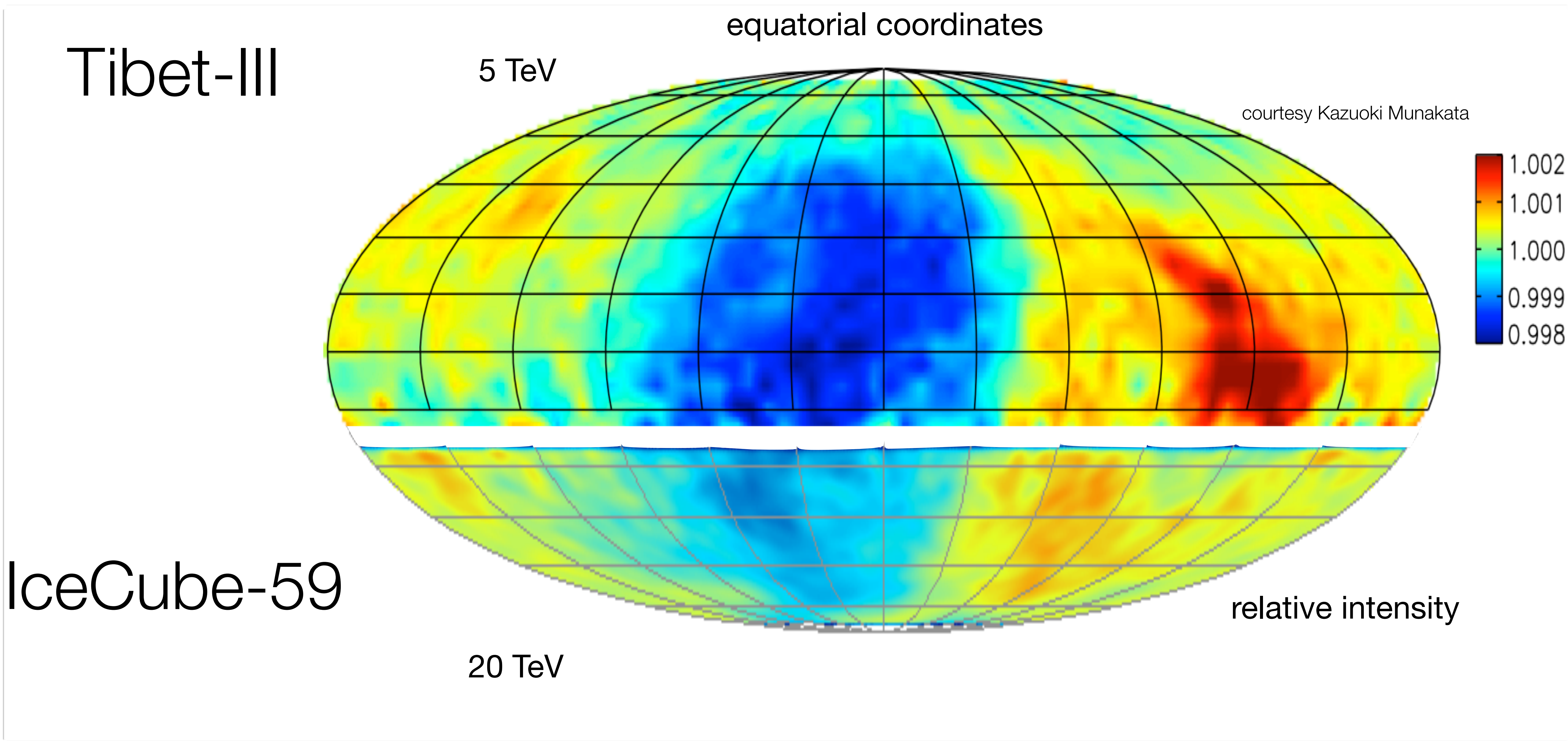

cosmic ray anisotropy vs energy in IceCube-59

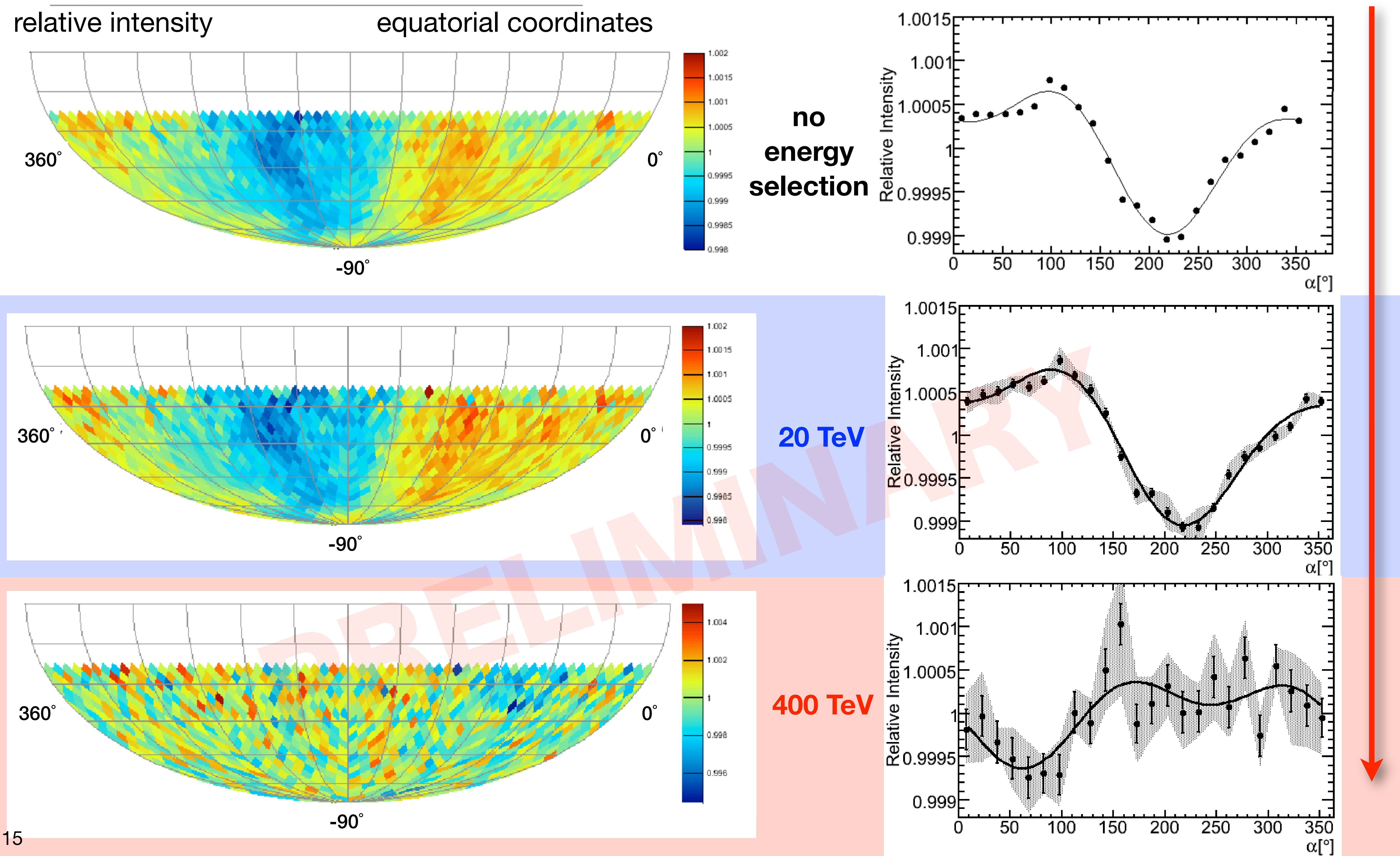

cosmic ray anisotropy vs energy in IceCube-59

energy

- reference map derived from data with time scrambling
- smoothing radius optimized on highest significance in excess/deficit region

$$s = \sqrt{2}\left\{ N_{\rm on} \ln\left[\frac{1+\alpha}{\alpha}\left(\frac{N_{\rm on}}{N_{\rm on}+N_{\rm off}}\right)\right] + N_{\rm off}\ln\left[(1+\alpha)\left(\frac{N_{\rm off}}{N_{\rm on}+N_{\rm off}}\right)\right]\right\}^{1/2} \qquad \alpha = 1/20$$

Li, T., & Ma, Y. 1983, ApJ, 272, 317

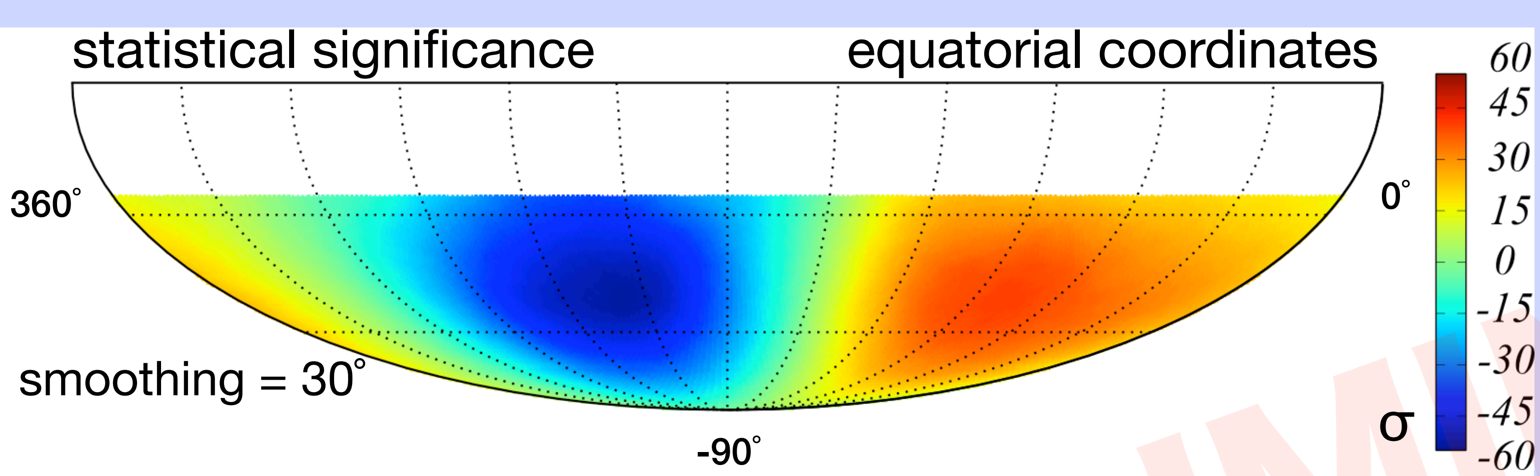

20 TeV

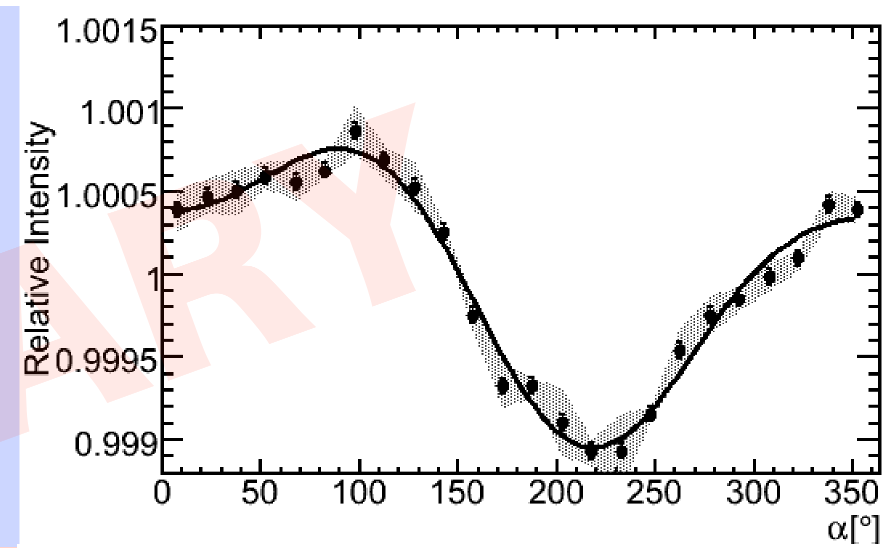

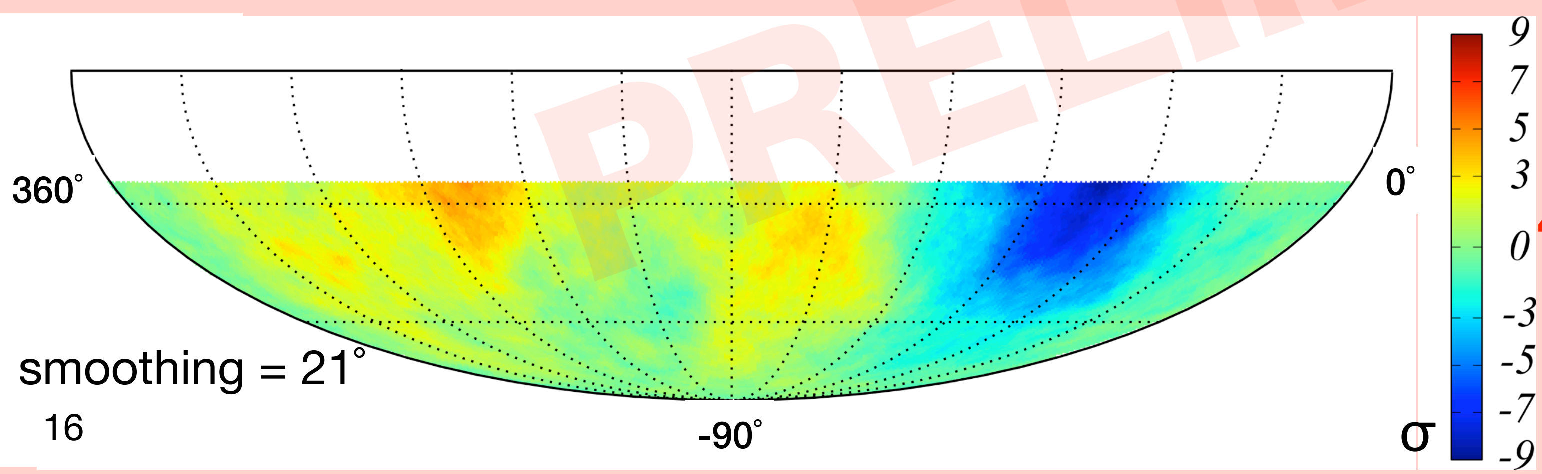

400 TeV

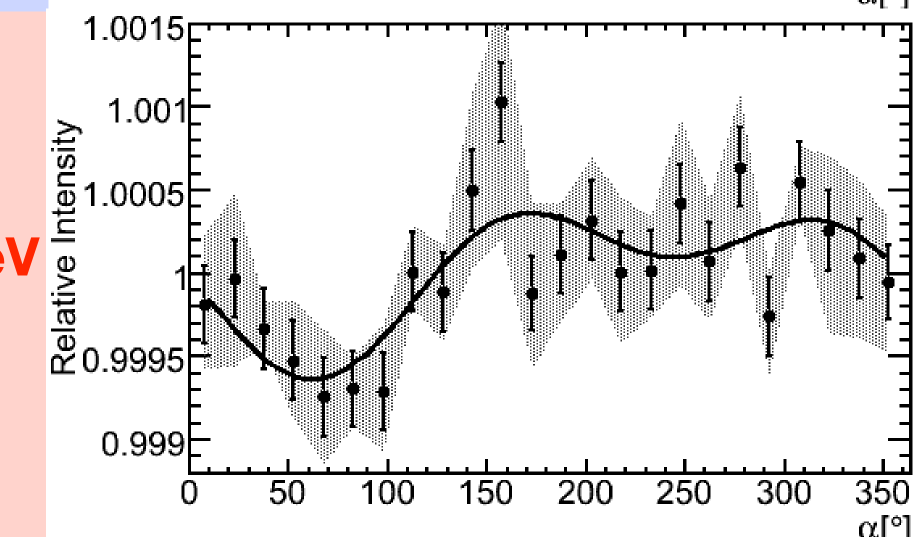

cosmic ray anisotropy vs energy in IceCube-59

EAS-TOP

370 TeV

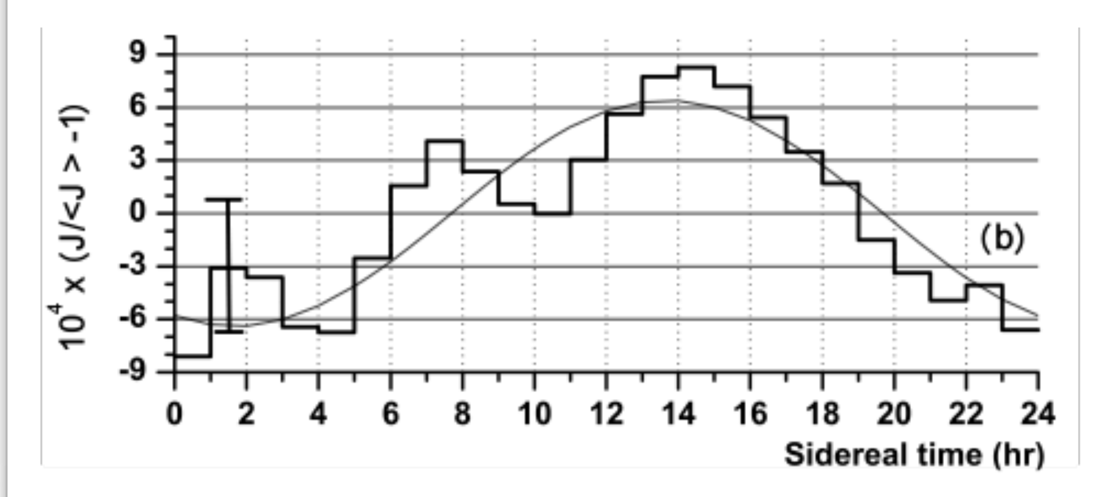

Tibet-III

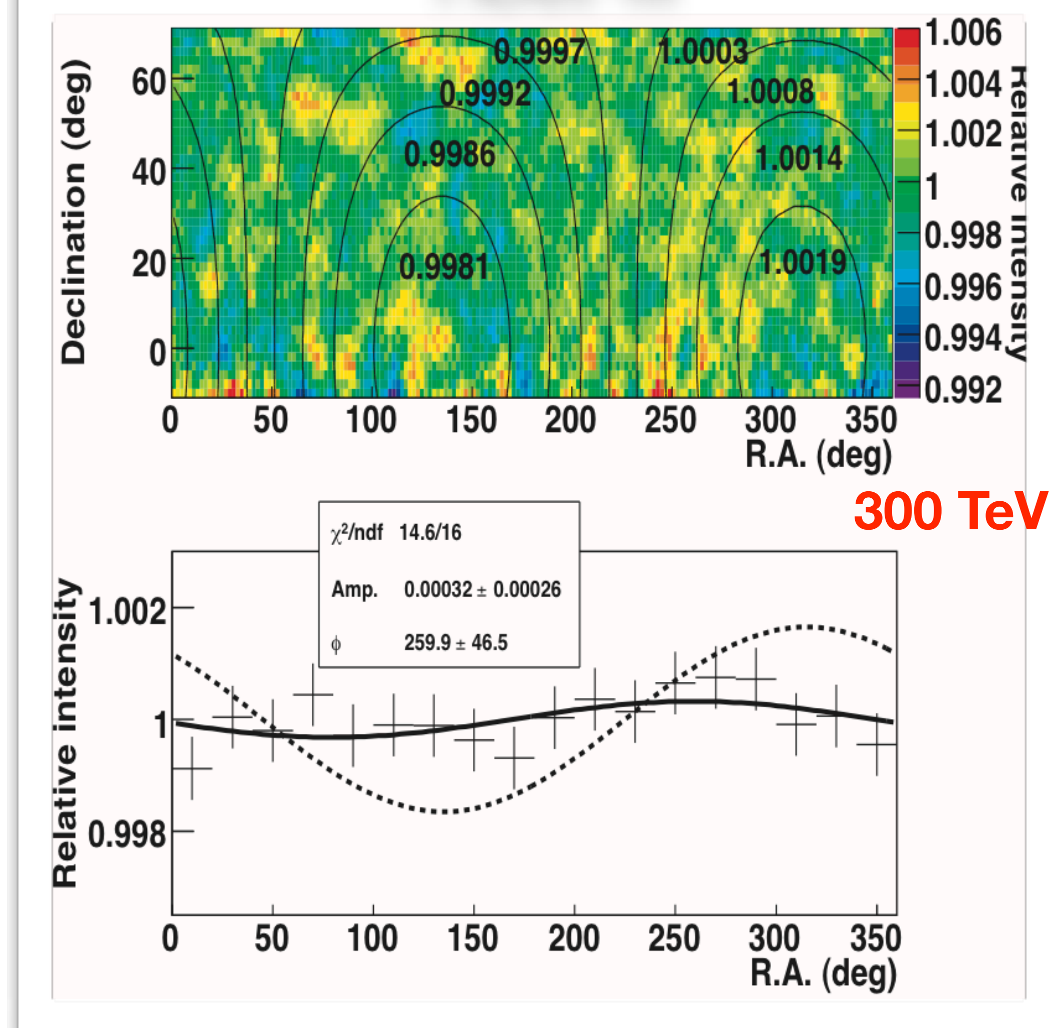

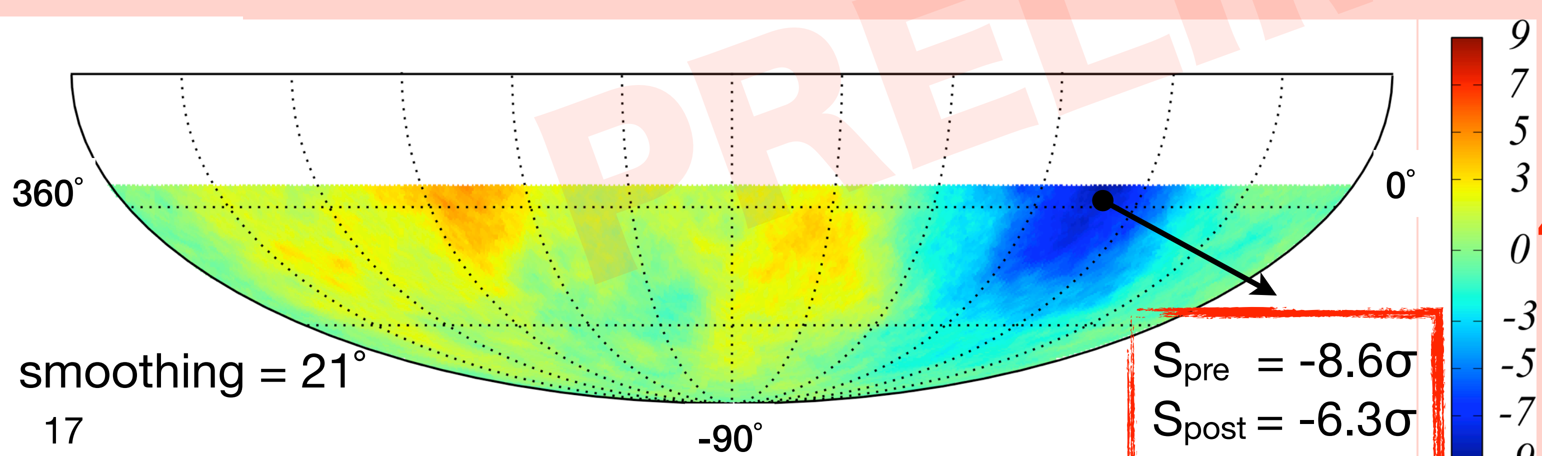

400 TeV

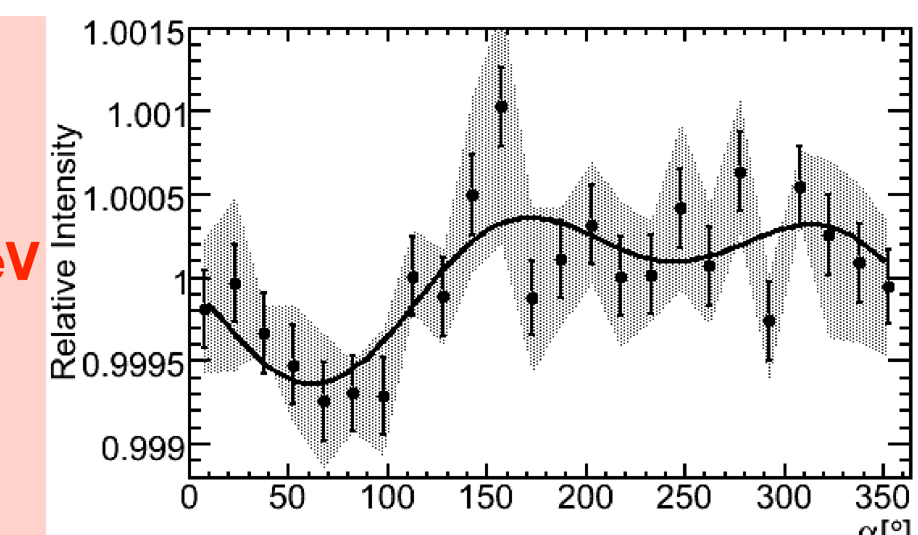

Earth's motion around the Sun

Compton & Getting, Phys. Rev. 47, 817 (1935)
Gleeson, & Axford, Ap&SS, 2, 43 (1968)

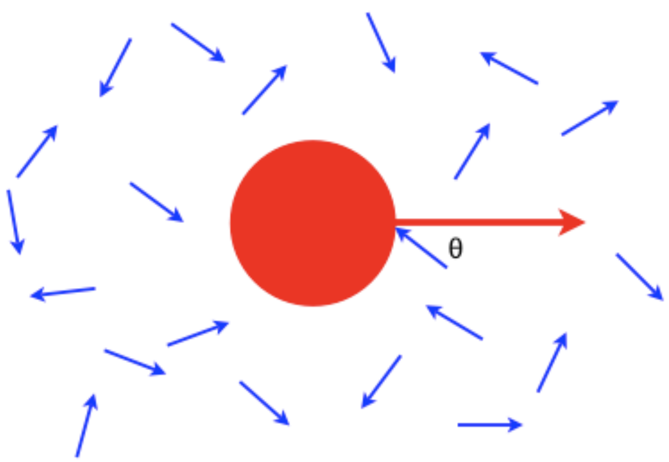

v = 29.8 ± 0.5 km/s

$$\frac{\Delta I}{I} = (\gamma + 2)\frac{v}{c}\cos\theta$$

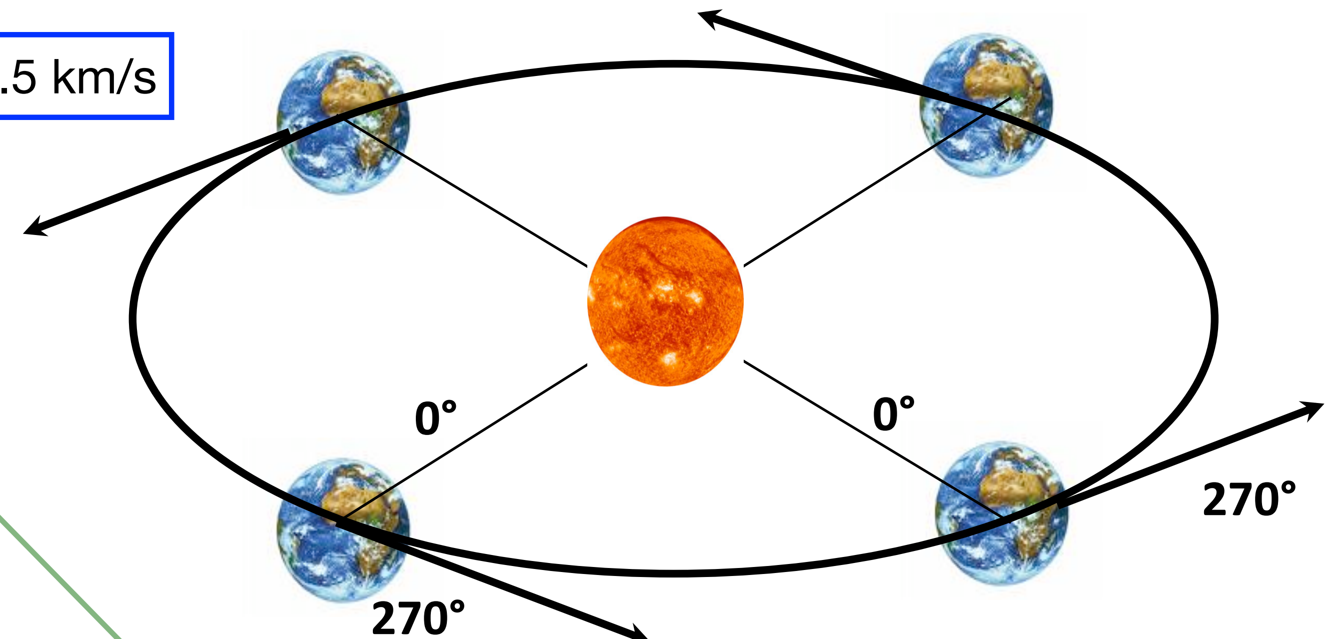

Hörandel, Astrop. Phys. 19, 193, 2003

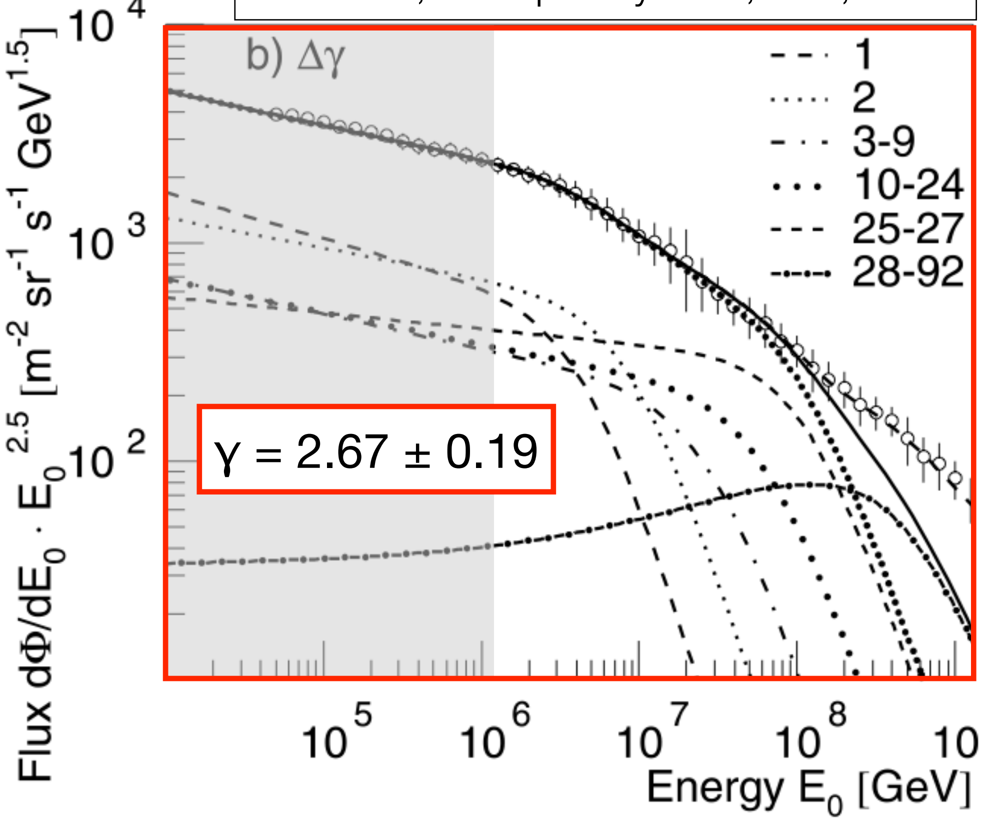

point spread function

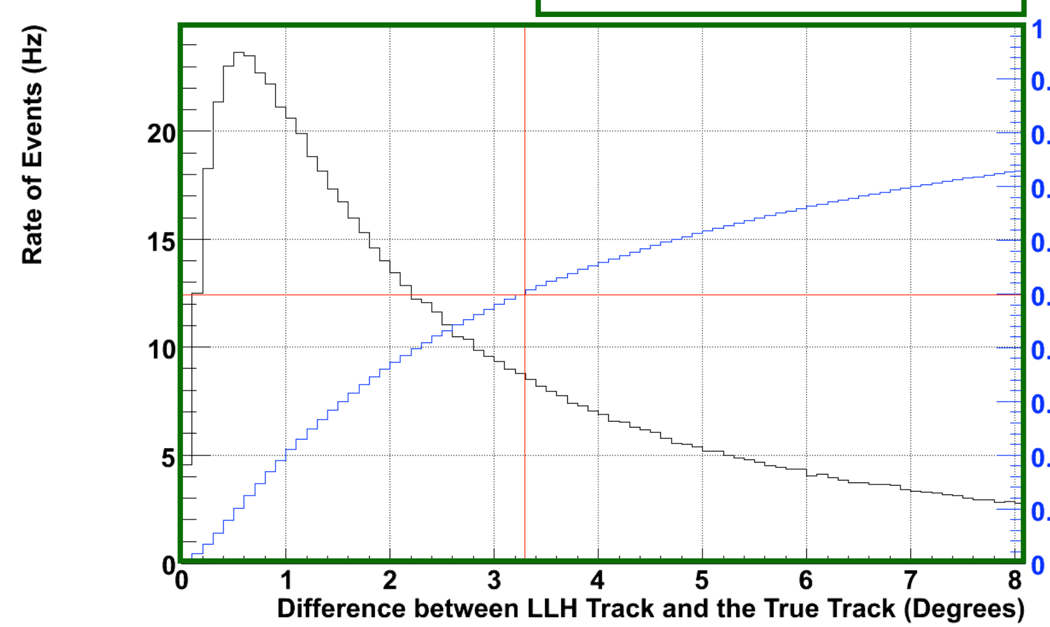

solar dipole anisotropy vs energy in IceCube-59

The observation of the solar dipole supports the observation of the sidereal anisotropy in cosmic ray arrival direction

relative intensity

α [°] - α_{SUN} [°]

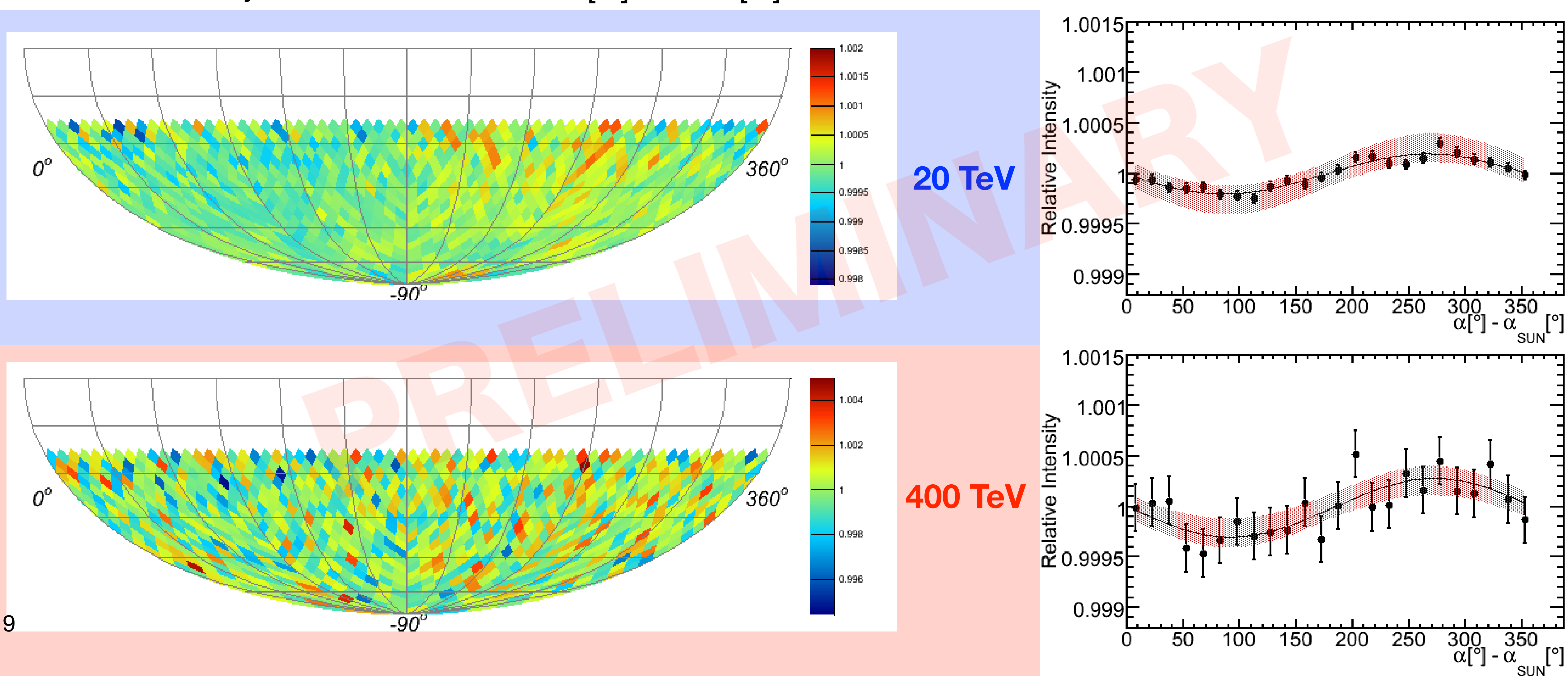

anti-/extended-sidereal distributions vs energy in IceCube-59

anti-sidereal distribution ~ solar dipole variability

extended-sidereal distribution ~ sid. anis. variability

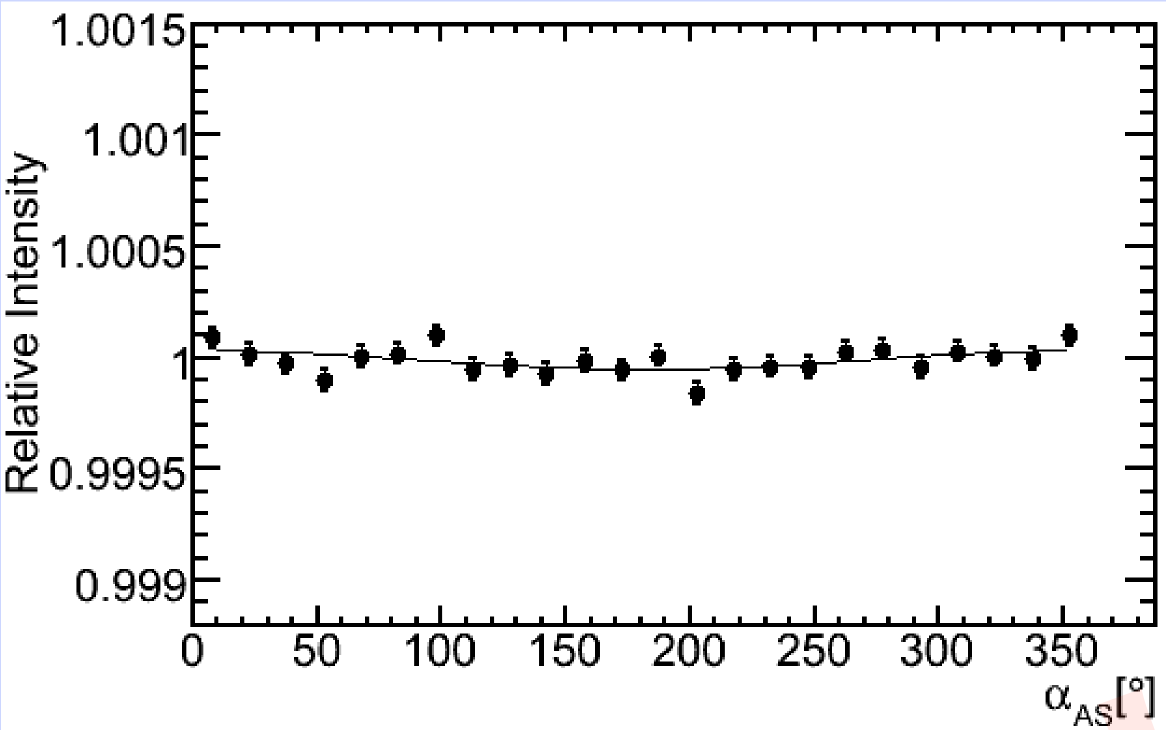

20 TeV

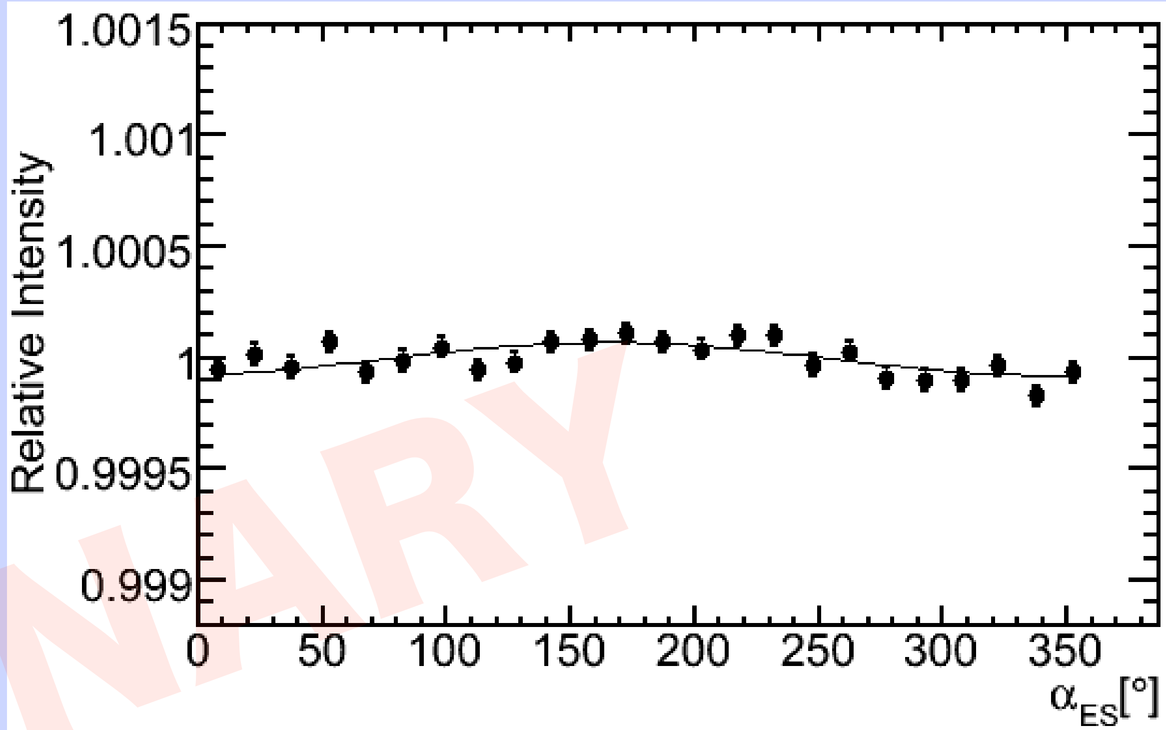

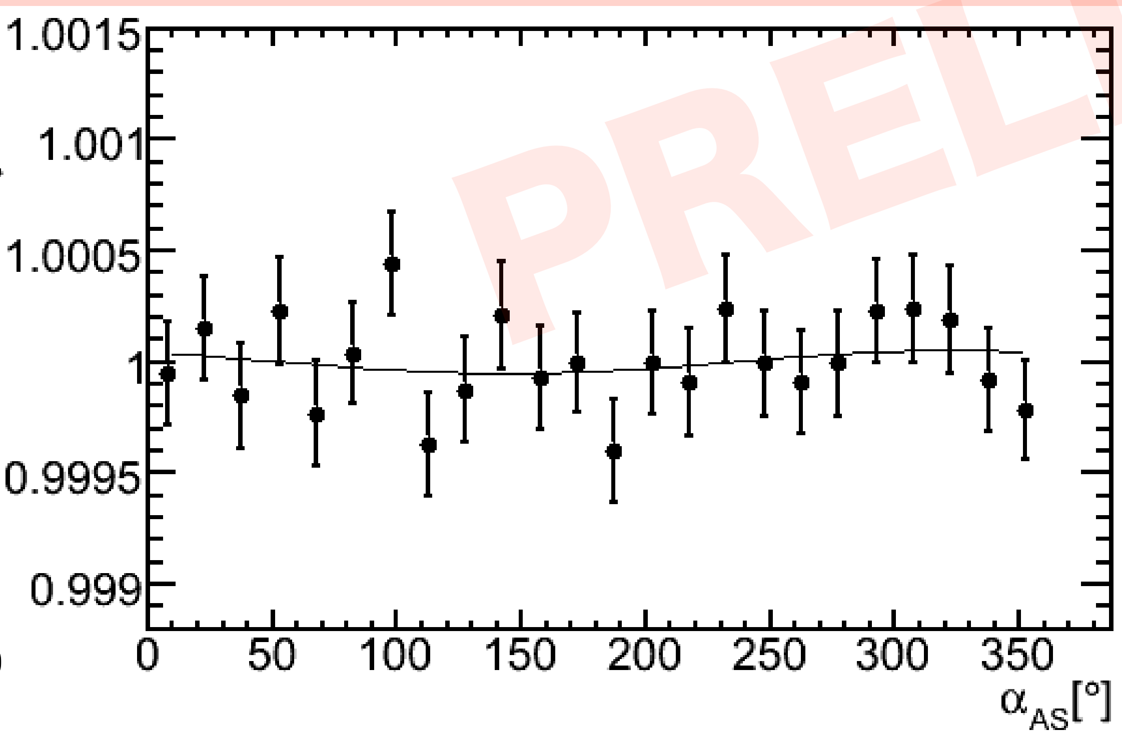

400 TeV

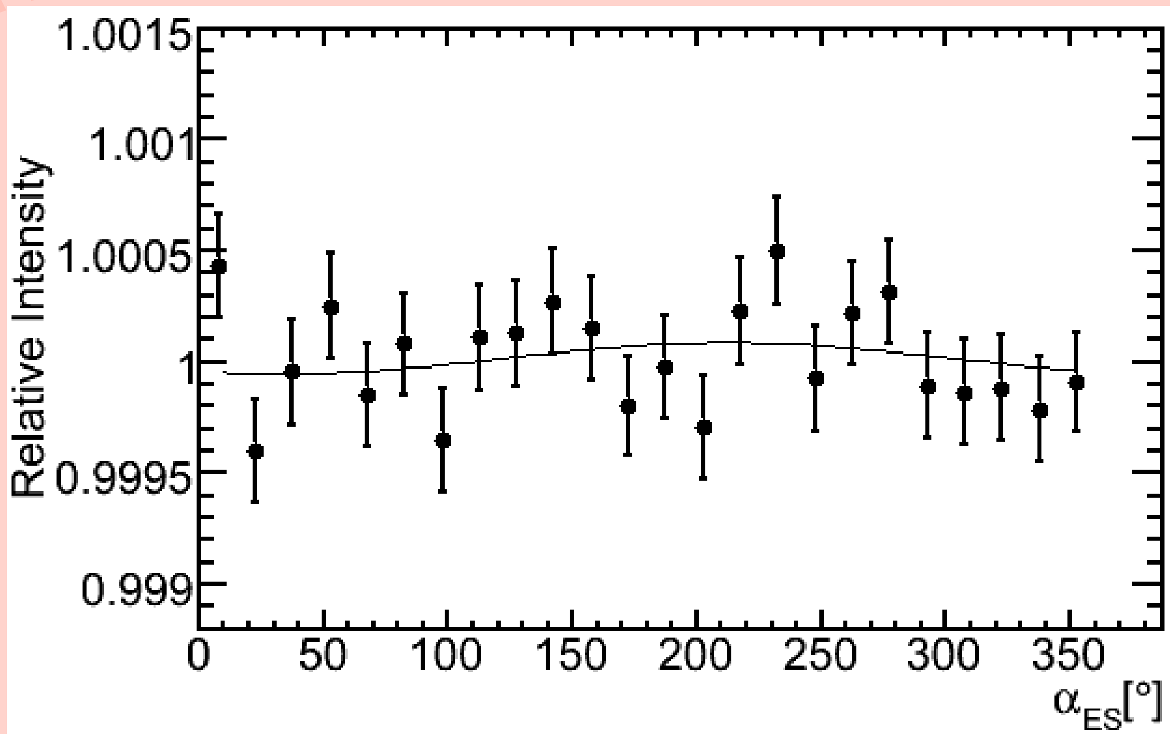

cosmic ray anisotropy vs angular scale

Abdo A.A. et al., Phys. Rev. Lett., 101, 221101 (2008)

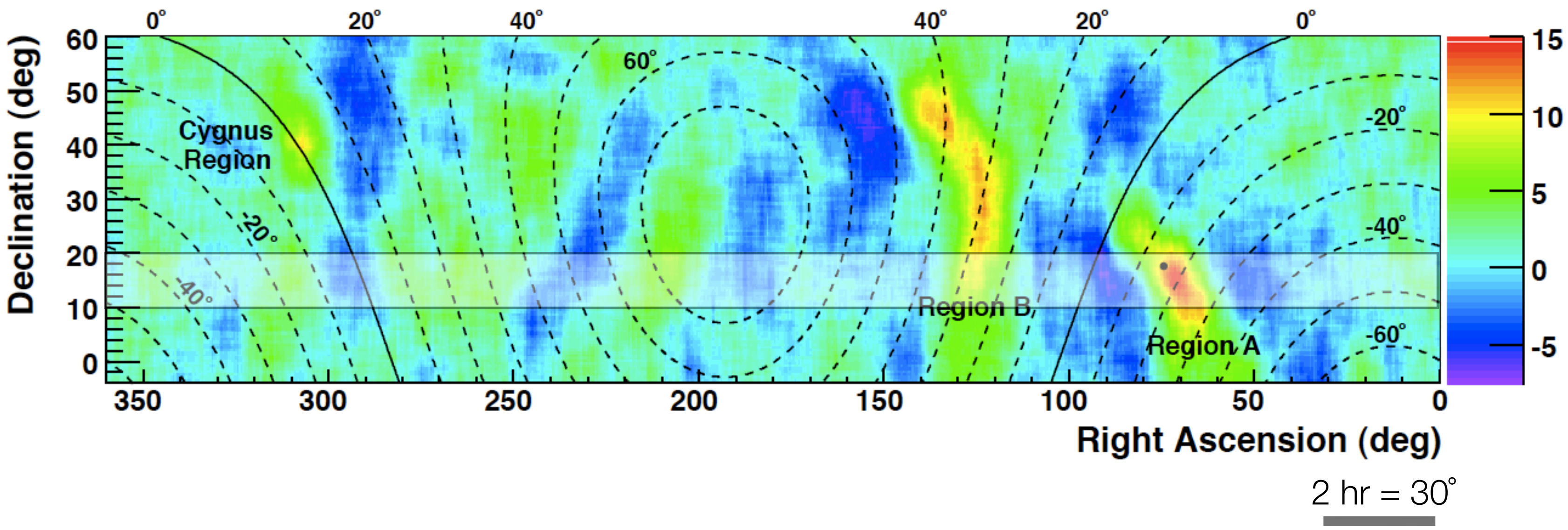

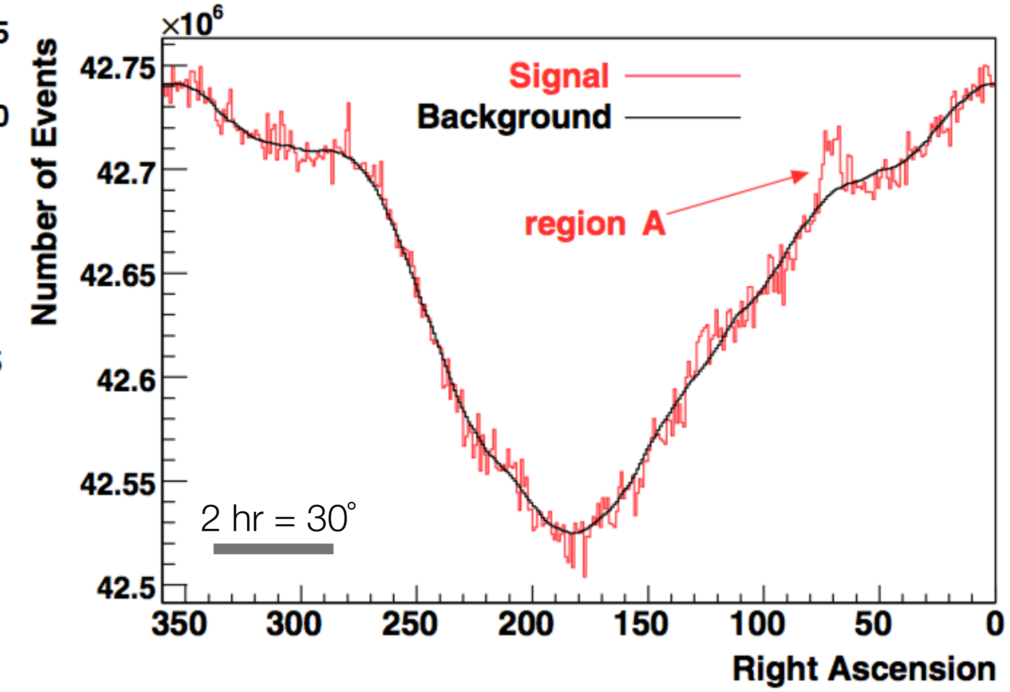

Milagro

$2.2 \cdot 10^{11}$ events
median CR energy ~ 1 TeV = 10^{12} eV
average angular resolution < 1^{o}

2hr time window
10° smoothing

- filter all angular features > 30°
- technique used in gamma ray searches

cosmic ray anisotropy vs angular scale

Abdo A.A. et al., Phys. Rev. Lett., 101, 221101 (2008)

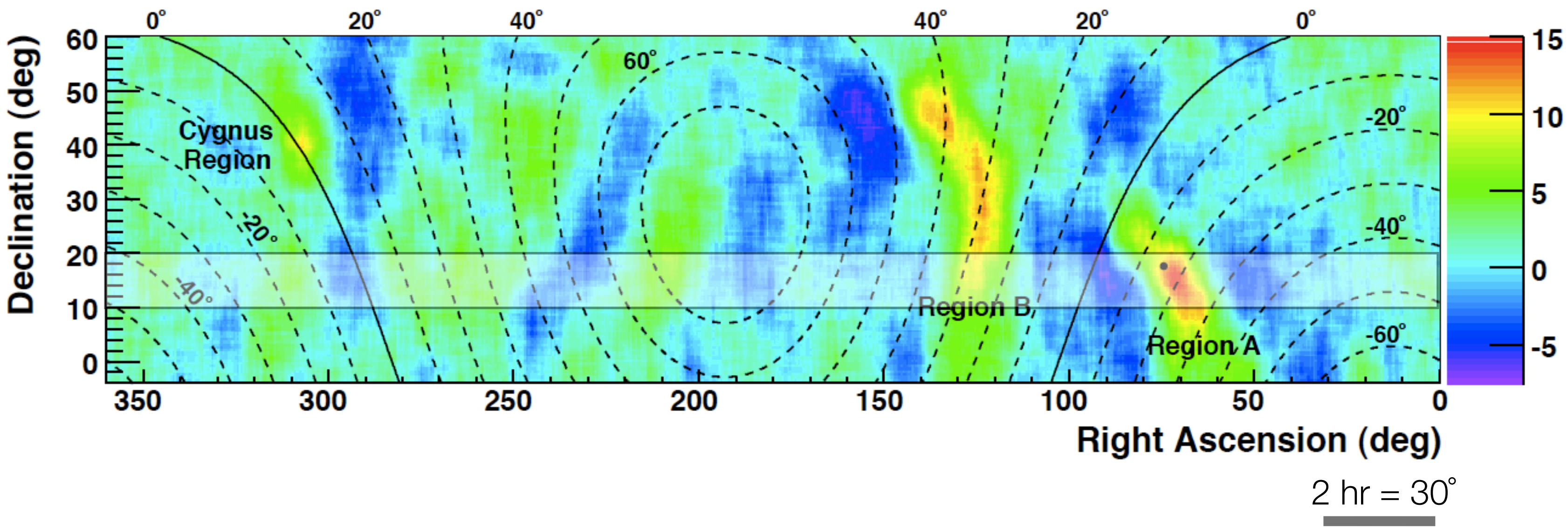

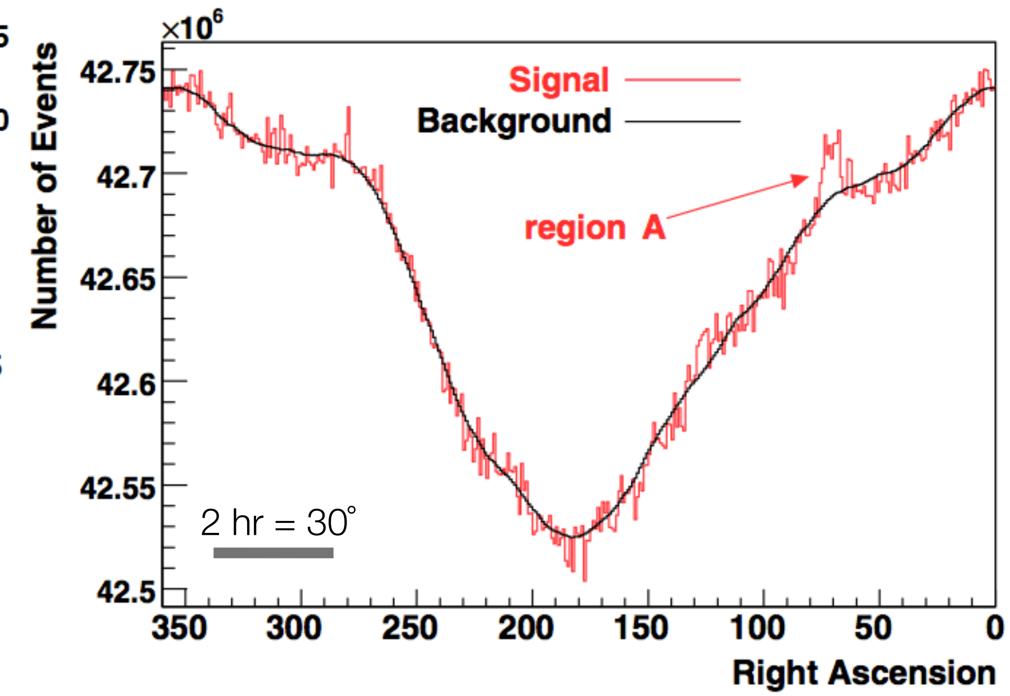

Milagro

$2.2 \cdot 10^{11}$ events
median CR energy ~ 1 TeV = 10^{12} eV
average angular resolution < 1°

2hr time window
10° smoothing

- filter all angular features > 30°
- technique used in gamma ray searches

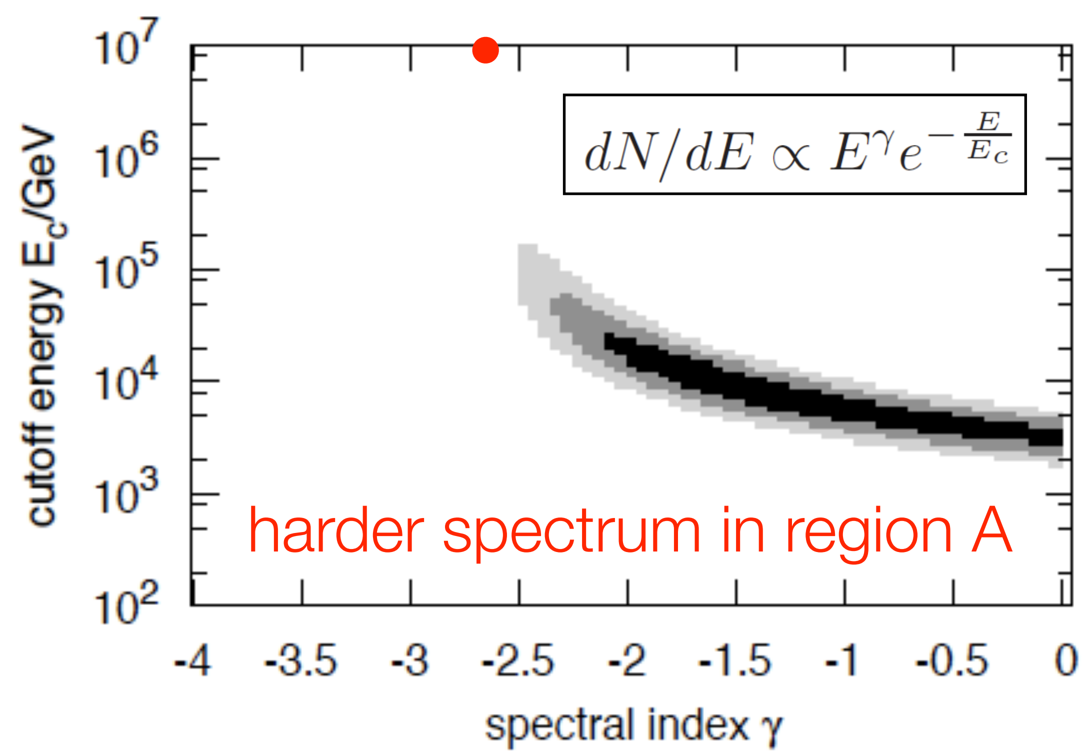

medium / small scale anisotropy for different experiments

Milagro

(direct integration)

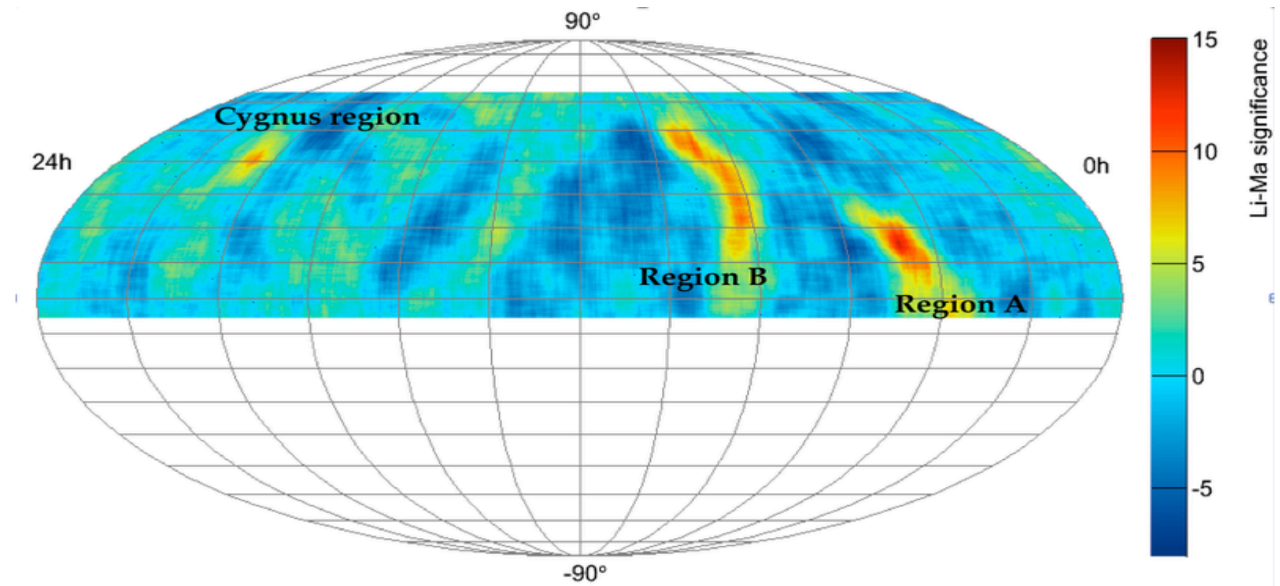

ARGO-YBJ

(time scrambling)

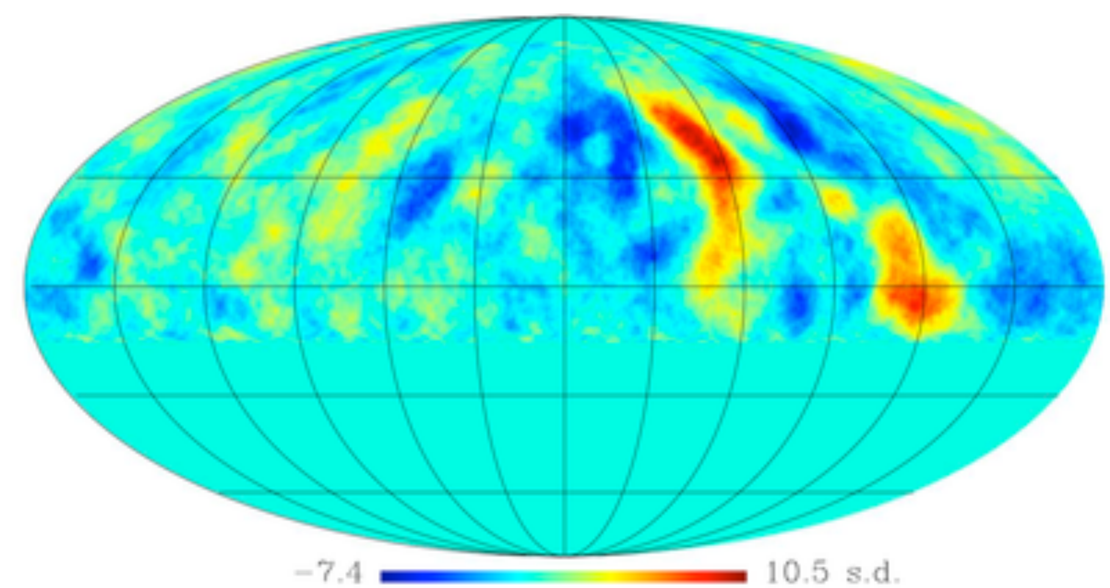

Tibet-III

(global fit)

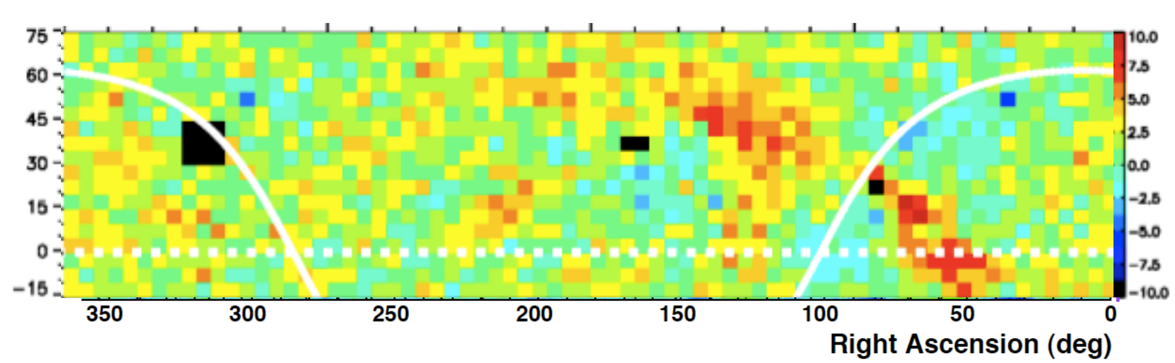

cosmic ray anisotropy vs angular scale

statistical significance equatorial coordinates

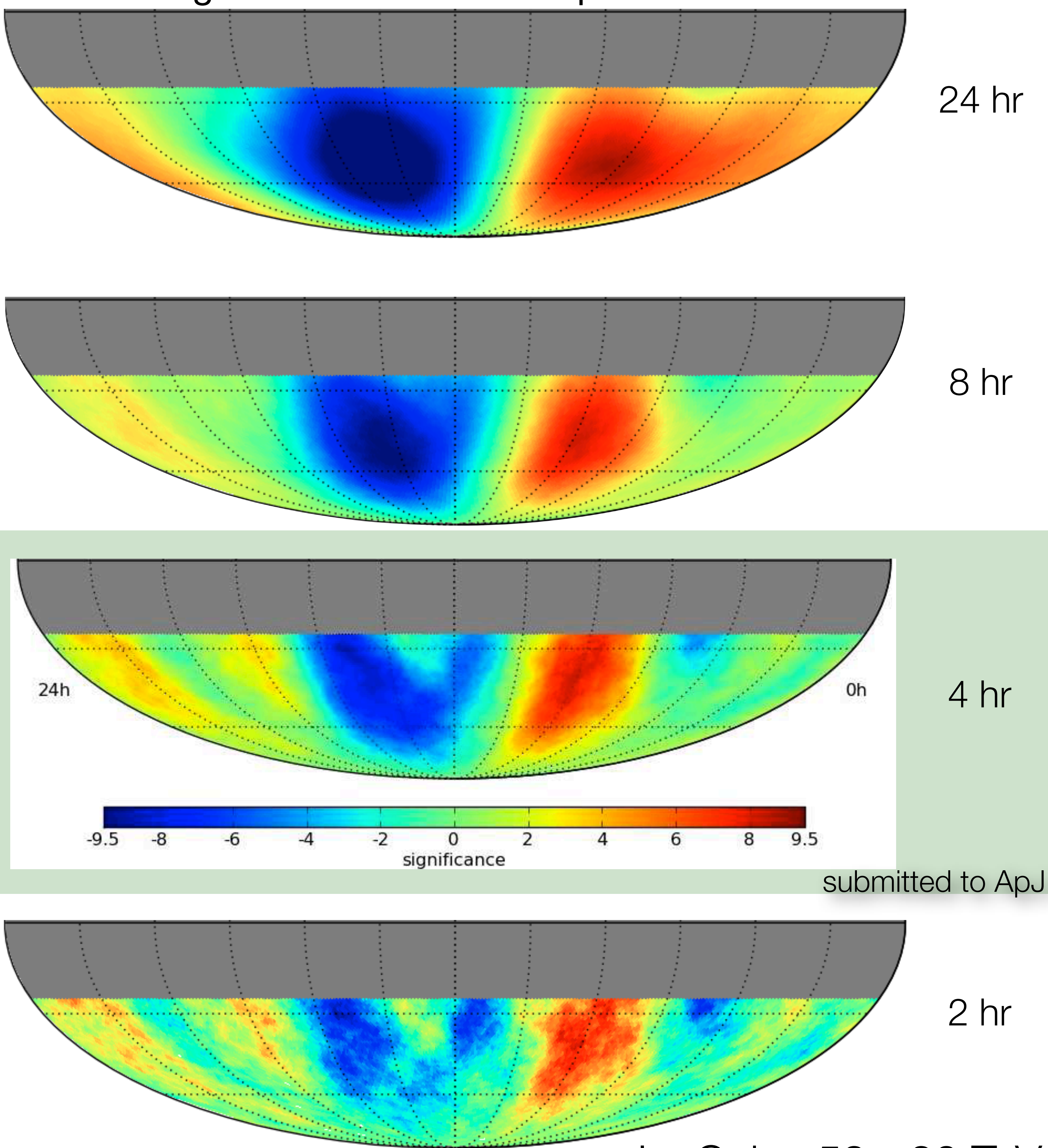

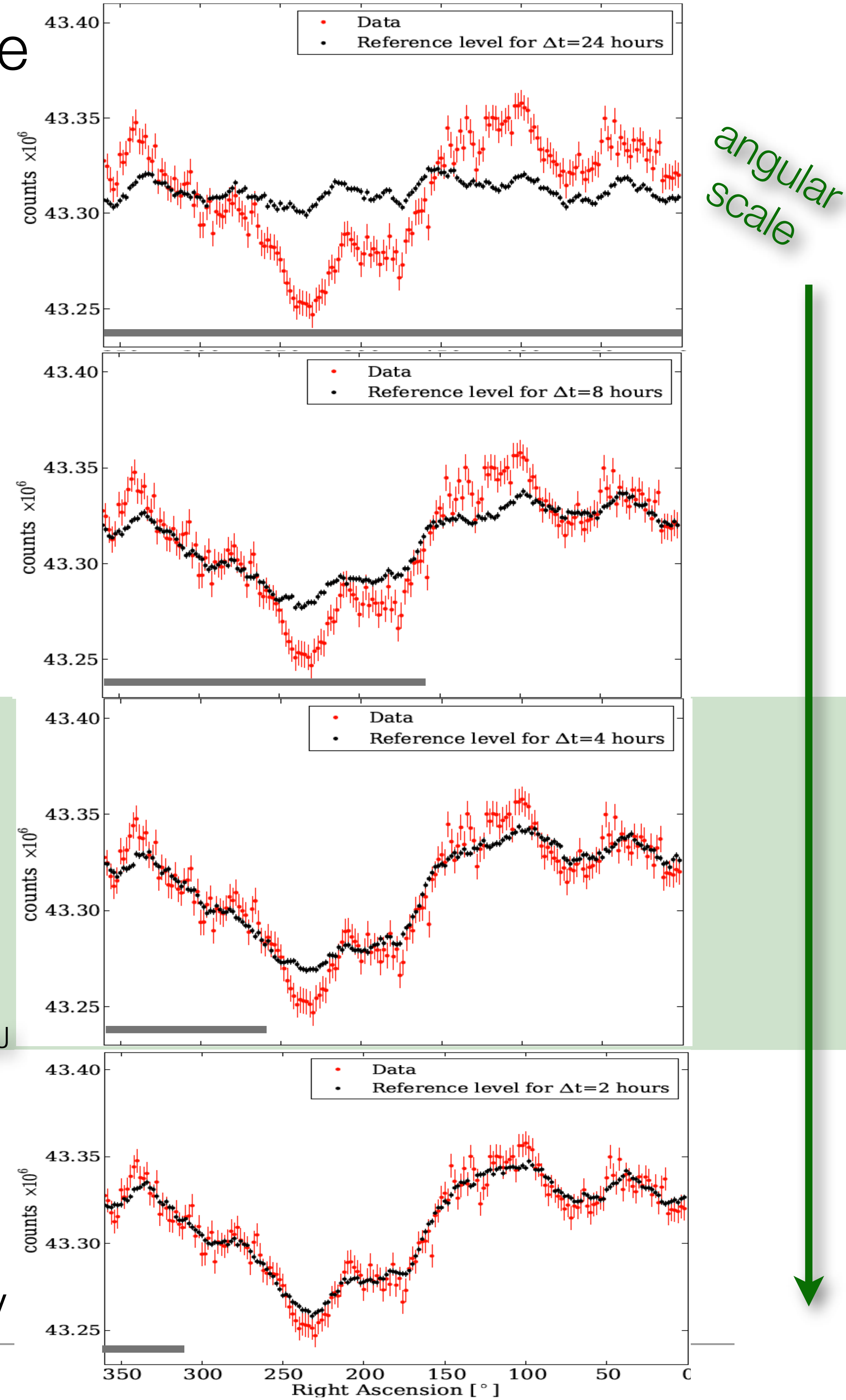

IceCube-59 - 20 TeV

medium scale anisotropy

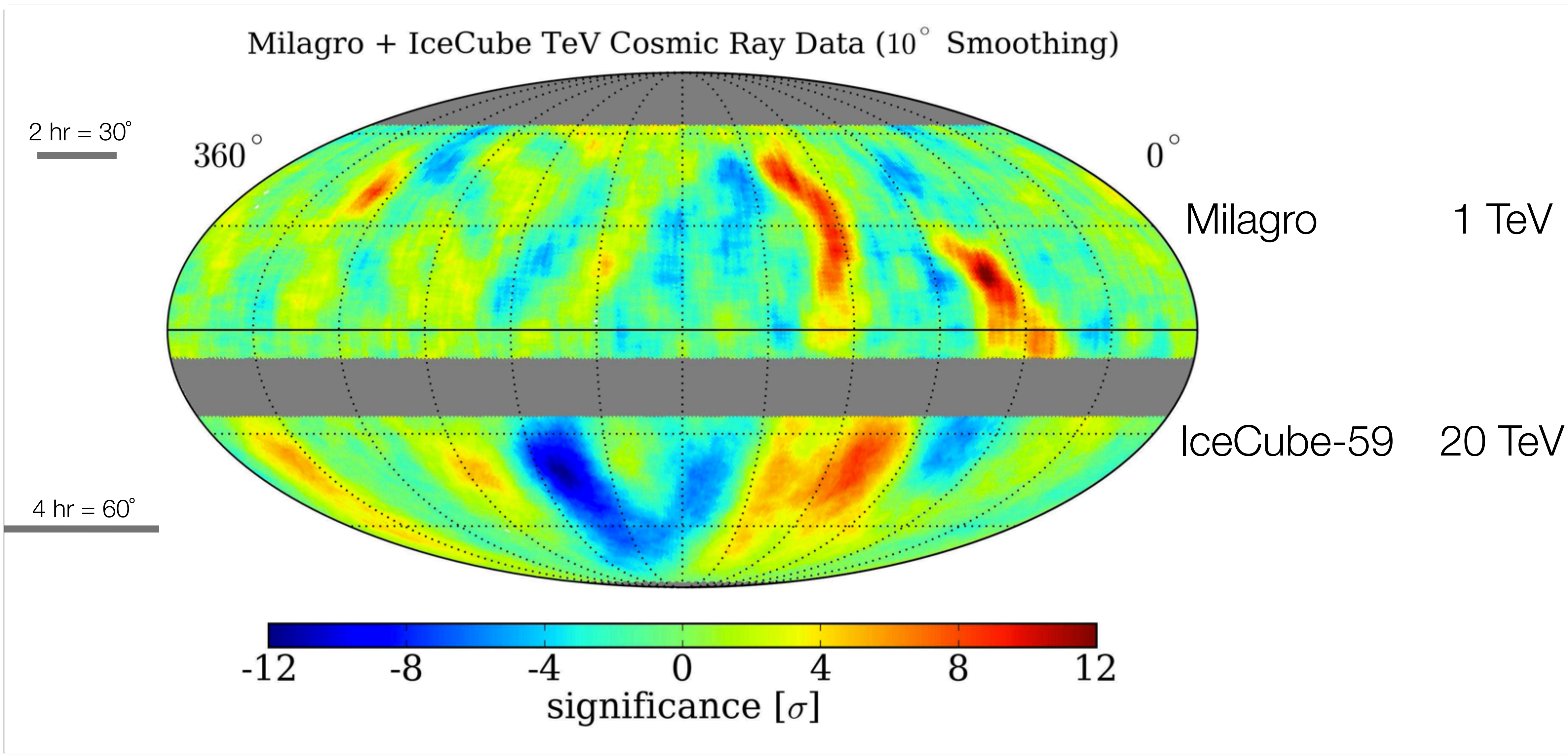

dipole & quadrupole fit

$$\delta I(\alpha,\delta) = m_0 + p_x \cos\delta\cos\alpha + p_y \cos\delta\sin\alpha + p_z \sin\delta + \frac{1}{2}Q_1(3\cos^2\delta - 1) + Q_2 \sin 2\delta\cos\alpha + Q_3 \sin 2\delta \sin\alpha + Q_4 \cos^2\delta\cos 2\alpha + Q_5 \cos^2\delta \sin 2\alpha$$

monopole

dipole

quadrupole

Coefficient	Fit Value
m_0	0.320 ± 2.264
p_x	2.435 ± 0.707
p_y	-3.856 ± 0.707
p_z	0.548 ± 3.872
Q_1	0.233 ± 1.702
Q_2	-2.949 ± 0.494
Q_3	-8.797 ± 0.494
Q_4	-2.148 ± 0.200
Q_5	-5.268 ± 0.200

$$\chi^2/\mathrm{ndf} = 14743.4/14187$$
$$\Pr(\chi^2|\mathrm{ndf}) = 5.5 \times 10^{-4}$$

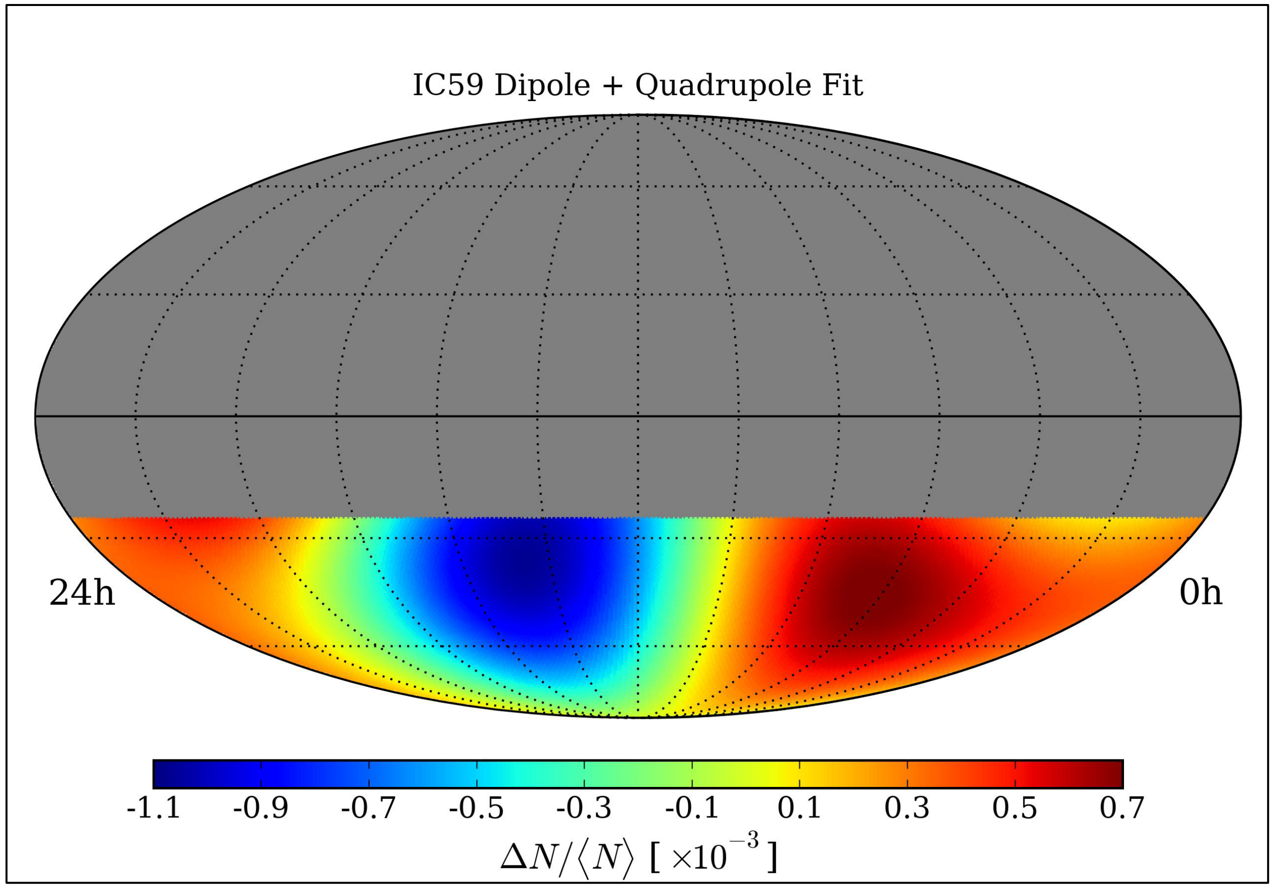

dipole & quadrupole fit

$$\delta I(\alpha,\delta) = m_0 \\ + p_x \cos\delta\cos\alpha + p_y\cos\delta\sin\alpha + p_z\sin\delta \\ + \frac{1}{2}Q_1(3\cos^2\delta - 1) + Q_2\sin 2\delta\cos\alpha + Q_3\sin 2\delta\sin\alpha + Q_4\cos^2\delta\cos 2\alpha + Q_5\cos^2\delta\sin 2\alpha$$

monopole
dipole
quadrupole

Coefficient	Fit Value
m_0	0.320 ± 2.264
p_x	2.435 ± 0.707
p_y	-3.856 ± 0.707
p_z	0.548 ± 3.872
Q_1	0.233 ± 1.702
Q_2	-2.949 ± 0.494
Q_3	-8.797 ± 0.494
Q_4	-2.148 ± 0.200
Q_5	-5.268 ± 0.200

$$\chi^2/\mathrm{ndf} = 14743.4/14187$$
$$\Pr(\chi^2|\mathrm{ndf}) = 5.5\times 10^{-4}$$

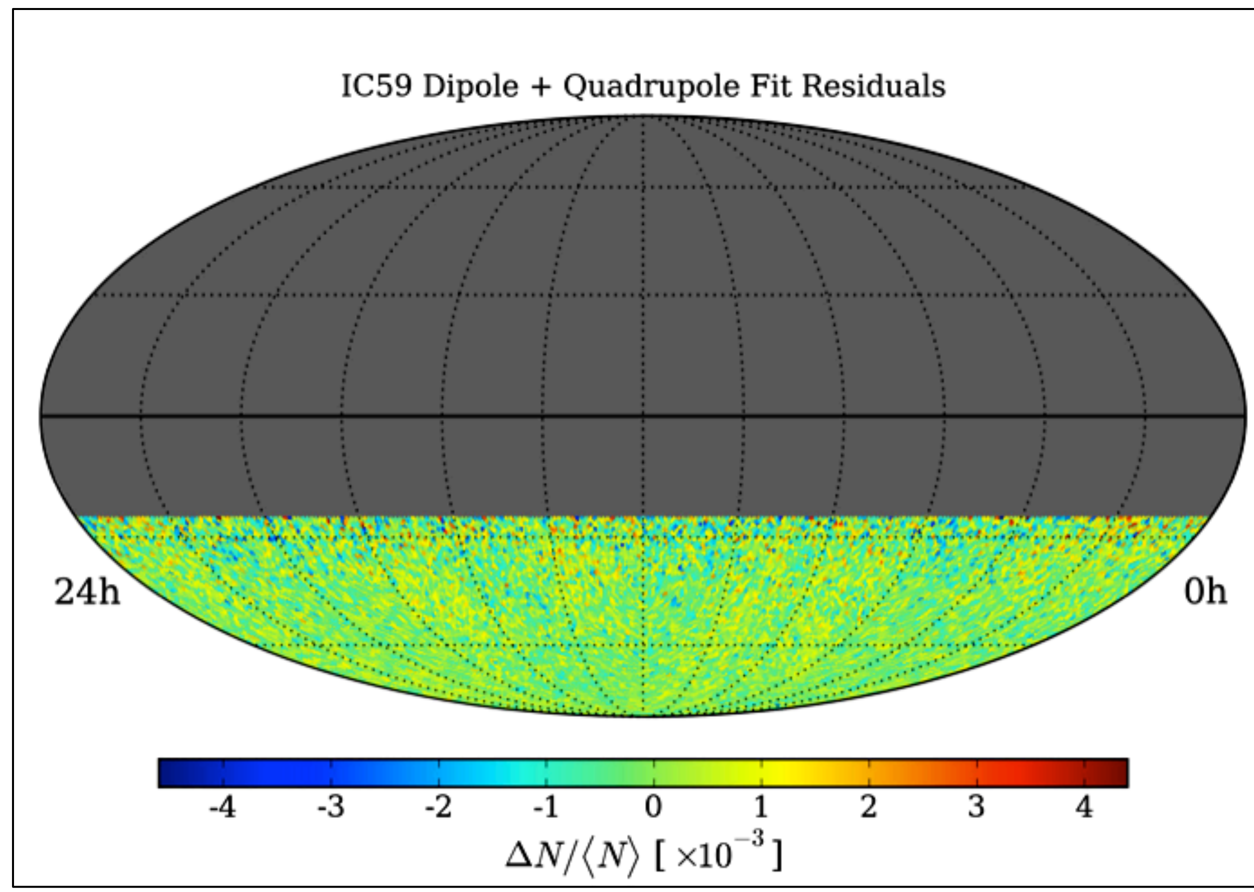

smoothing scan

region	right ascension	declination	optimal scale	peak significance	post-trials
1	$(122.4^{+4.1}_{-4.7})^\circ$	$(-47.4^{+7.5}_{-3.2})^\circ$	22°	7.0σ	5.3σ
2	$(263.0^{+3.7}_{-3.8})^\circ$	$(-44.1^{+5.3}_{-5.1})^\circ$	13°	6.7σ	4.9σ
3	$(201.6^{+6.0}_{-1.1})^\circ$	$(-37.0^{+2.2}_{-1.9})^\circ$	11°	6.3σ	4.4σ
4	$(332.4^{+9.5}_{-7.1})^\circ$	$(-70.0^{+4.2}_{-7.6})^\circ$	12°	6.2σ	4.2σ
5	$(217.7^{+10.2}_{-7.8})^\circ$	$(-70.0^{+3.6}_{-2.3})^\circ$	12°	-6.4σ	-4.5σ
6	$(77.6^{+3.9}_{-8.4})^\circ$	$(-31.9^{+3.2}_{-8.6})^\circ$	13°	-6.1σ	-4.1σ
7	$(308.2^{+4.8}_{-7.7})^\circ$	$(-34.5^{+9.6}_{-6.9})^\circ$	20°	-6.1σ	-4.1σ
8	$(166.5^{+4.5}_{-5.7})^\circ$	$(-37.2^{+5.0}_{-5.7})^\circ$	12°	-6.0σ	-4.0σ

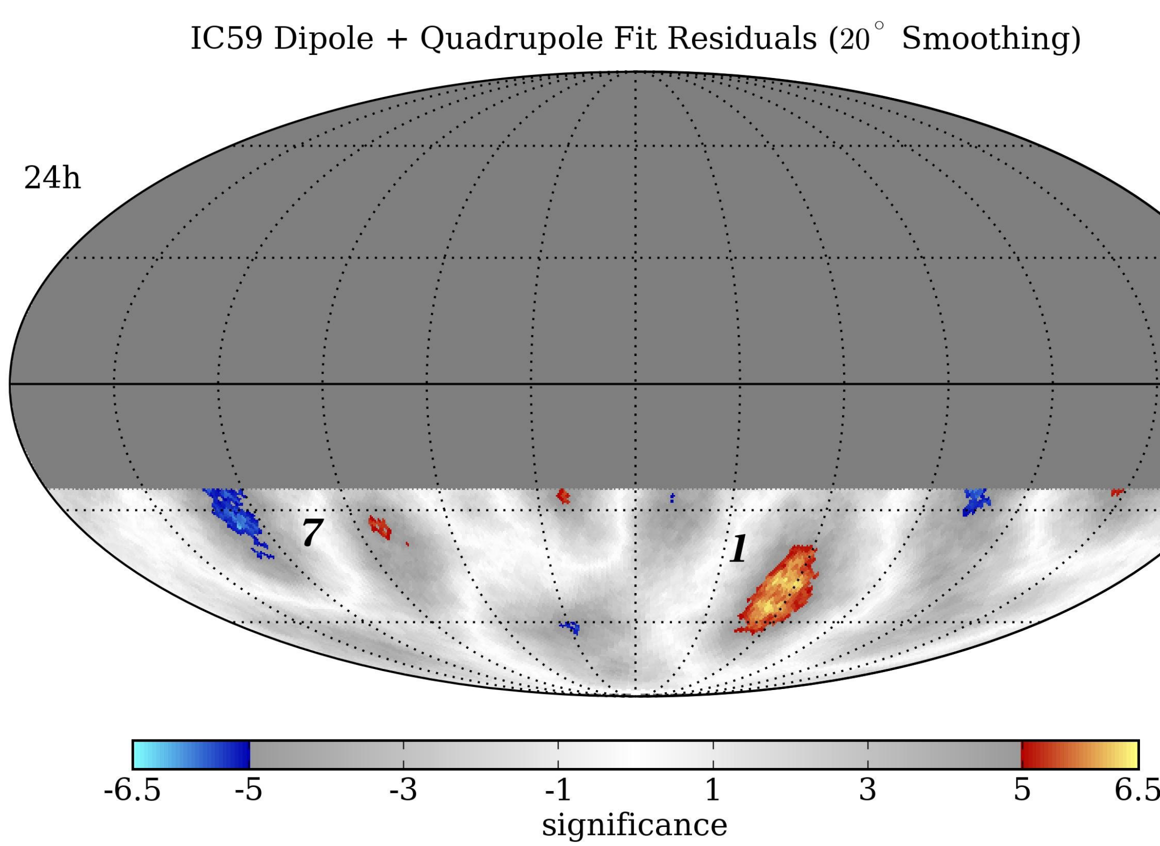

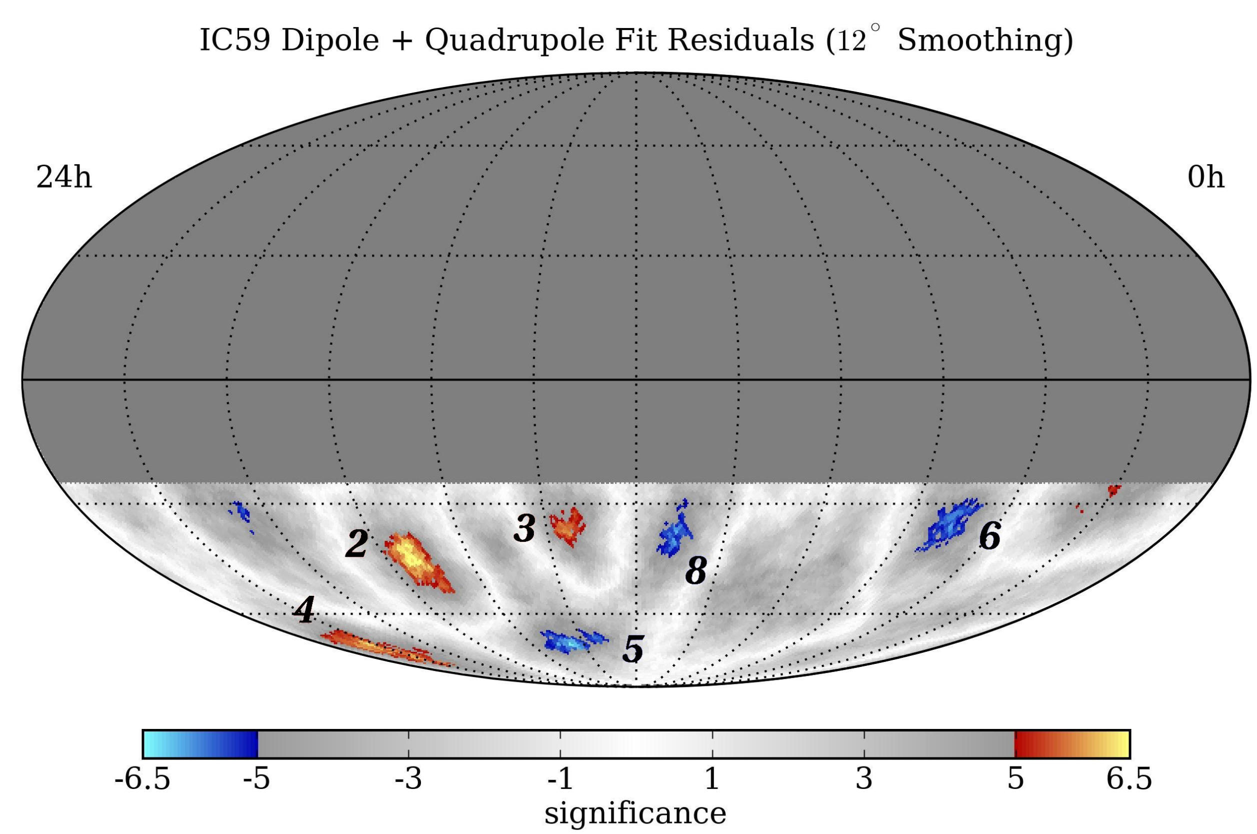

cosmic ray anisotropy

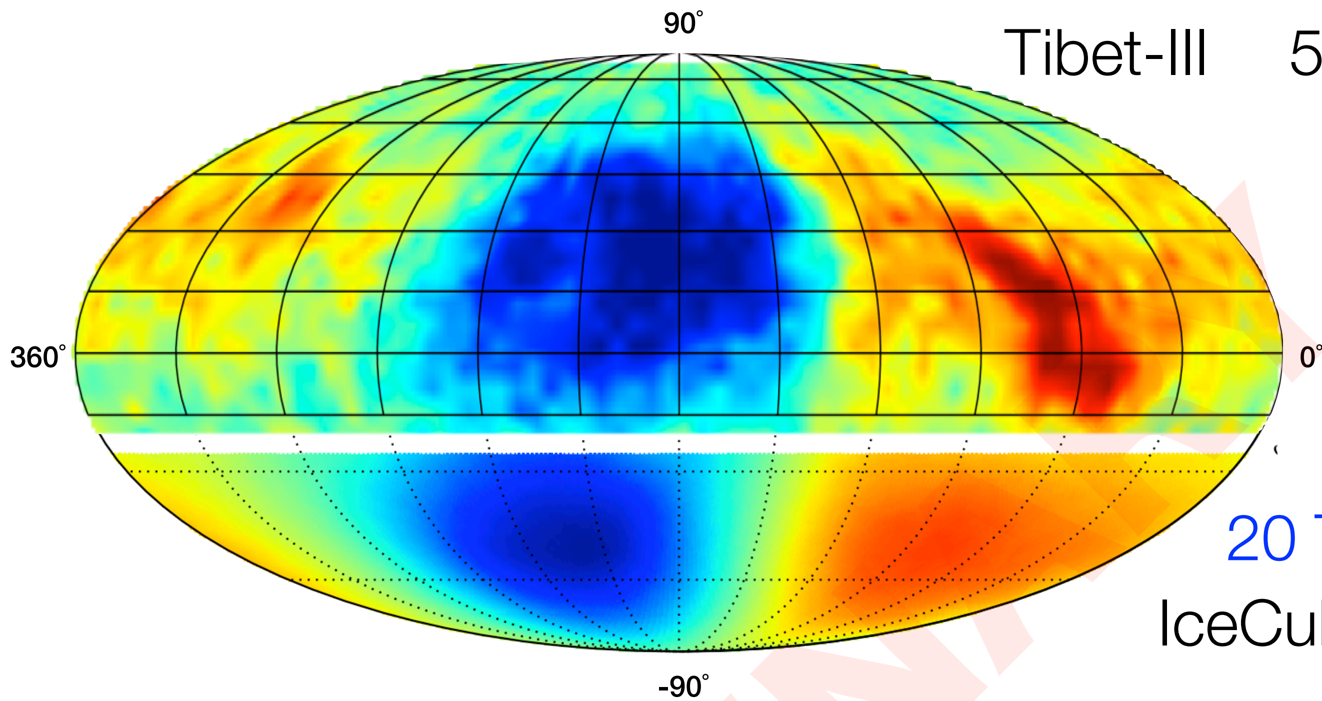

Tibet-III 5 TeV

20 TeV
IceCube-59

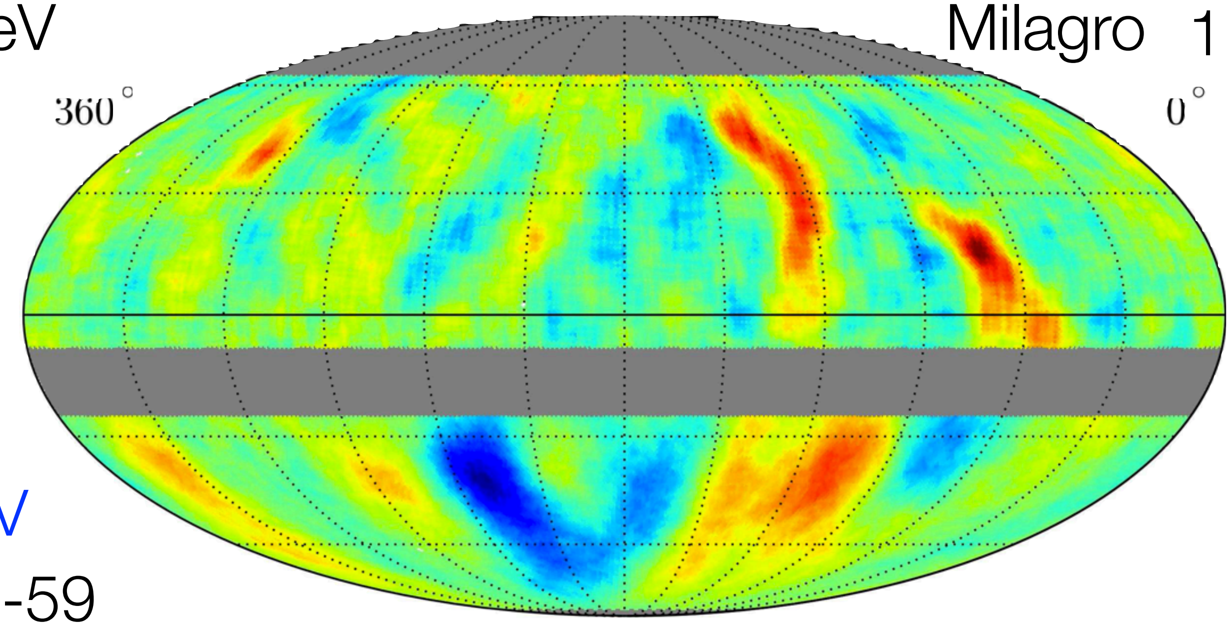

Milagro 1 TeV

statistical significance equatorial coordinates

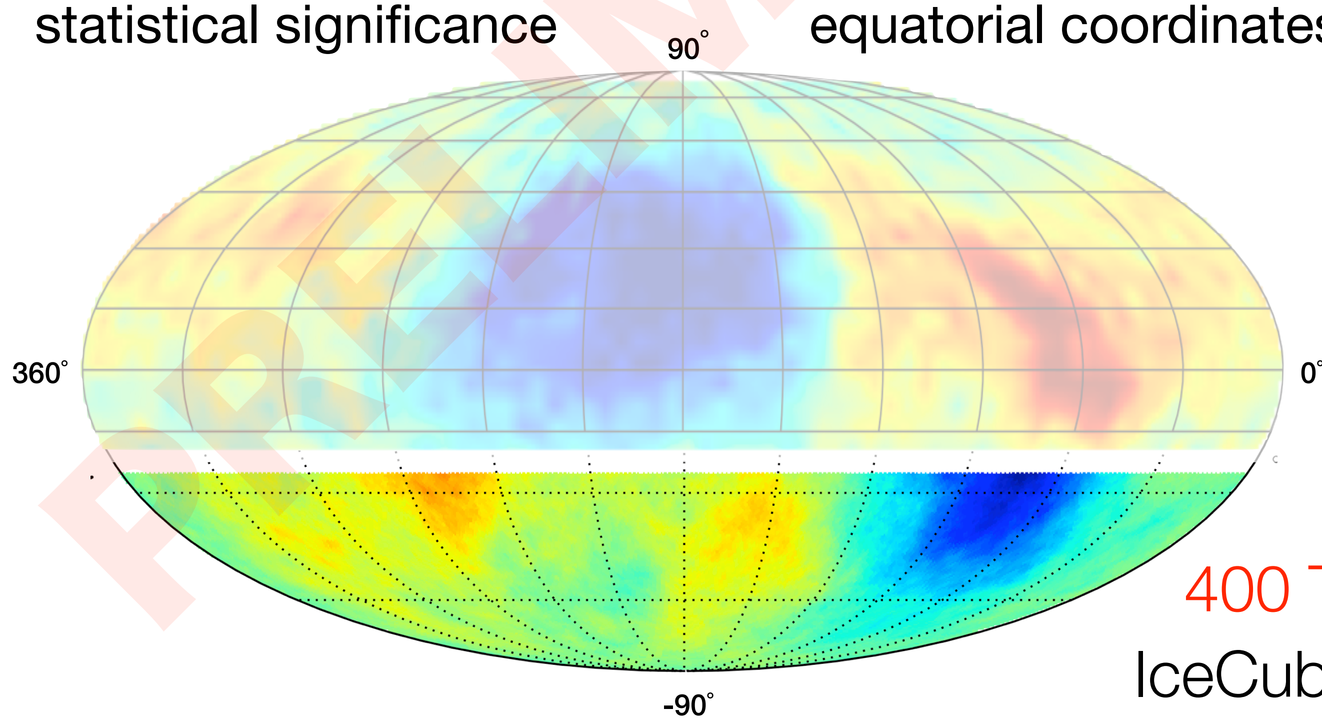

400 TeV
IceCube-59

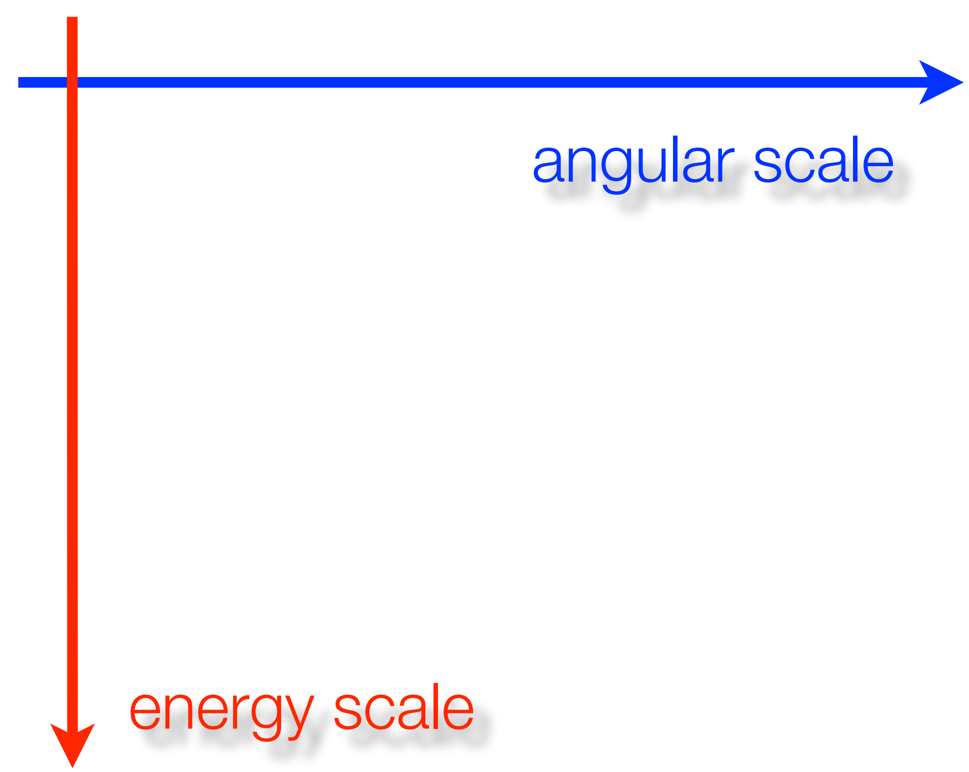

anisotropy and local interstellar medium

scale : 100-1,000 pc

Ackermann et al., Phys. Rev D82, 092003 (2010)

e^-e^+
Fermi-LAT

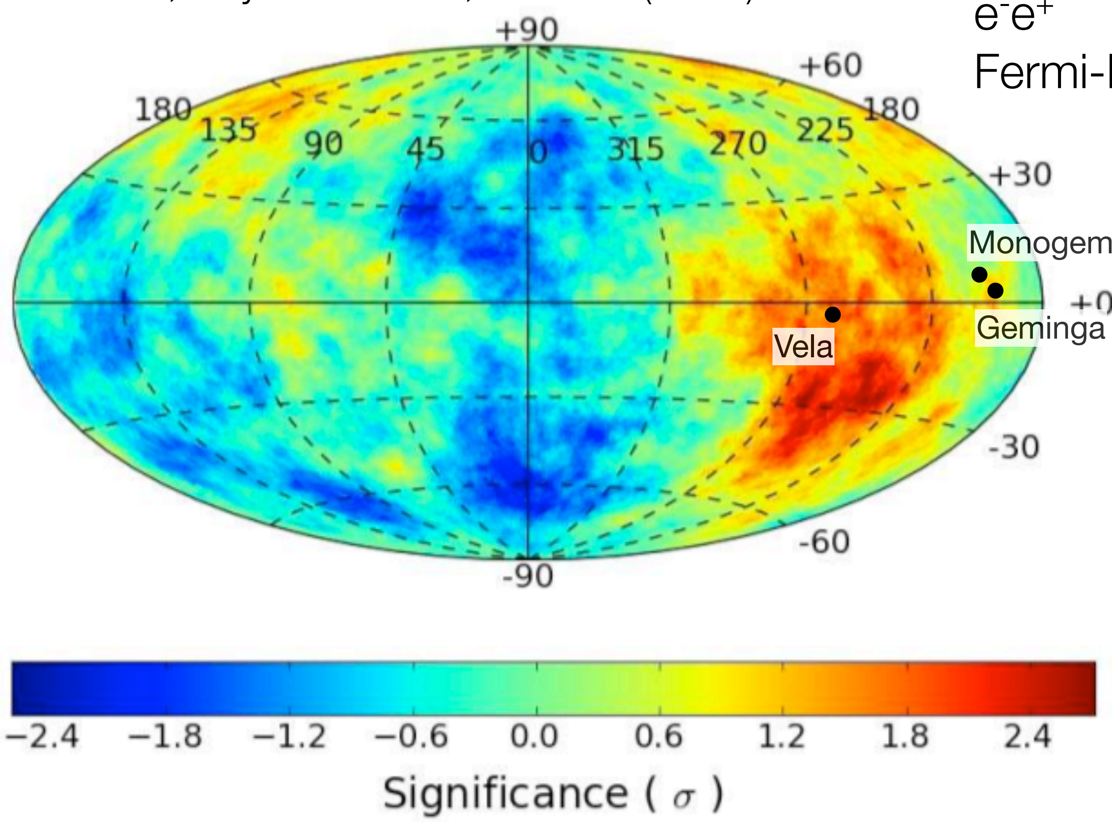

scale : < 40 pc

Frisch P. et al., ApJ, 724, 1473 (2010)

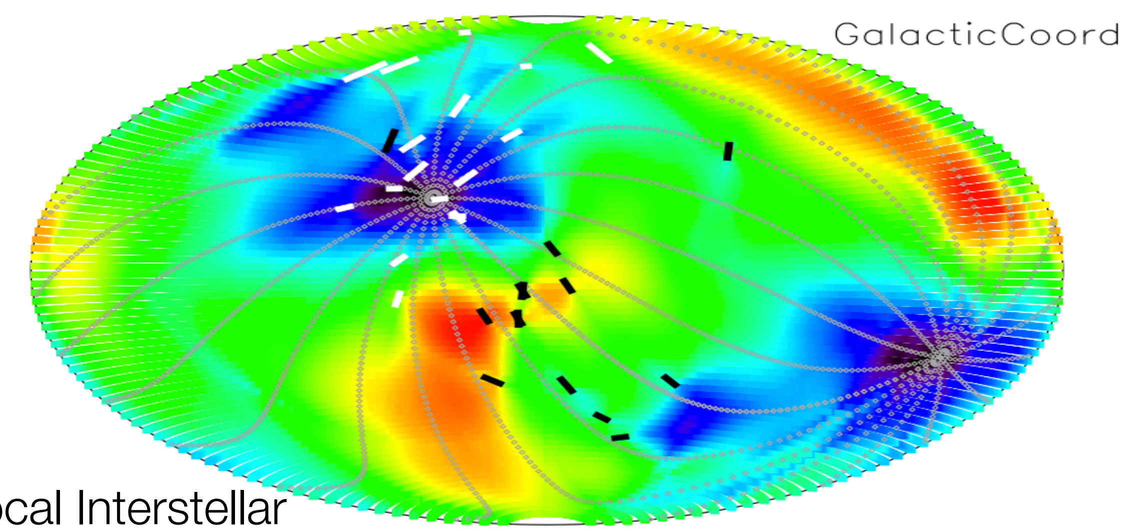

Local Interstellar Magnetic Field

Tibet-III - ~3 TeV

(Zhang Yi)

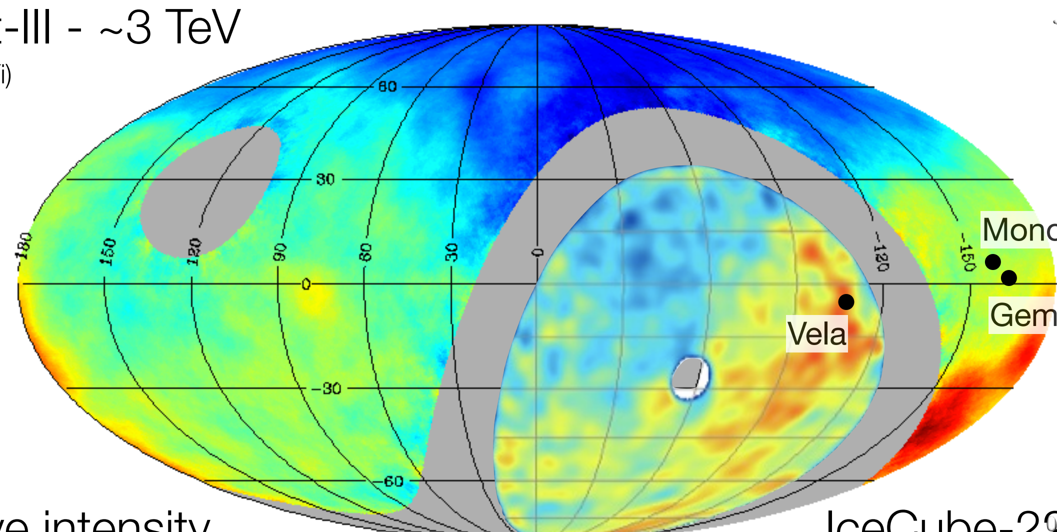

relative intensity

IceCube-22 - ~20 TeV

Abbasi et al., ApJ, 718, L194 (2010)

scale : 10^{-3}-100 pc

Redfield & Linsky, ApJ, Vol 673, pag 283 (2008)

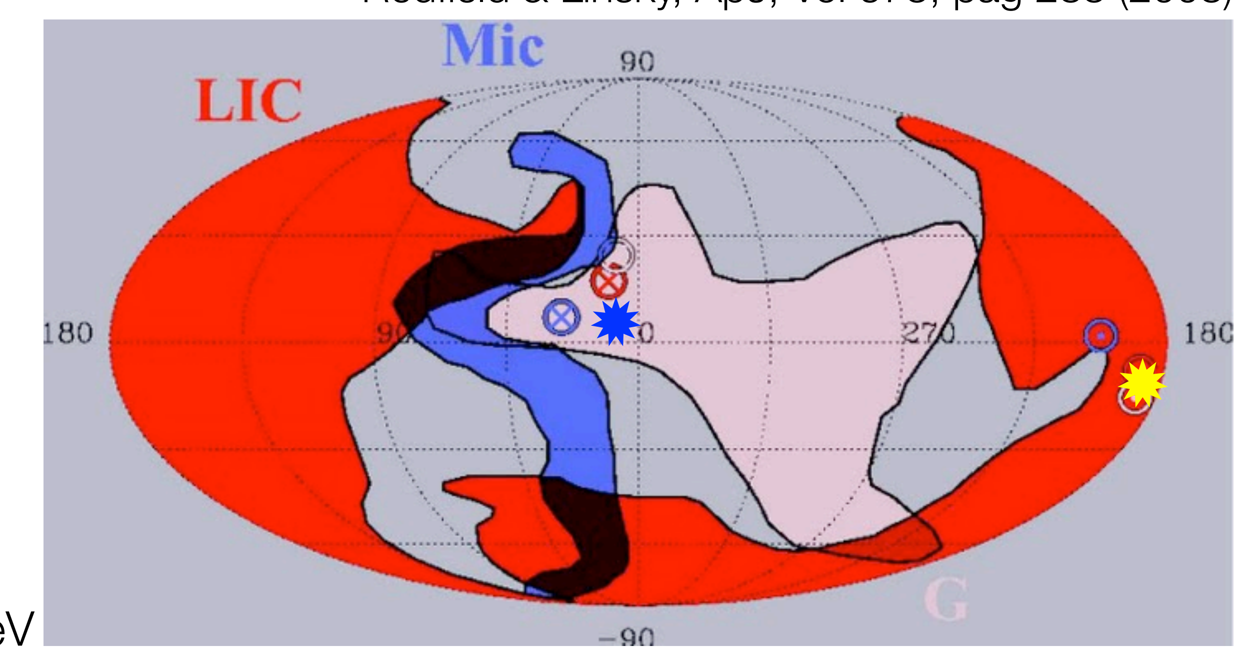

Local Interstellar Medium & Heliosphere

our galactic neighborhood

Lallement et al., Science, Vol 307, page 1447 (2005)

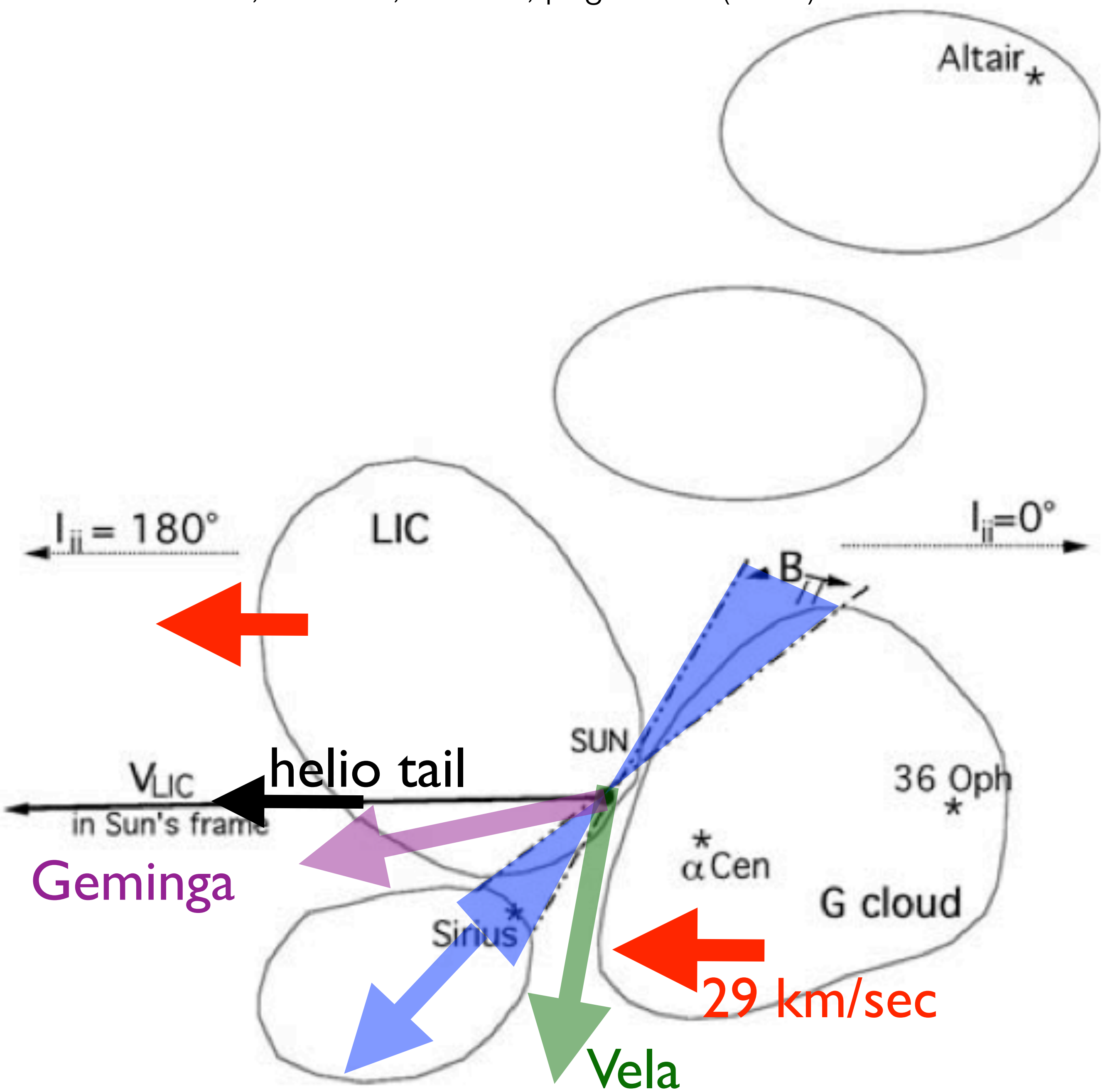

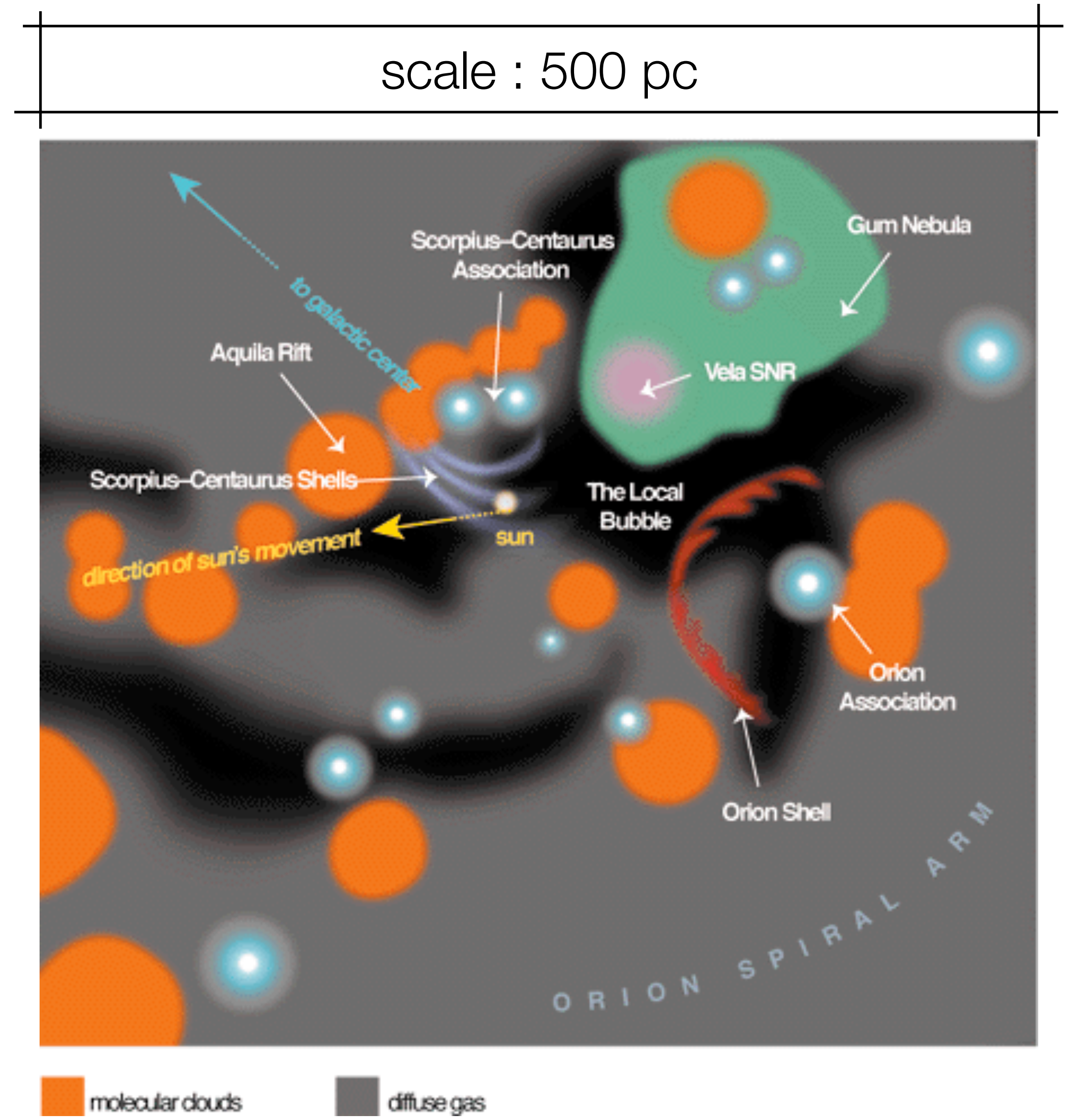

Priscilla Frisch - University of Chicago

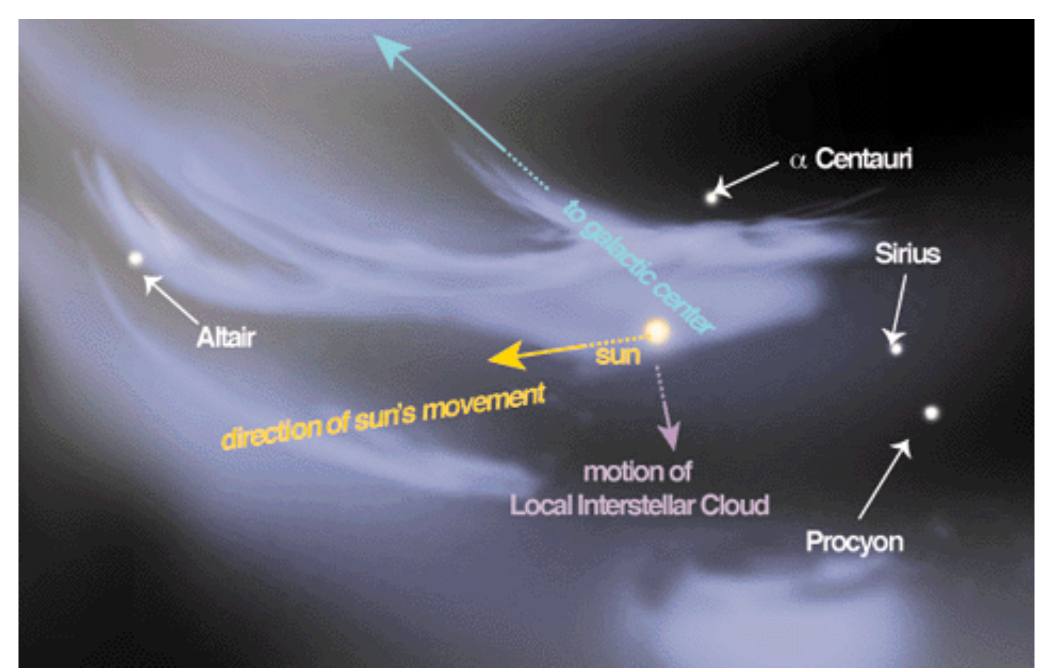

origin of *large scale* anisotropy

- stochastic effect from <0.1-1kpc young SNR & propagation — Erlykin & Wolfendale, Astropart. Phys., 25, 183 (2006); Blasi & Amato, arXiv:1105.4529
- escape from galaxy — Butt, Nature, 460, 701 (2009)
- galactic magnetic field induced by cosmic ray flow along the arms — X.B.Qu et al., arXiv:1101.5273
- combined effect of regular galactic and turbulent IS magnetic field < 10 pc: isotropy broken in our vicinity due to propagation in turbulent magnetic field — Battaner, Castellano & Masip ApJ, 703, L90 (2009)
- effect from Local Interstellar Cloud (LIC) and local IS magnetic field < 1 pc — Amenomori et al., ICRC 2007, Mérida, México (2007)
- Heliosphere and the sub-GeV cosmic rays — Nagashima et al., J. Geophys. Res., Vol 103, No. A8, Pag. 17,429 (1998)

origin of *small scale* anisotropy : CR source

Salvati & Sacco, arXiv:0802.2181
Drury & Aharonian, Astropart. Phys. 29, 420 (2008)

- **CR from Geminga:** ~90-200 pc, 340,000 yr ago
  - energy passband (cutoff HE, delays LE) ~ hard spectrum
- **magnetic connection & propagation in turbulent LIMF**

Salvati, Astron. & Astrophys. arXiv:1001.4947

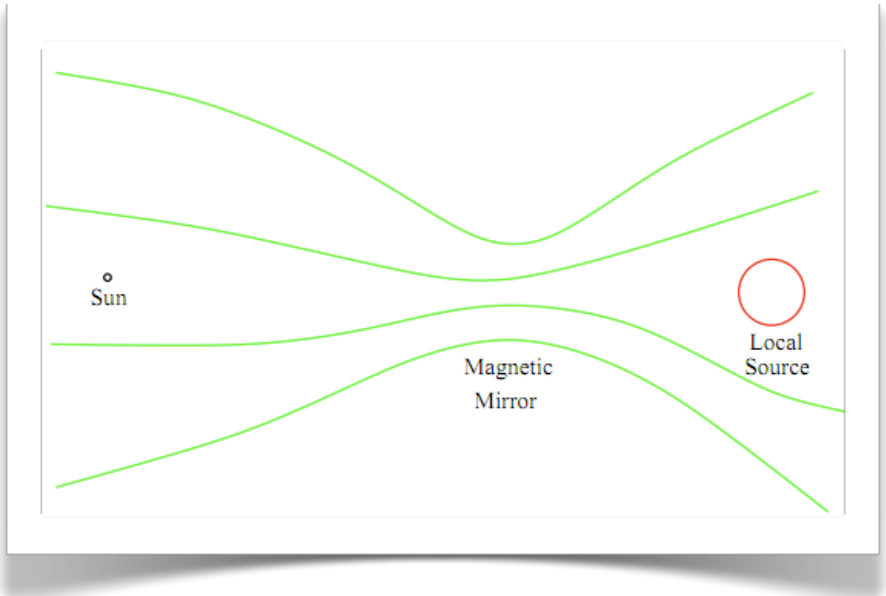

- **anisotropic MHD turbulence in the ISM**
  - large scale anisotropy is "perturbed" by faint beam of collimated particles along the "magnetic" tube that connects to the source (~100 pc)
  - pitch angle scattering peaked near the direction of LIMF
  - outer scale of perturbation ~1 pc determines beam angular width and strength

Malkov et al., ApJ 721, 750, 2010

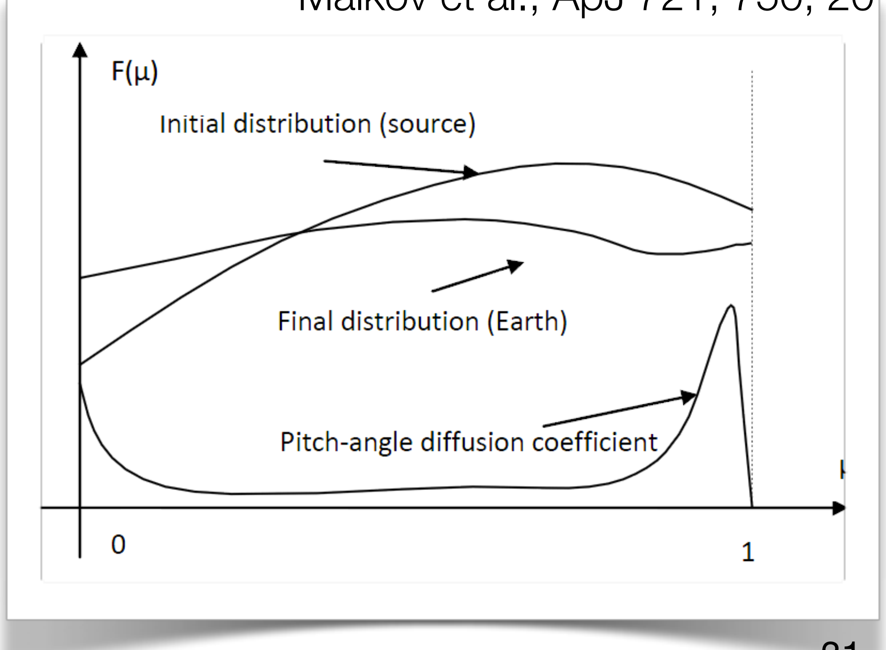

the heliosphere

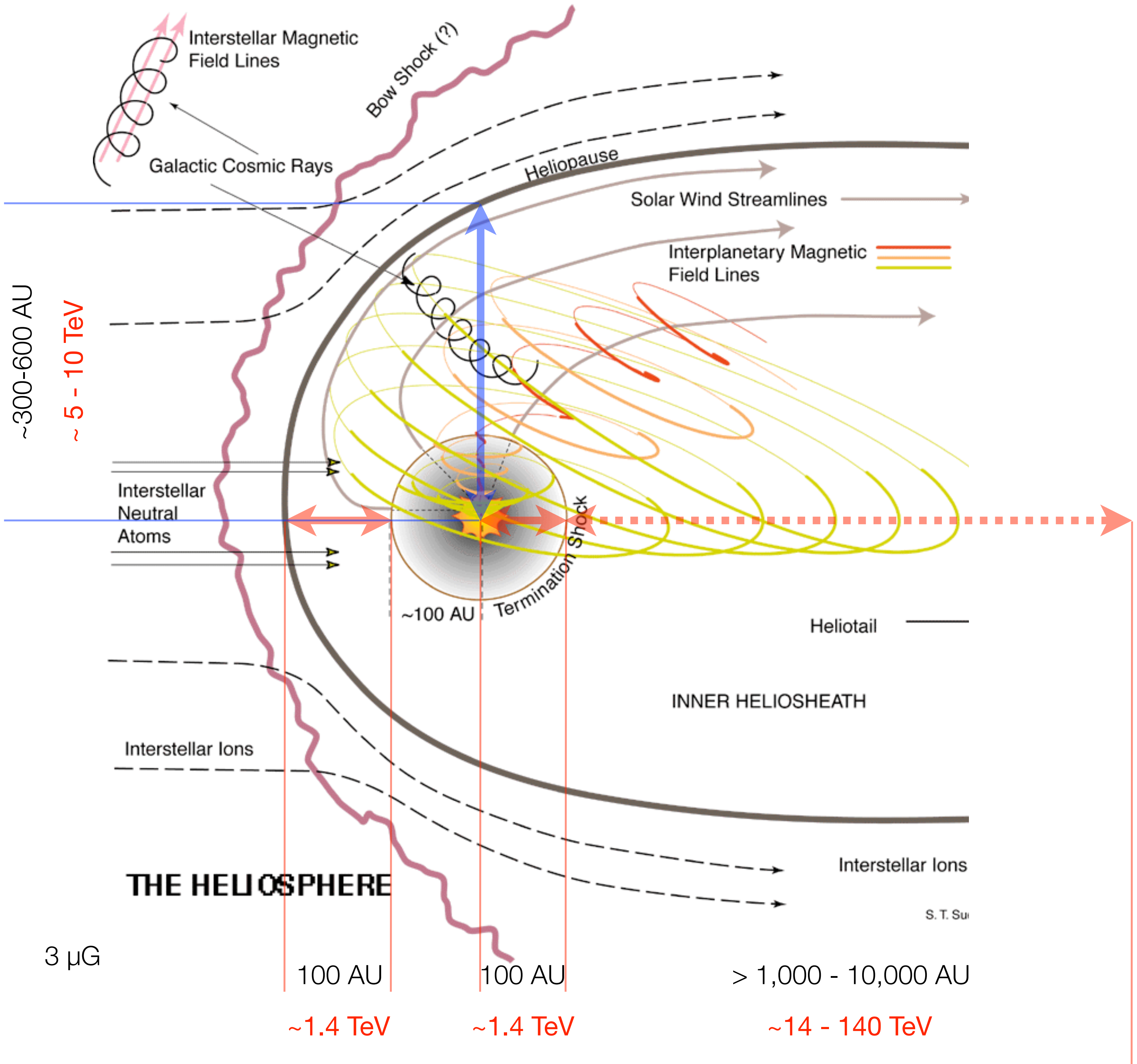

Izmodenov et al., Astron. Lett., 29, 1, 58 (2003)

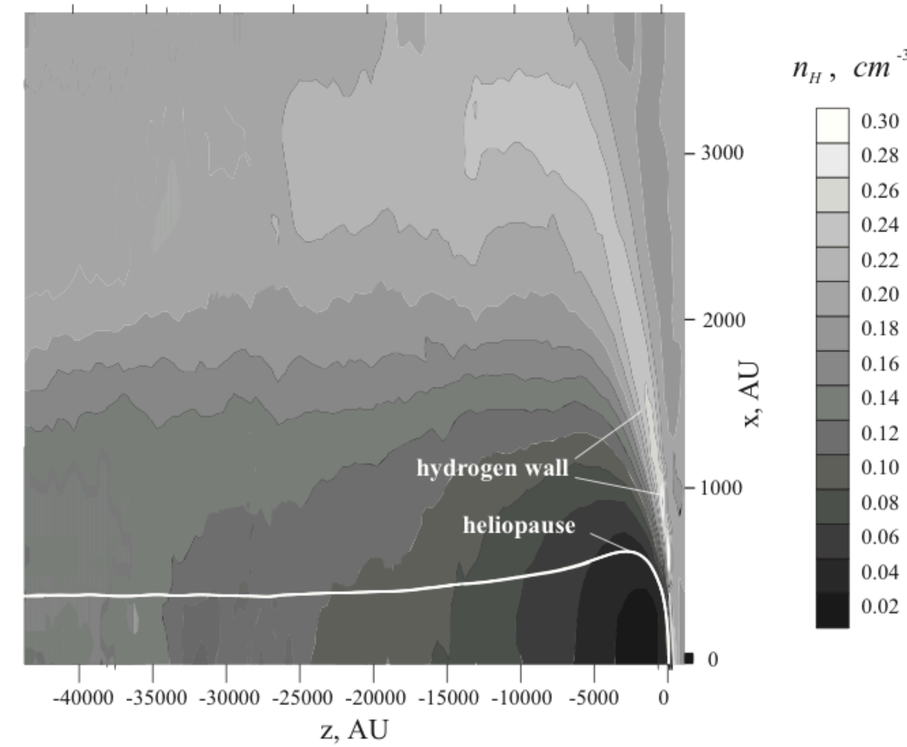

3D simulation of heliosphere/heliotail
Pogorelov et al., ApJ, 696, 1478 (2009)

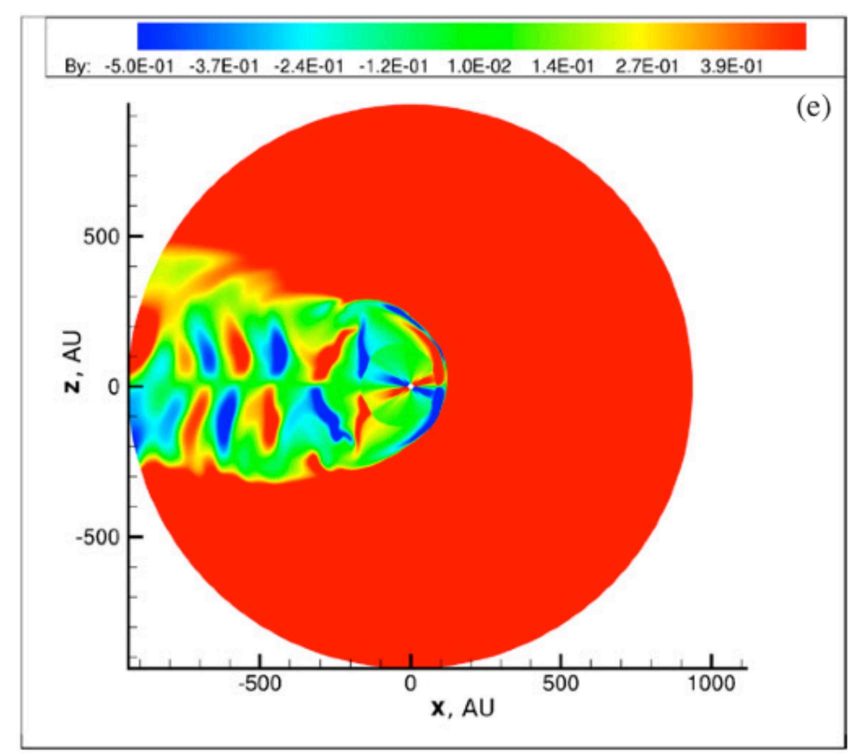

origin of “tail-in anisotropy”

- first-order Fermi acceleration in magnetic reconnection regions in the heliotail
- magnetic polarity reversals due to the 11-year solar cycles compressed by the solar wind in the magneto-tail
- weakly stochastic magnetic reconnection
- harder spectrum up to ~10 TeV (Milagro, ARGO)

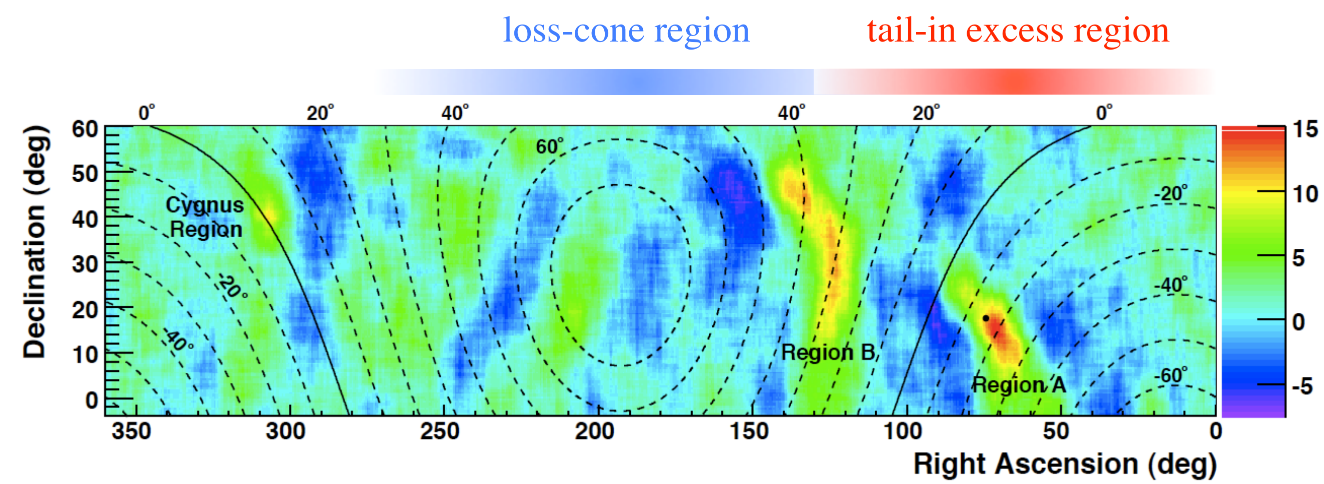

Abdo et al., Phys. Rev. Lett., 101, 221101, 2008

Lazarian & Desiati, ApJ, 722, 188, 2010

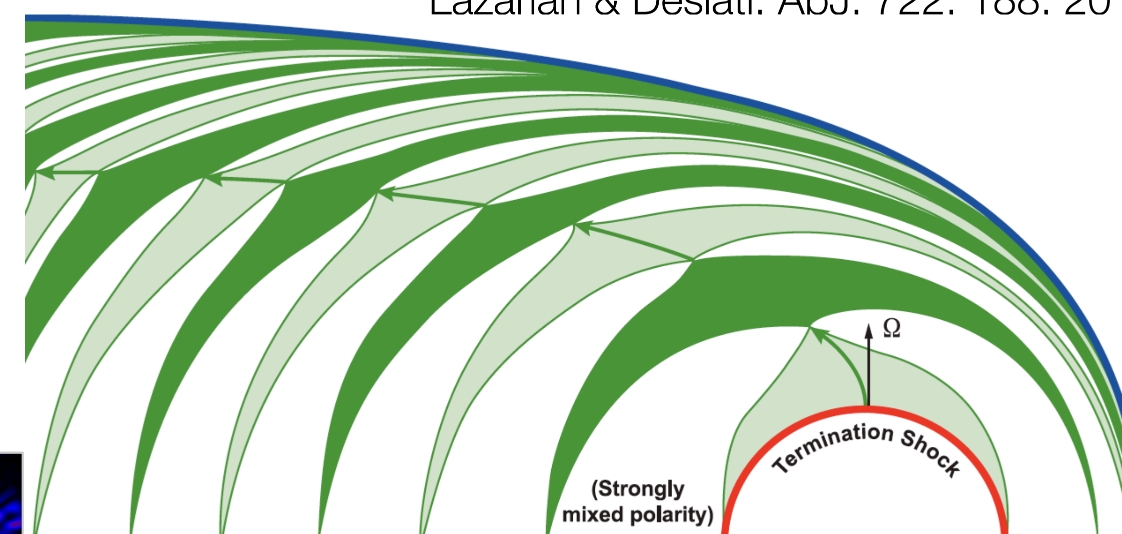

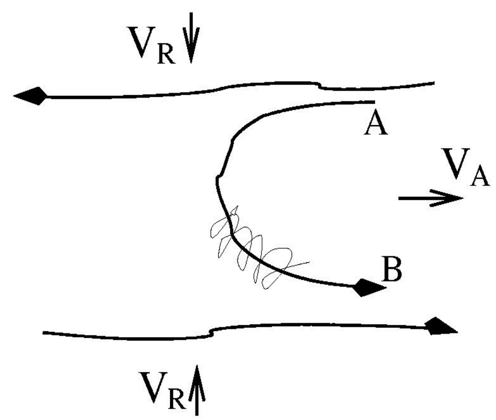

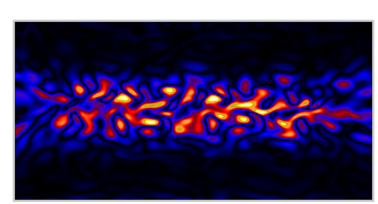

summary

- cosmic ray anisotropy **evolution** observed from 20 TeV to 400 TeV with high significance in the southern hemisphere
- significant angular structure of anisotropy is observed
- time variabilities and/or periodicities to be studied

- complexity of cosmic ray propagation in ISM and heliospheric boundary effects
- TeV cosmic rays as a new probe for outer heliospheric boundary and ISM
- anisotropy vs energy (>100's TeV) might uncover connection to nearby SNR

backup slides

drilling in the ice

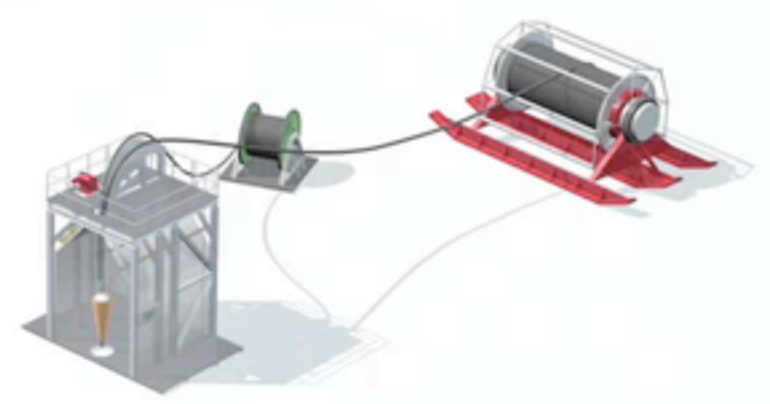

summary of measurement for IceCube-59

$$\sum_{j=1}^{n=2} A_j \cos[i(\alpha - \phi_j)] + B$$

	$E_{primary}$ (TeV)	events (10^9)	A_1 (10^{-4})	φ_1 (°)	A_2 (10^{-4})	φ_2 (°)	χ^2/ndf
sidereal	20	17.9	7.9 ± 0.1 ± 0.4	50°.5 ± 1°.0 ± 1°.1	2.9 ± 0.1 ± 0.4	299°.5 ± 1°.3 ± 1°.5	95/19
	400	0.5	3.7 ± 0.7 ± 0.7	239°.2 ± 10°.6 ± 10°.8	2.7 ± 0.7 ± 0.6	152°.7 ± 7°.0 ± 4°.2	34.19
solar	20		1.9 ± 0.1 ± 0.6	267°.1 ± 3°.8 ± 7°.5			23/21
	400		2.9 ± 0.7 ± 1.0	272°.1 ± 13°.3 ± 5°.0			12/21
anti-sidereal	20		0.4 ± 0.1	1°.5 ± 18°.5			29/21
	400		0.5 ± 0.7	324°.6 ± 75°.4			17/21
extended-sidereal	20		0.7 ± 0.1	165°.7 ± 10°.3			29/21
	400		0.7 ± 0.7	212°.9 ± 54°.5			23/21

cosmic ray energy estimation with muons

CR particle interacts in the atmosphere

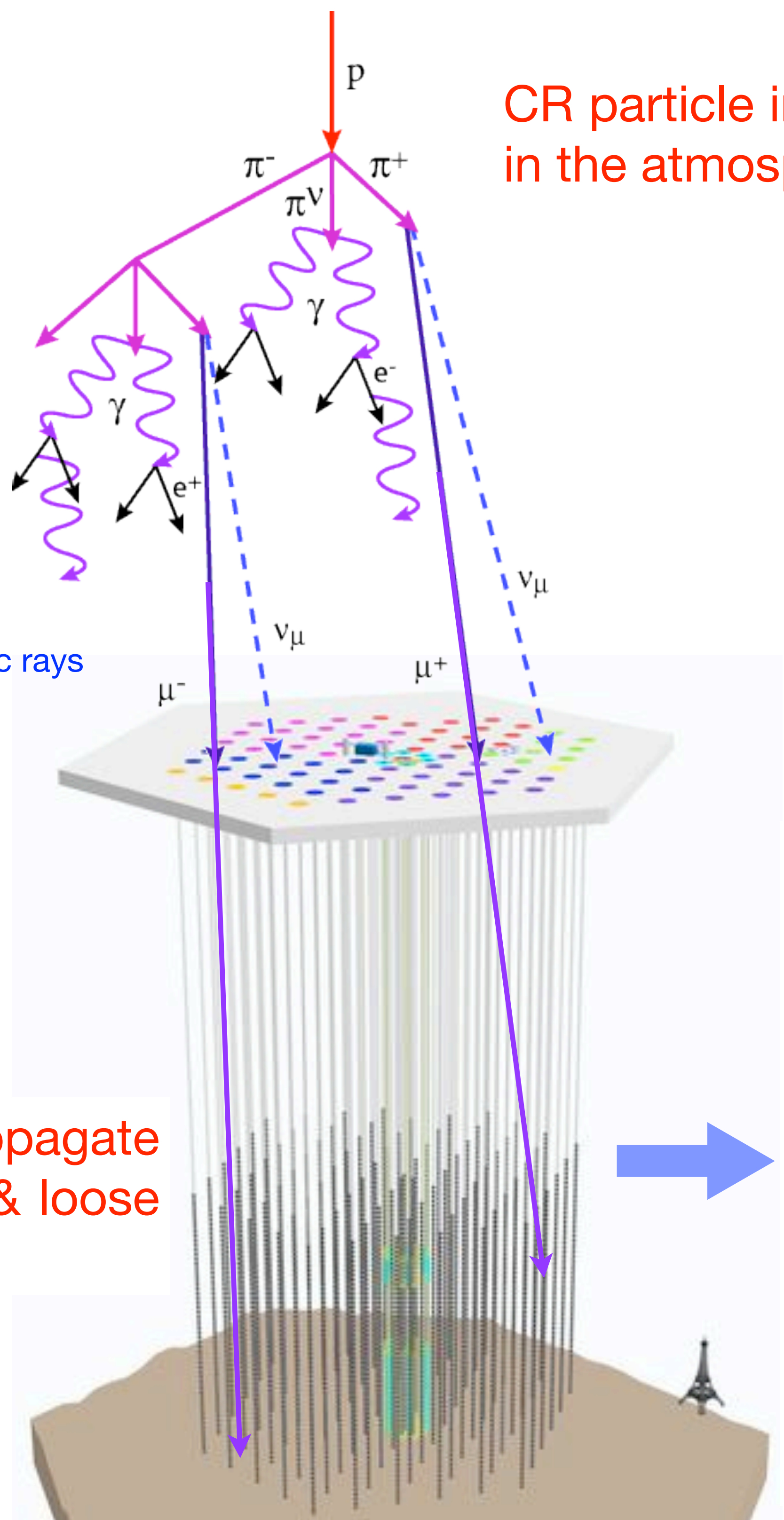

$E_\mu \propto E_{\text{cosmic rays}}$

muons propagate in the ice & loose energy

energy of secondaries $\propto E_\mu$

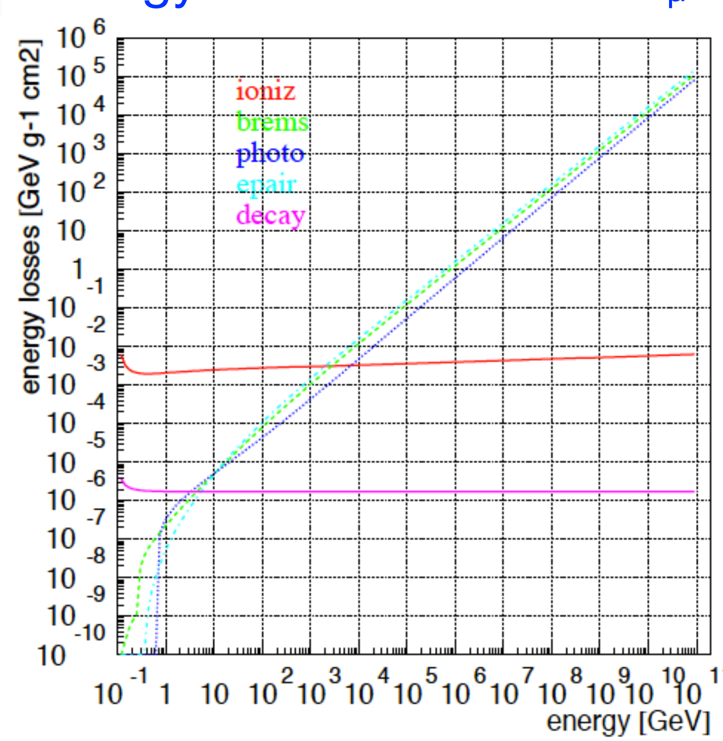

Cherenkov photons from μ and secondaries

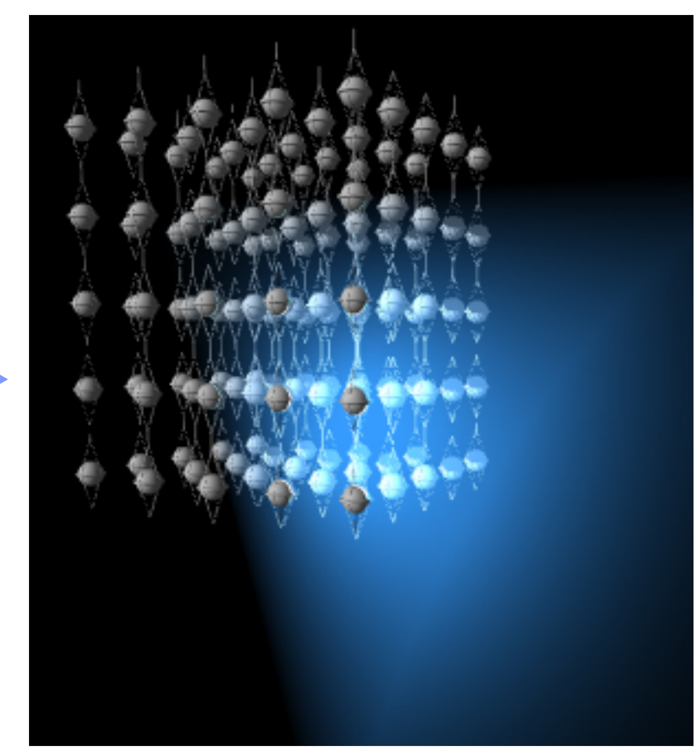

counts number of photons

$\propto$ energy of secondaries $\propto E_\mu$

$\propto E_{\text{cosmic rays}}$

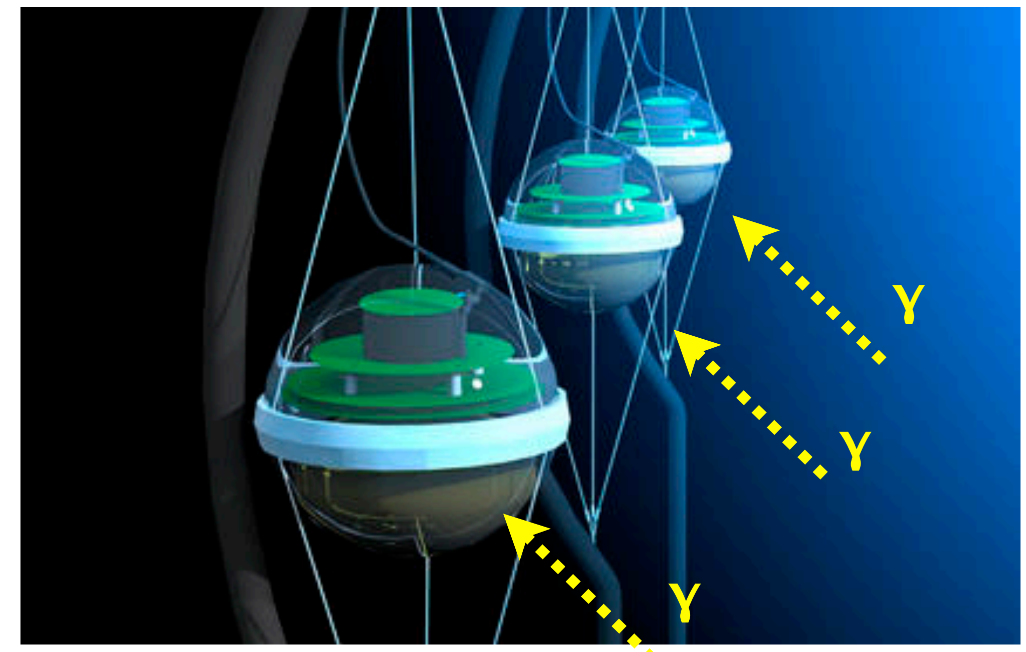

cosmic ray energy estimation with muons

Monte Carlo simulations

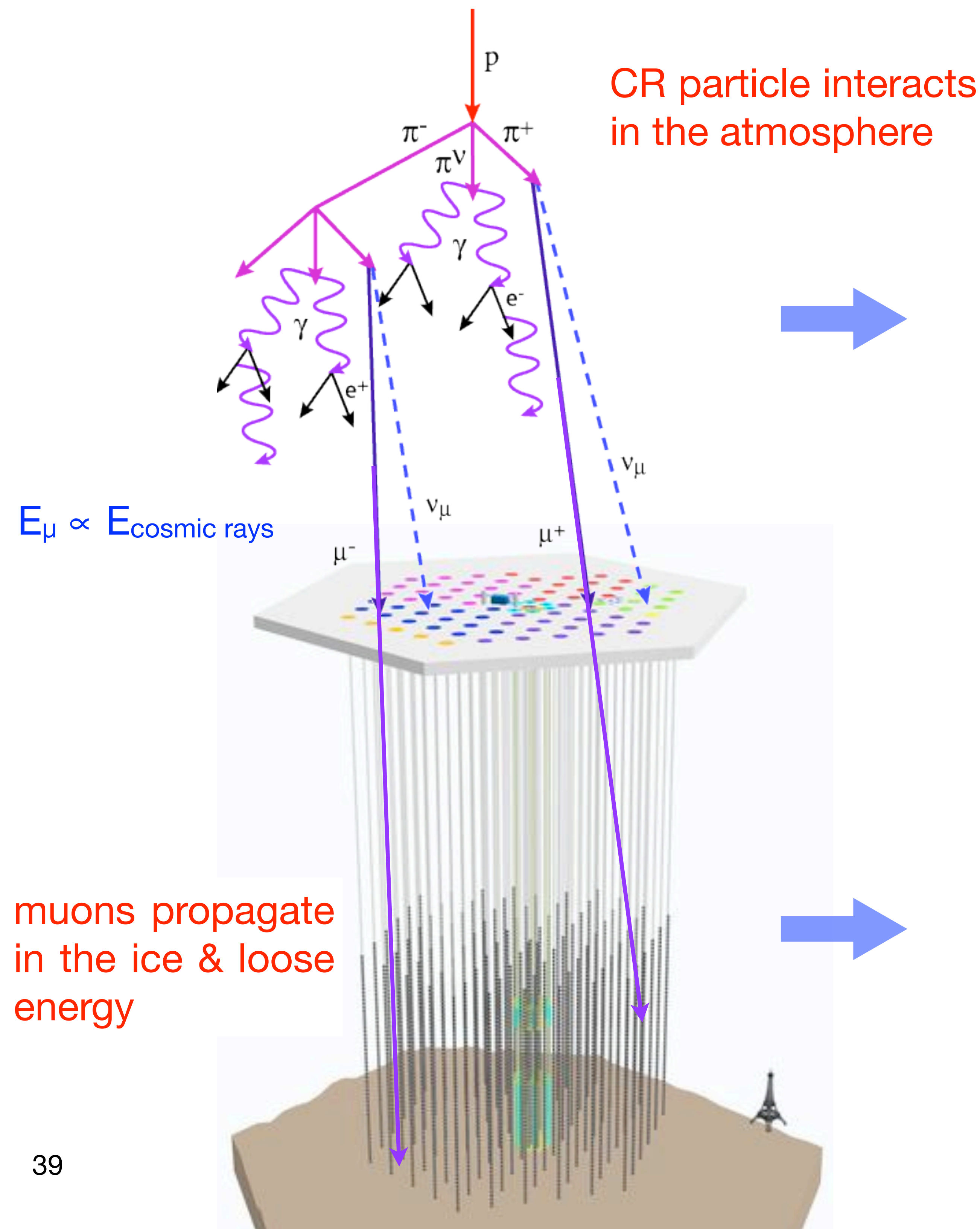

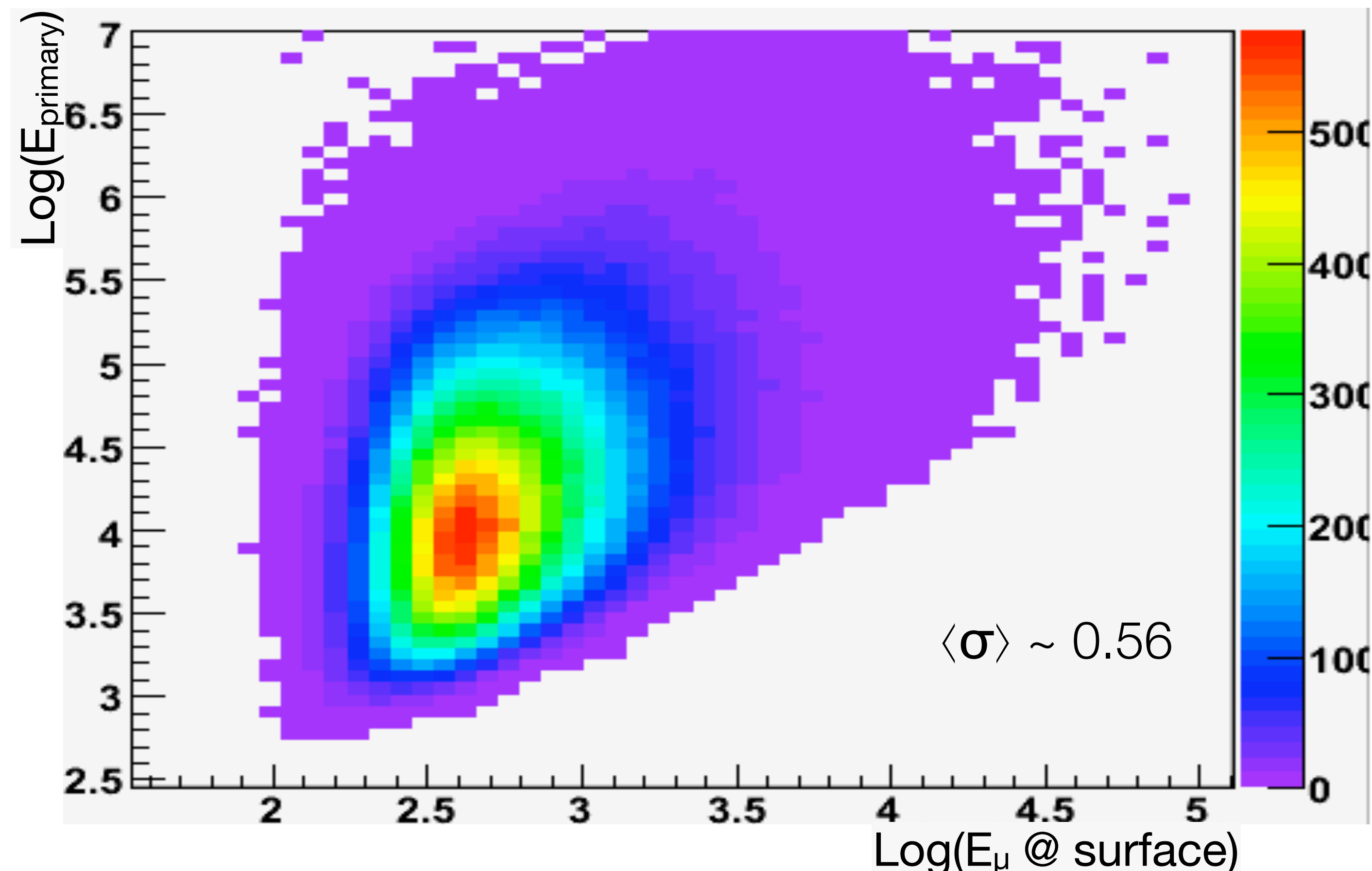

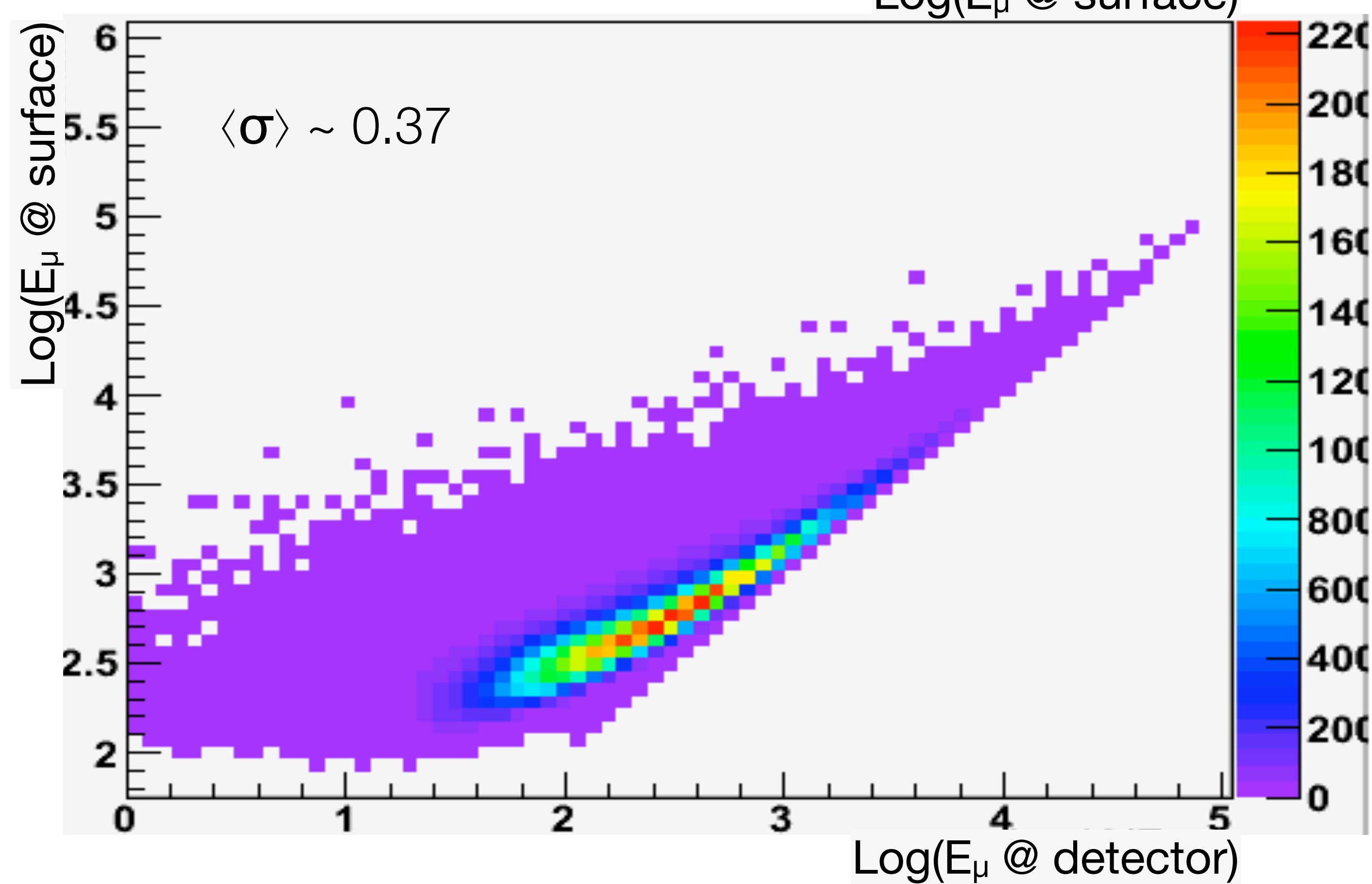

cosmic ray energy estimation with IceCube

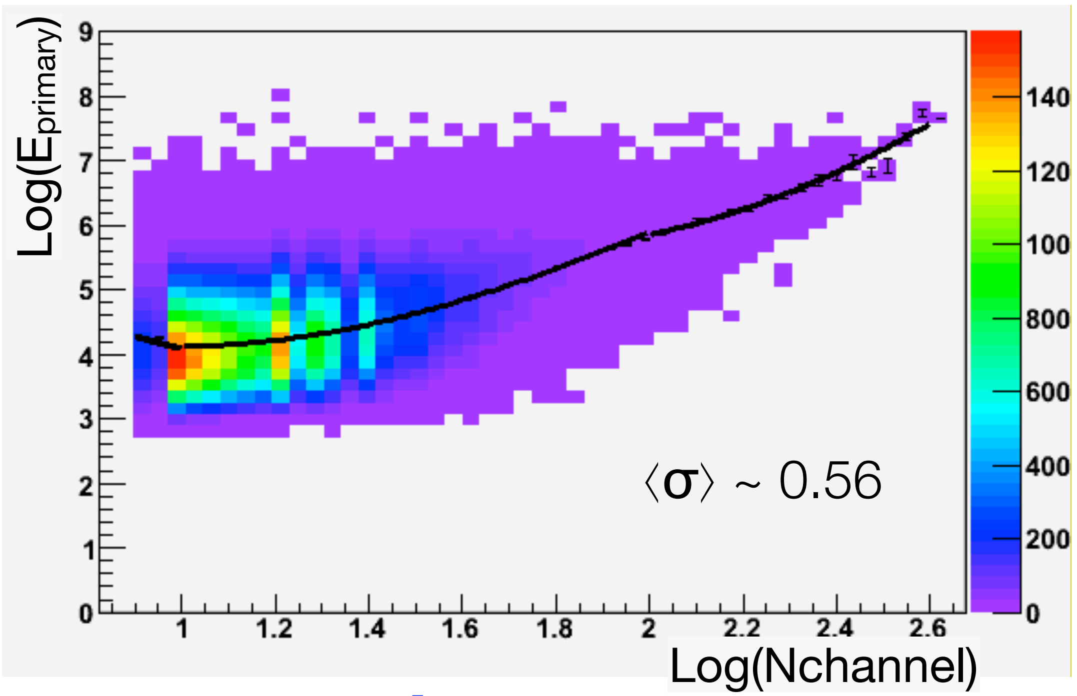

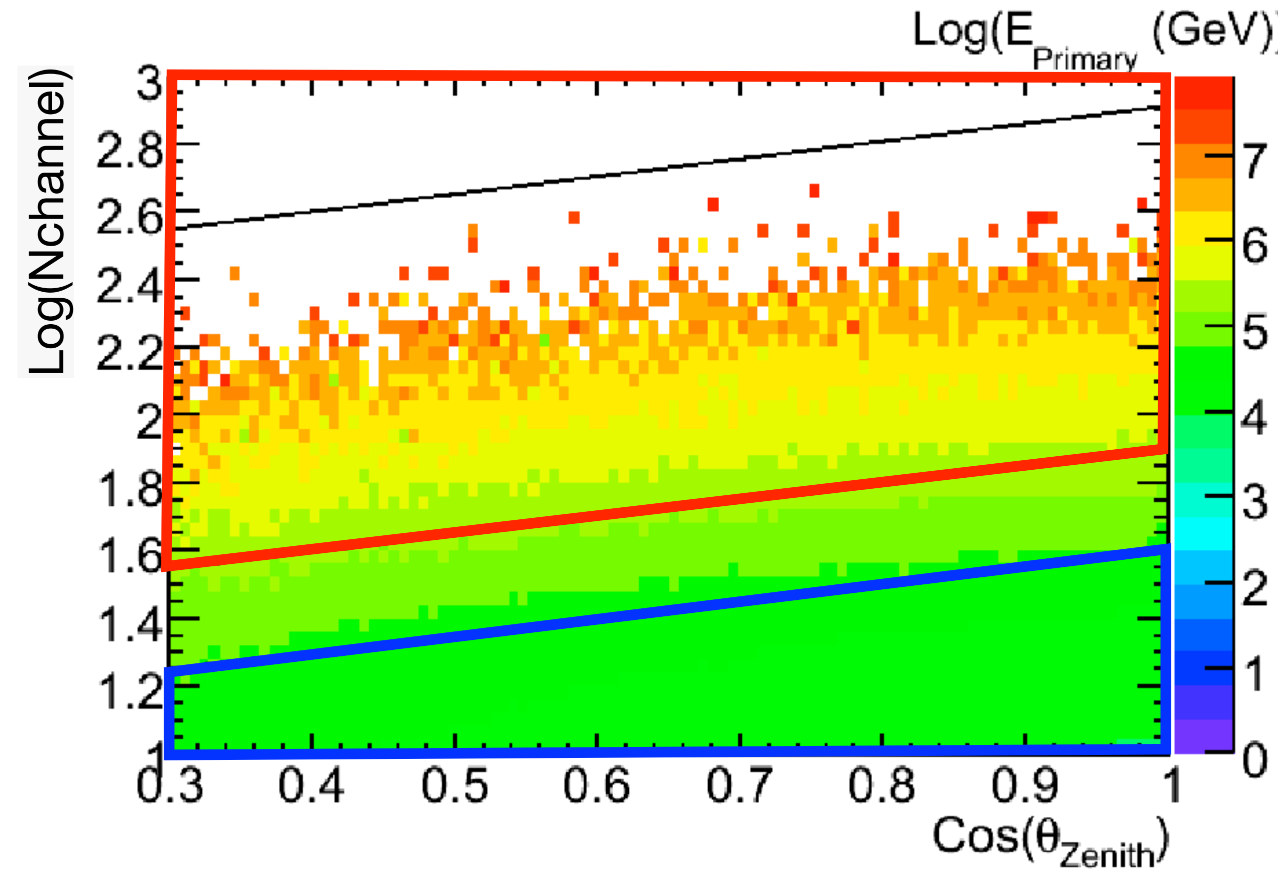

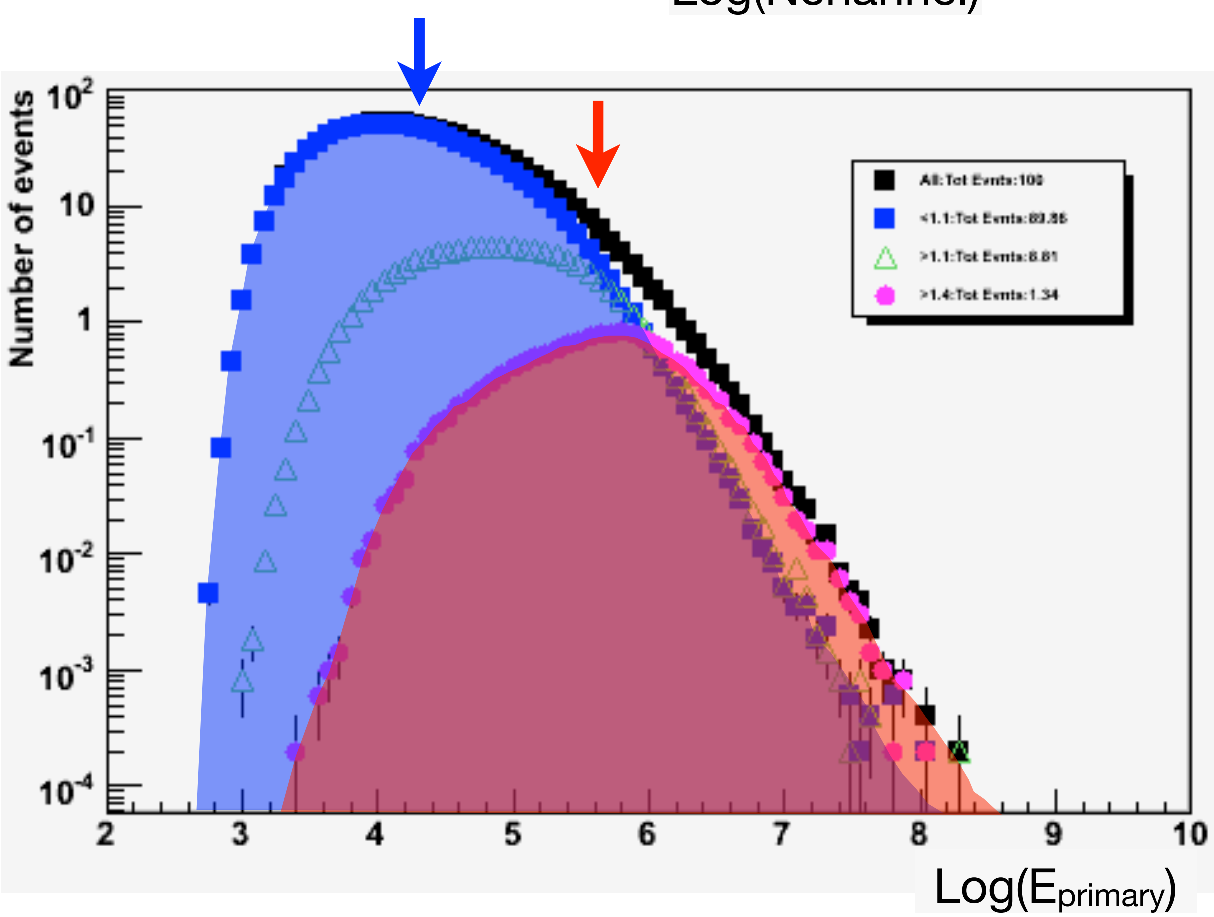

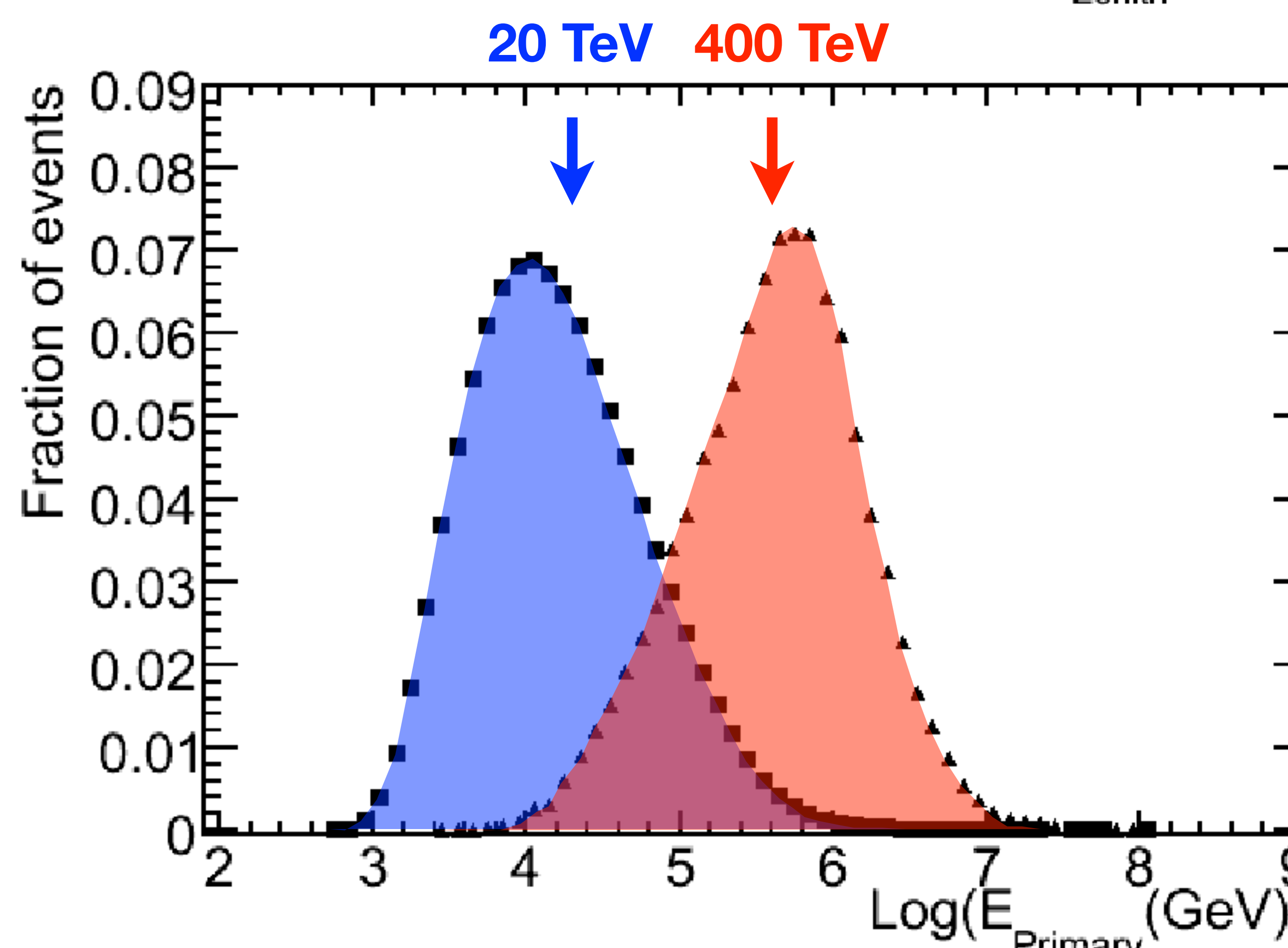

cosmic ray energy estimation with IceCube

$E_{primary}$ (TeV)	$N_{HE}(<E_{primary}) / N_{LE}(<E_{primary})$	$N_{HE}(>E_{primary}) / N_{LE}(>E_{primary})$
20	0.02%	4%
40	0.1%	6%
100	0.3%	14%
400	0.7%	64%

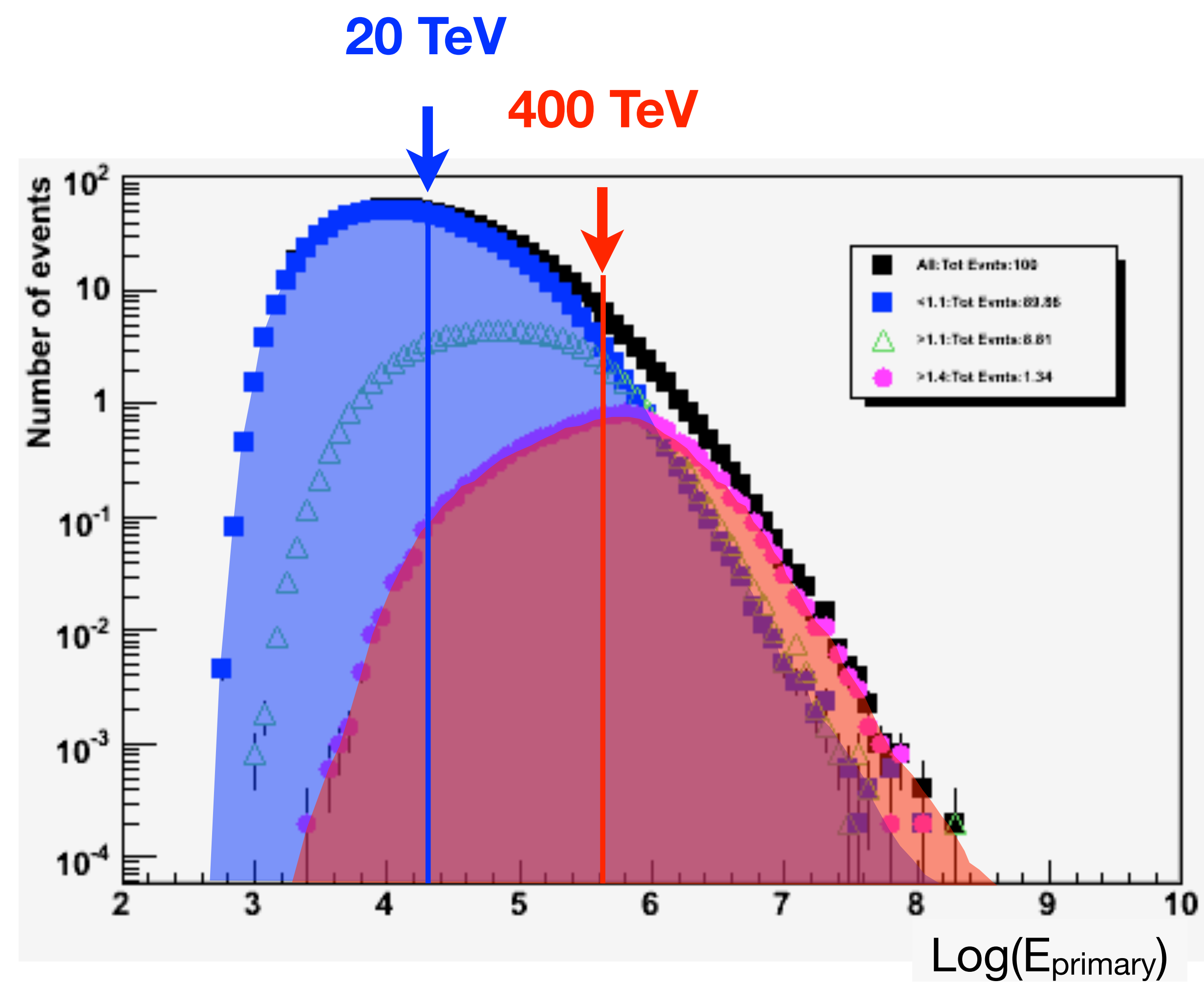

How much of the anisotropy observed @ 400 TeV is influenced by that @ 20 TeV ?

Does the anisotropy observation @ 20 TeV contain features from 400 TeV scale ?

MuE vs Nchannel

$$\mu E = \frac{\langle N_\gamma \rangle}{L_{track}} \cdot A_{eff}^{PMT}$$

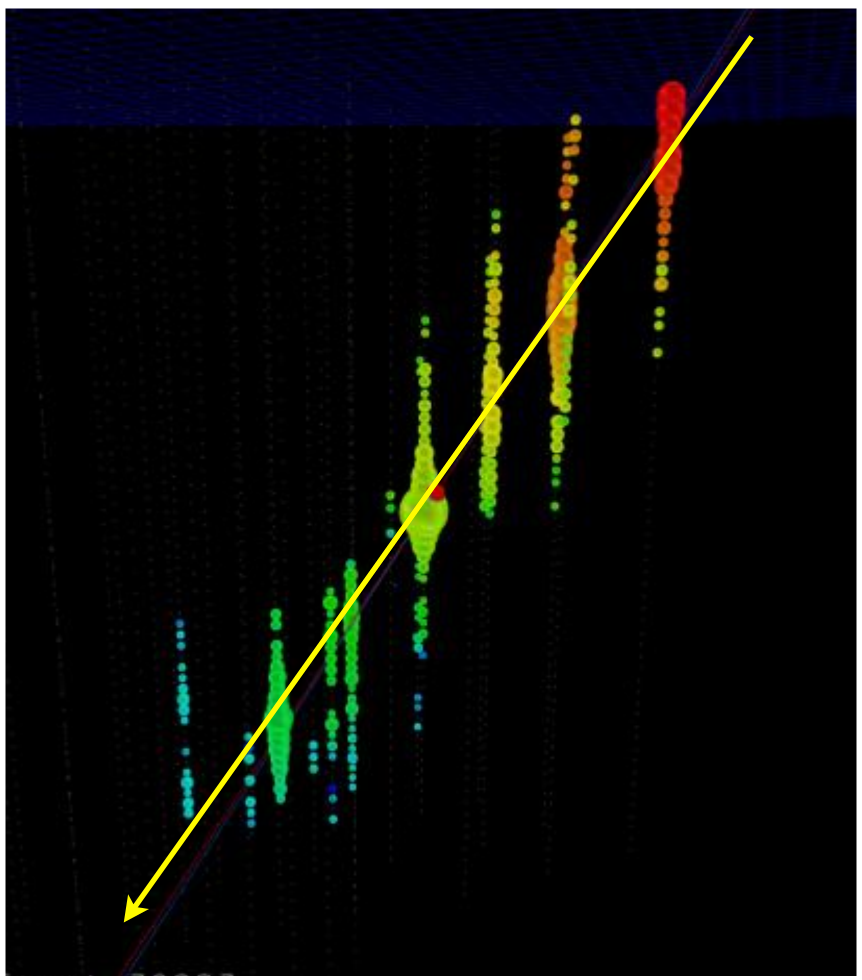

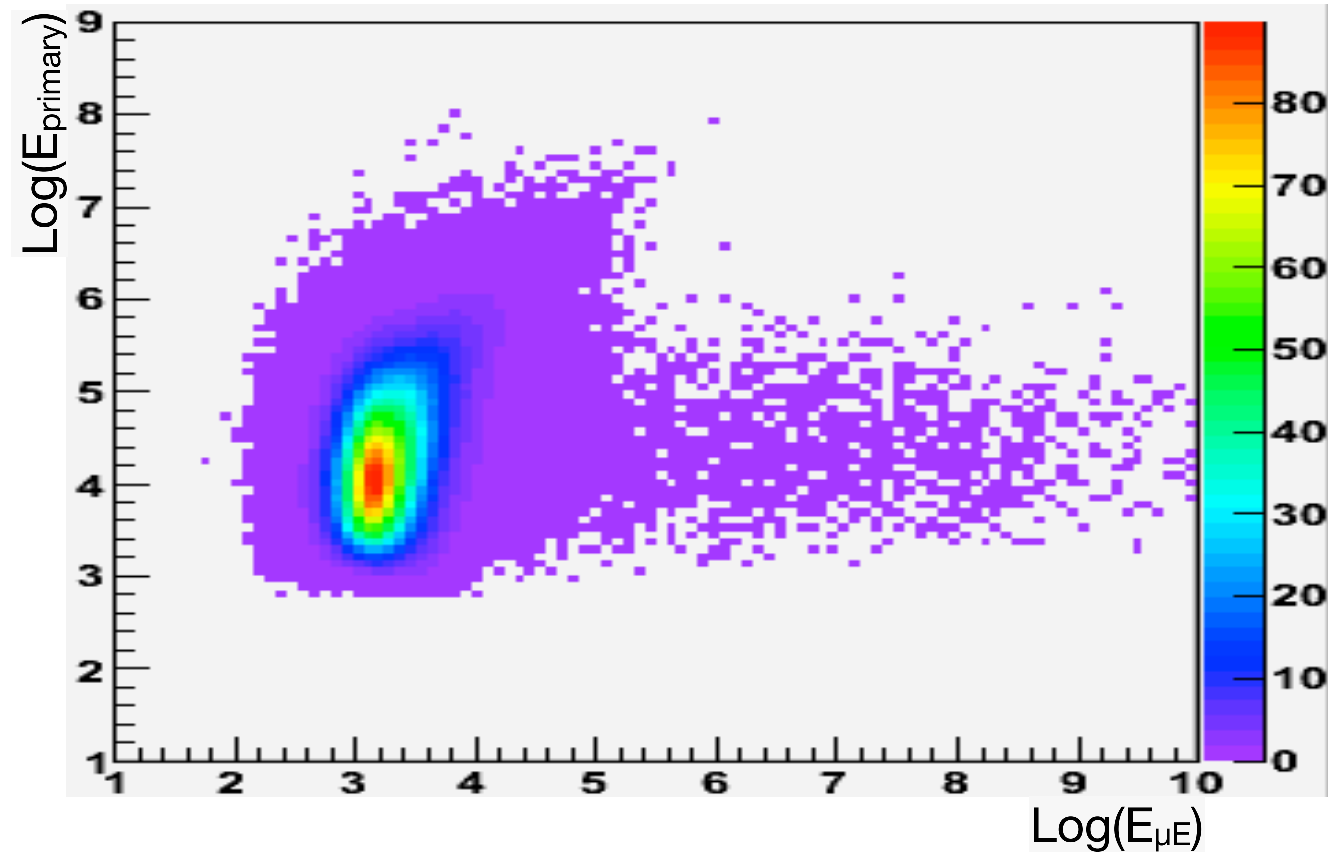

Optimized Cut Values on Angular Resolution					
NString	Opening Angle	LDirC	NChan	Rlogl	Distance to the COG
> 2	< 5 degrees	> 468	> 9	< 10	< 740

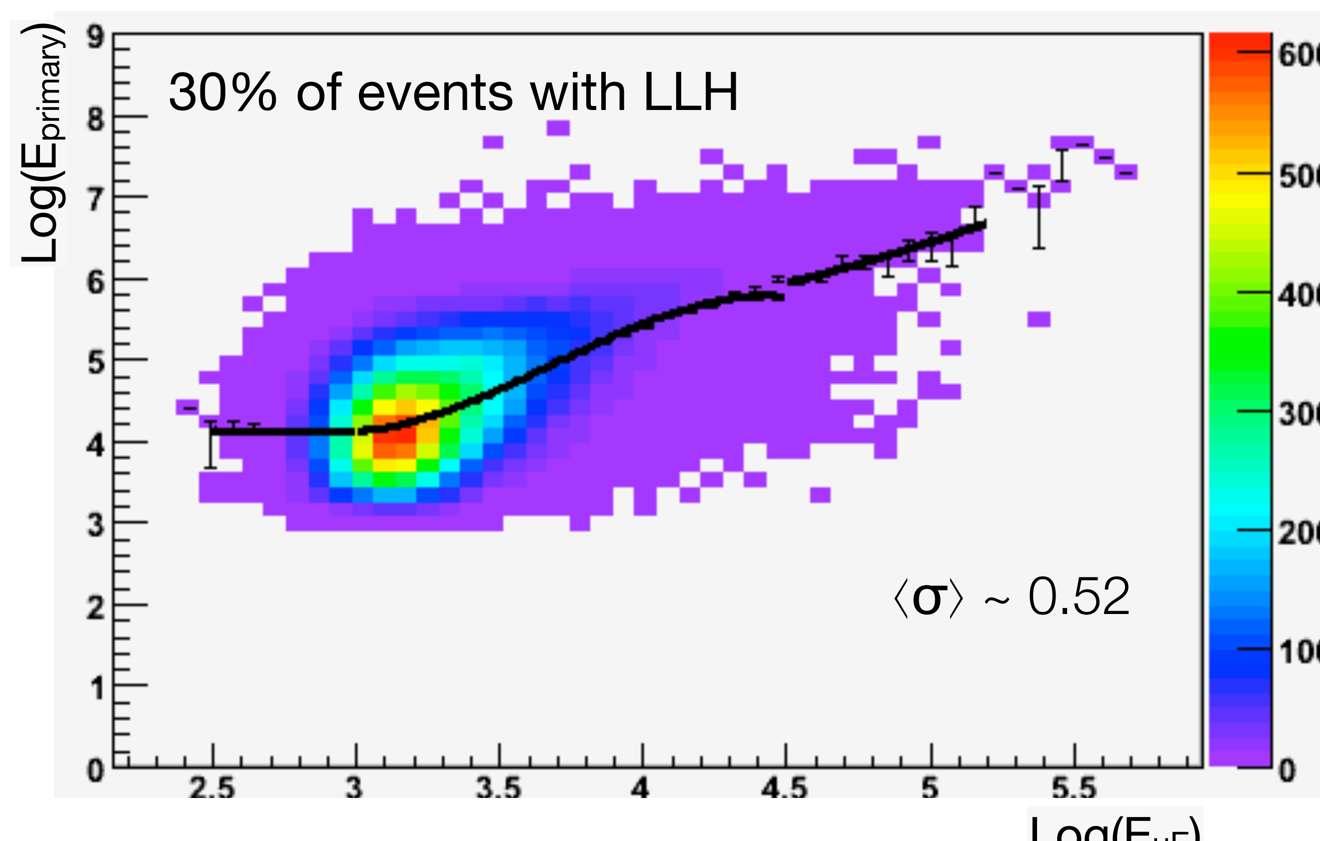

MuE vs Nchannel

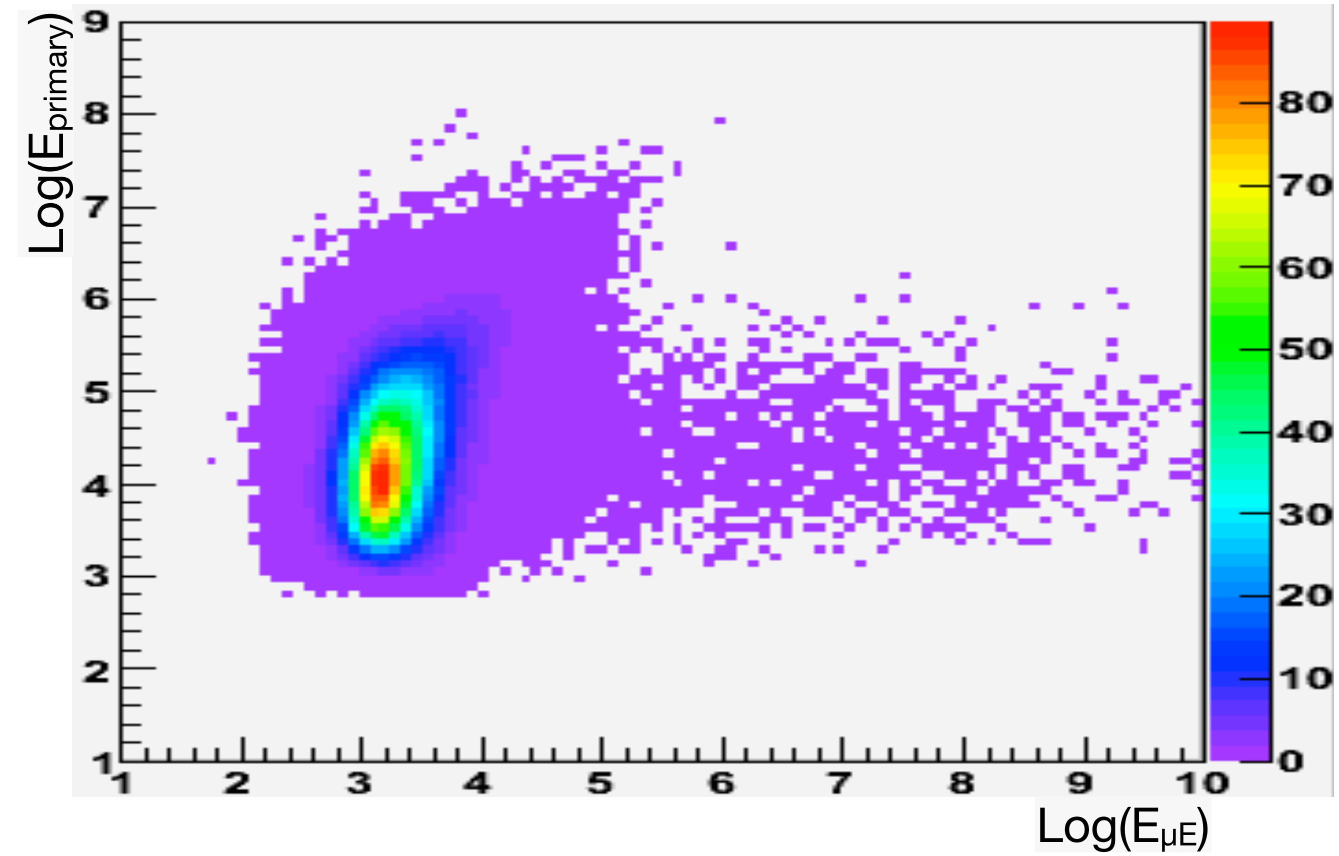

Optimized Cut Values on Angular Resolution					
NString	Opening Angle	LDirC	NChan	Rlogl	Distance to the COG
> 2	< 5 degrees	> 468	> 9	< 10	< 740

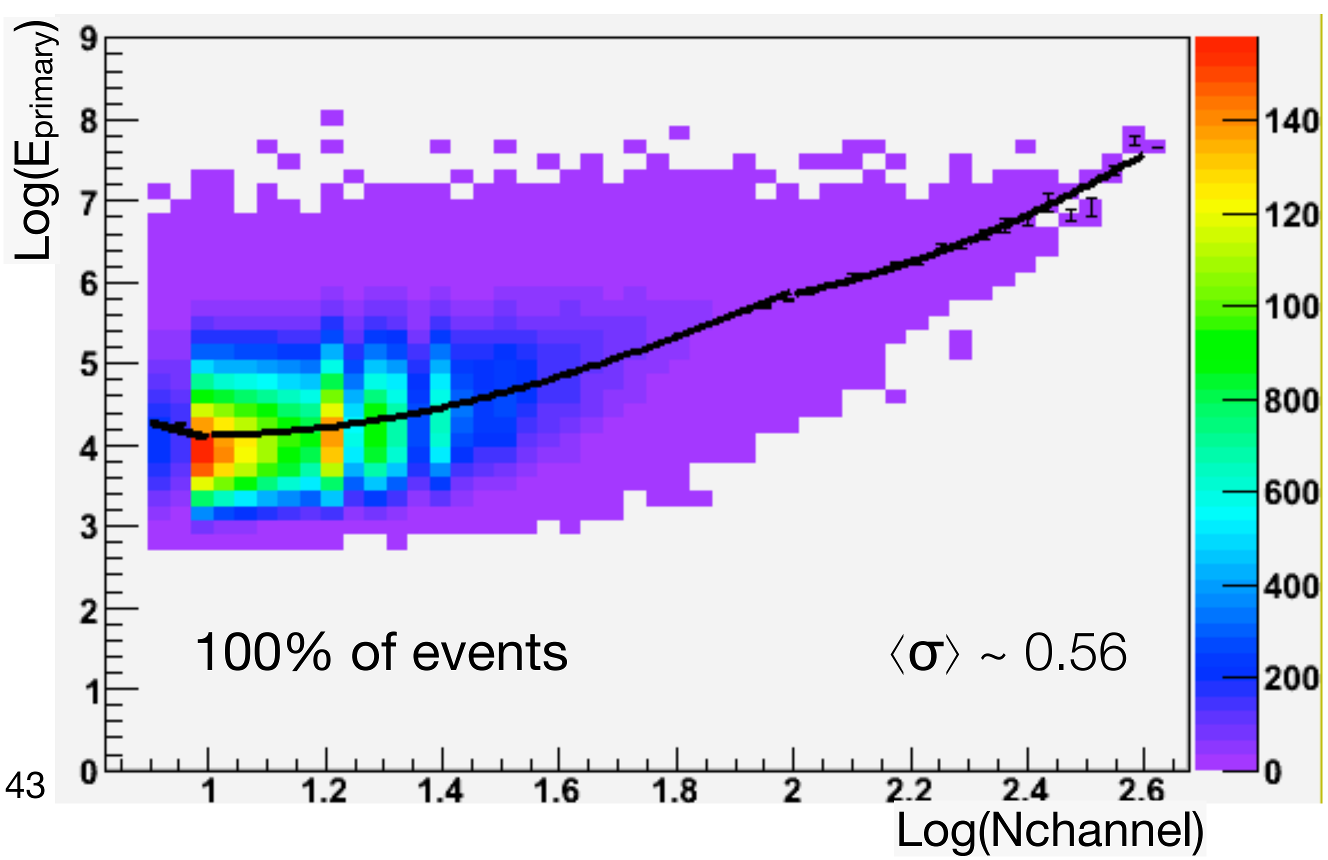

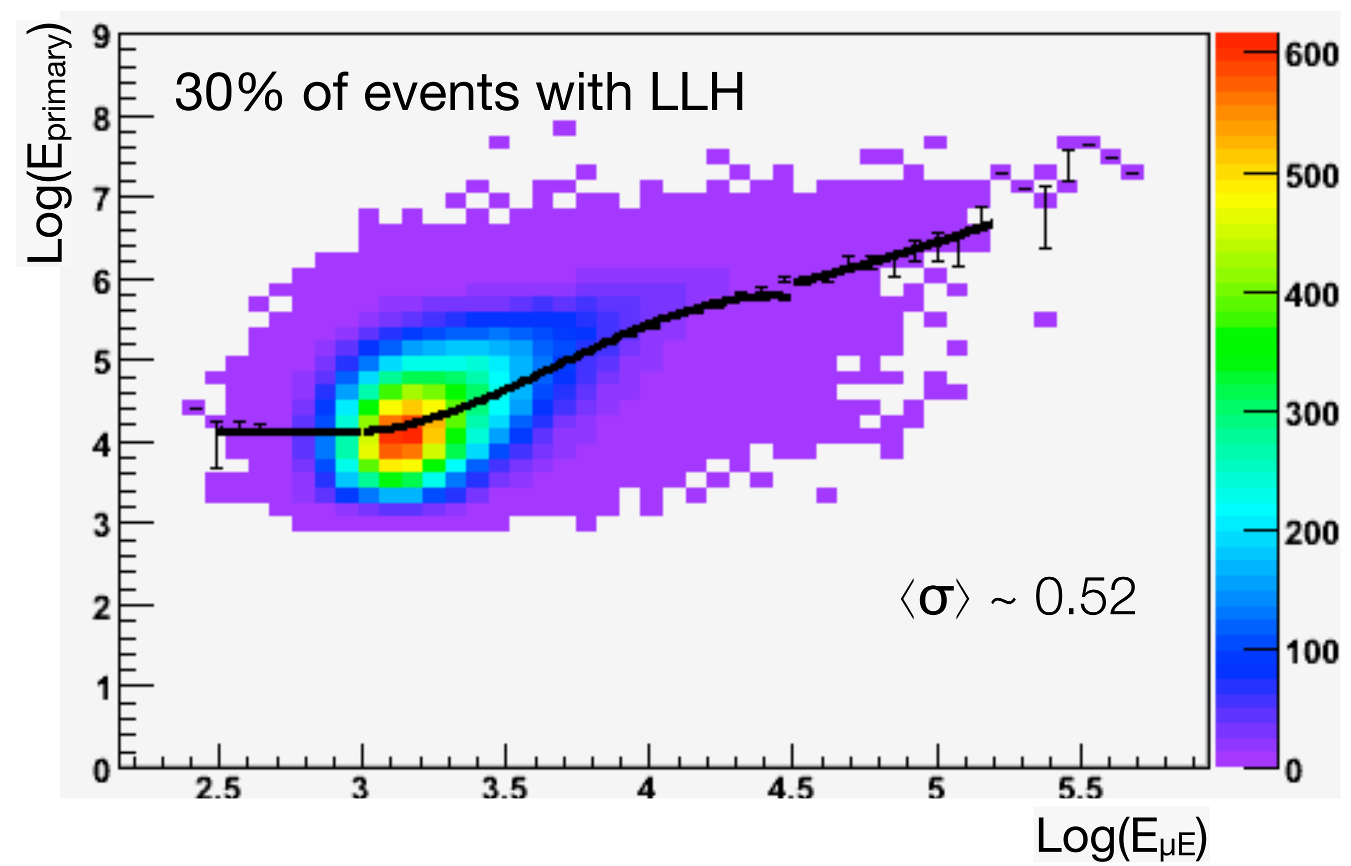

Craig Price

cut optimization

$$\epsilon = \frac{\Phi_{LLH,MC}}{\sqrt{\frac{N_{selected}}{N_{total}}}}$$

Optimized Cut Values on Angular Resolution					
NString	Opening Angle	LDirC	NChan	Rlogl	Distance to the COG
> 2	< 5 degrees	> 468	> 9	< 10	< 740

selection efficiency ~ 30%

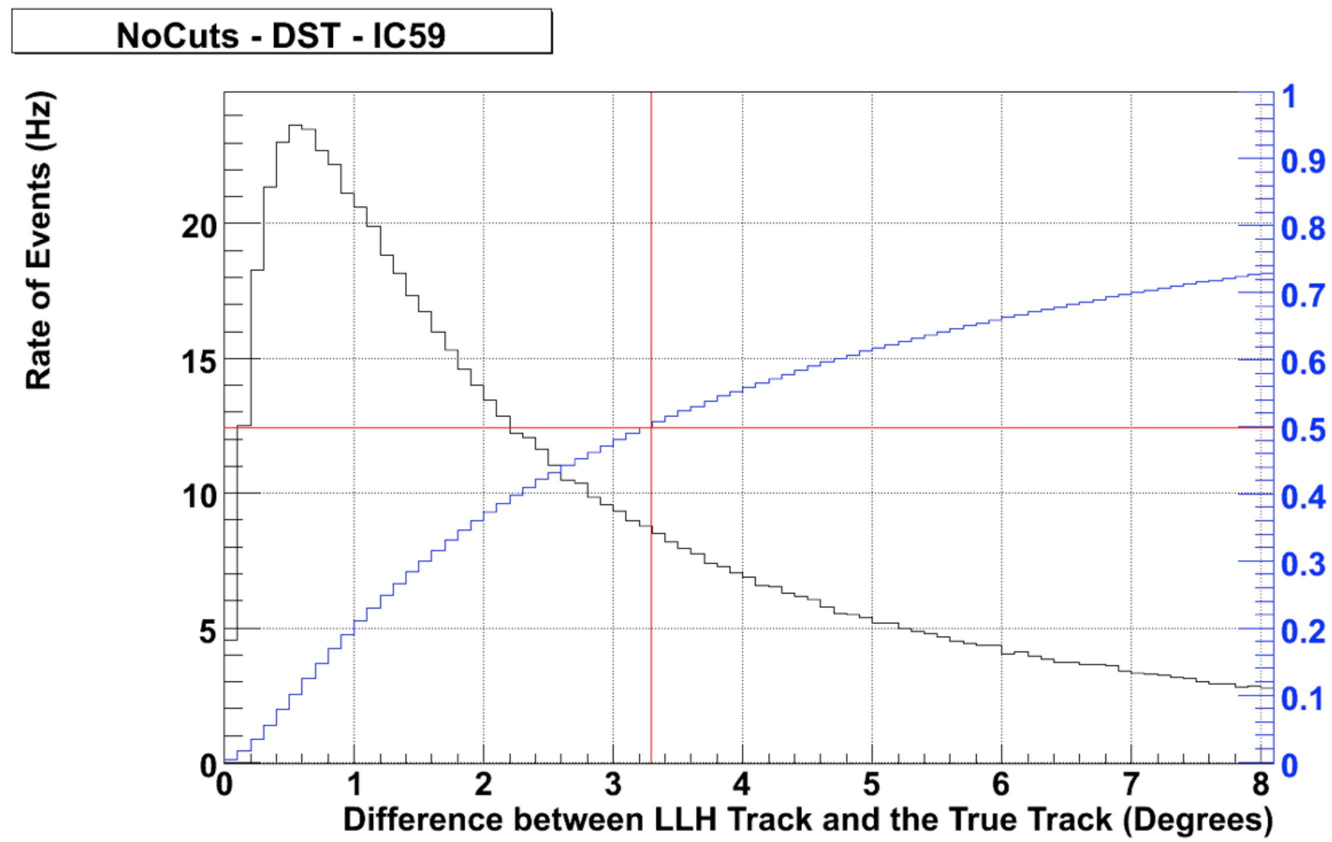

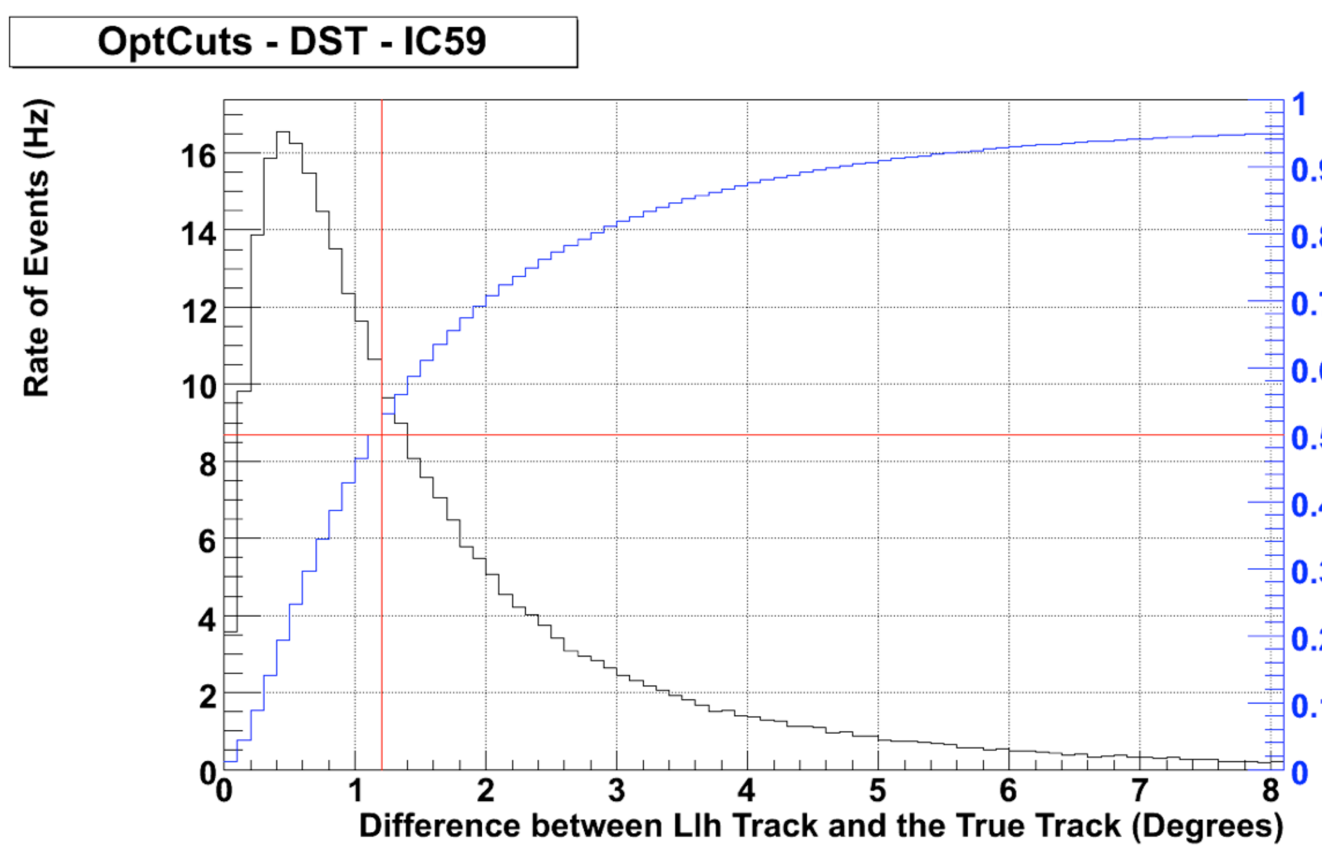

Craig Price

cut optimization

$$\epsilon = \frac{\Phi_{LLH,MC}}{\sqrt{\frac{N_{selected}}{N_{total}}}}$$

Optimized Cut Values on Angular Resolution					
NString	Opening Angle	LDirC	NChan	Rlogl	Distance to the COG
> 2	< 5 degrees	> 468	> 9	< 10	< 740

selection efficiency ~ 30%

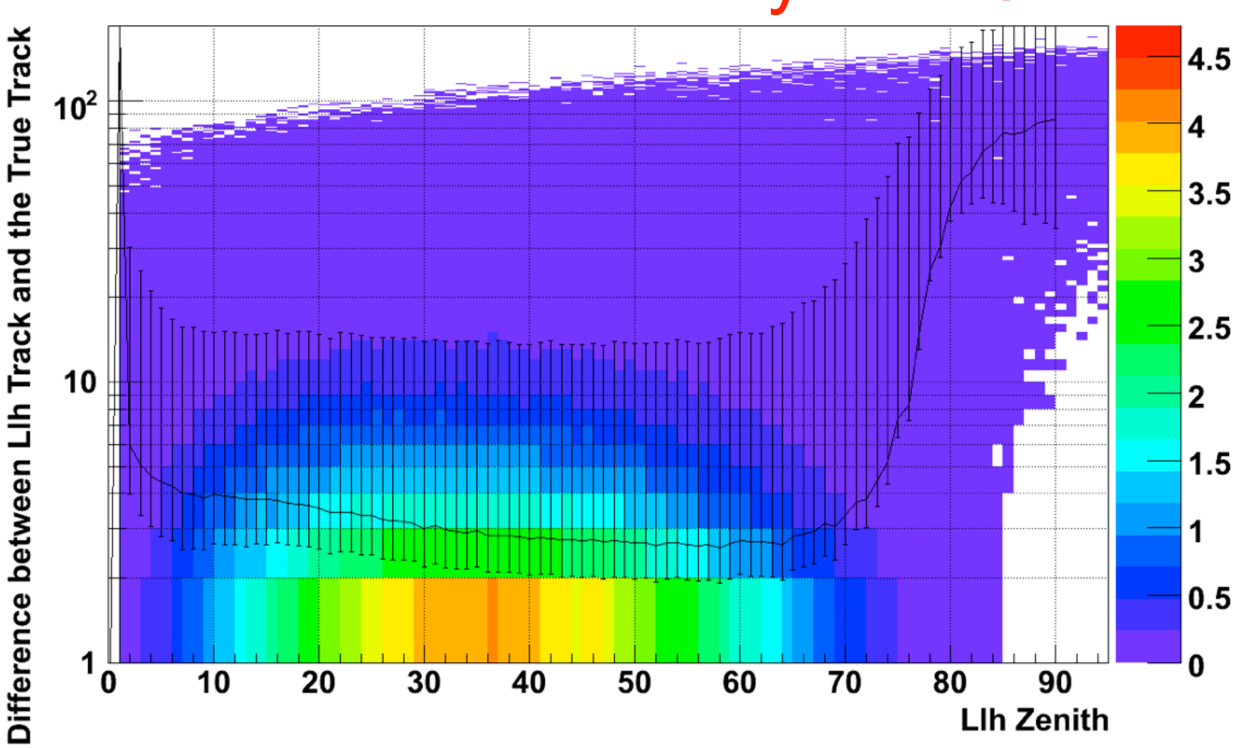

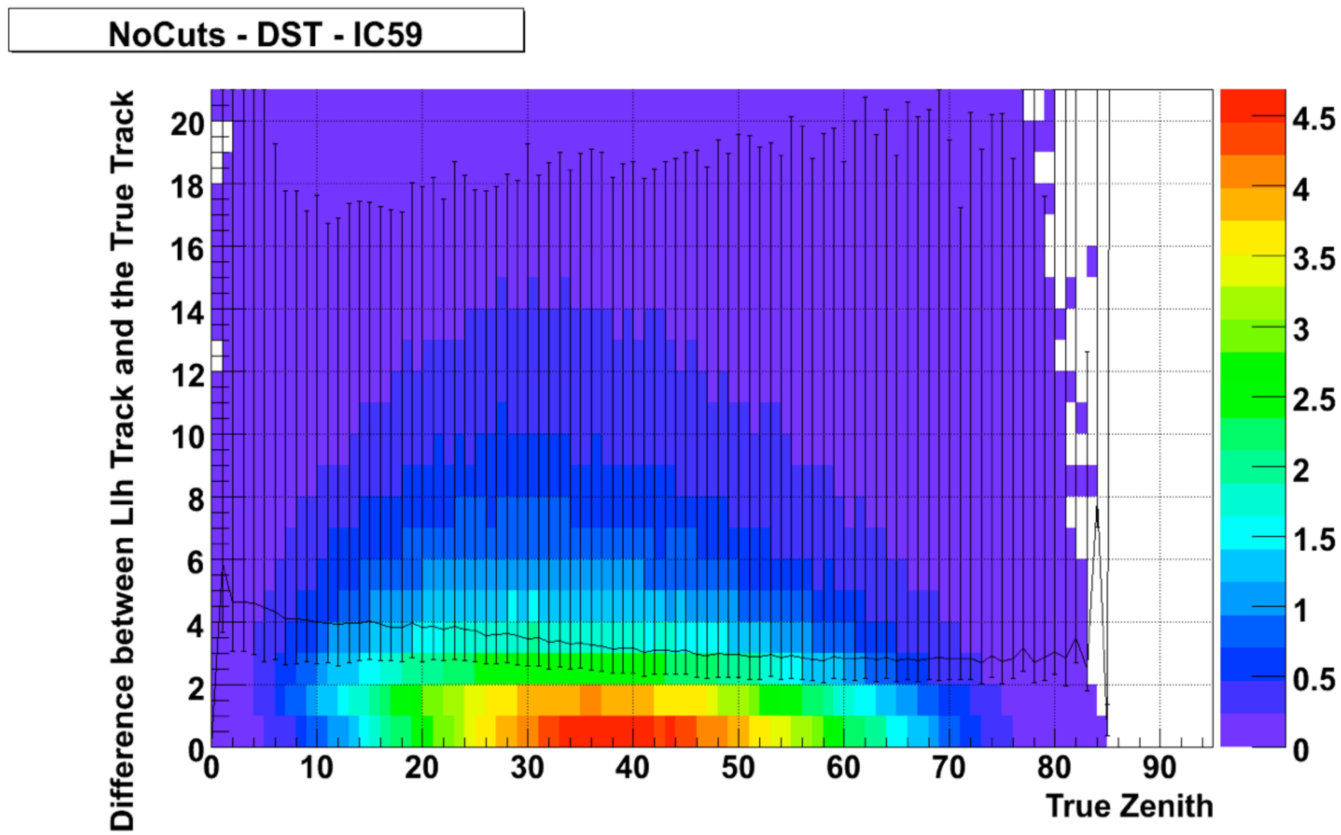

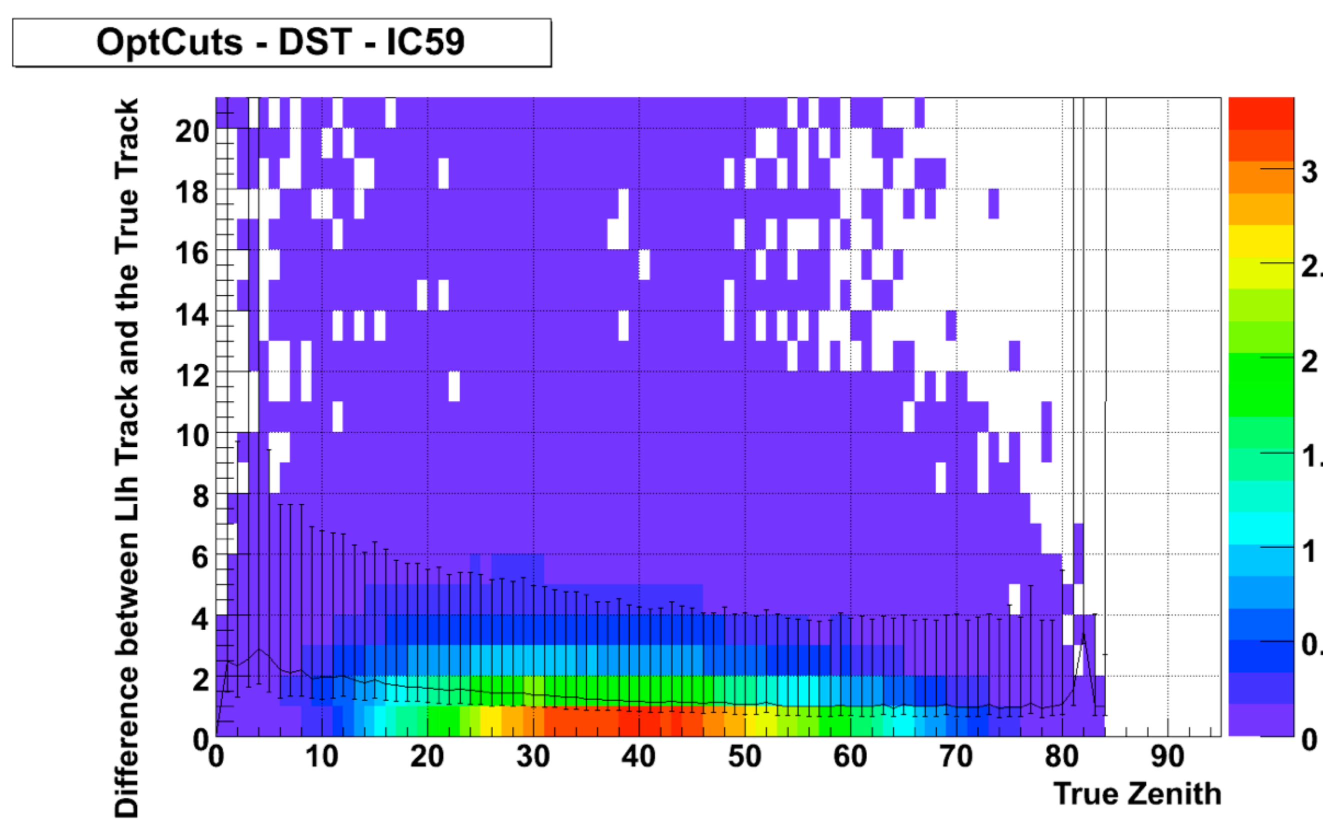

detector acceptance correction

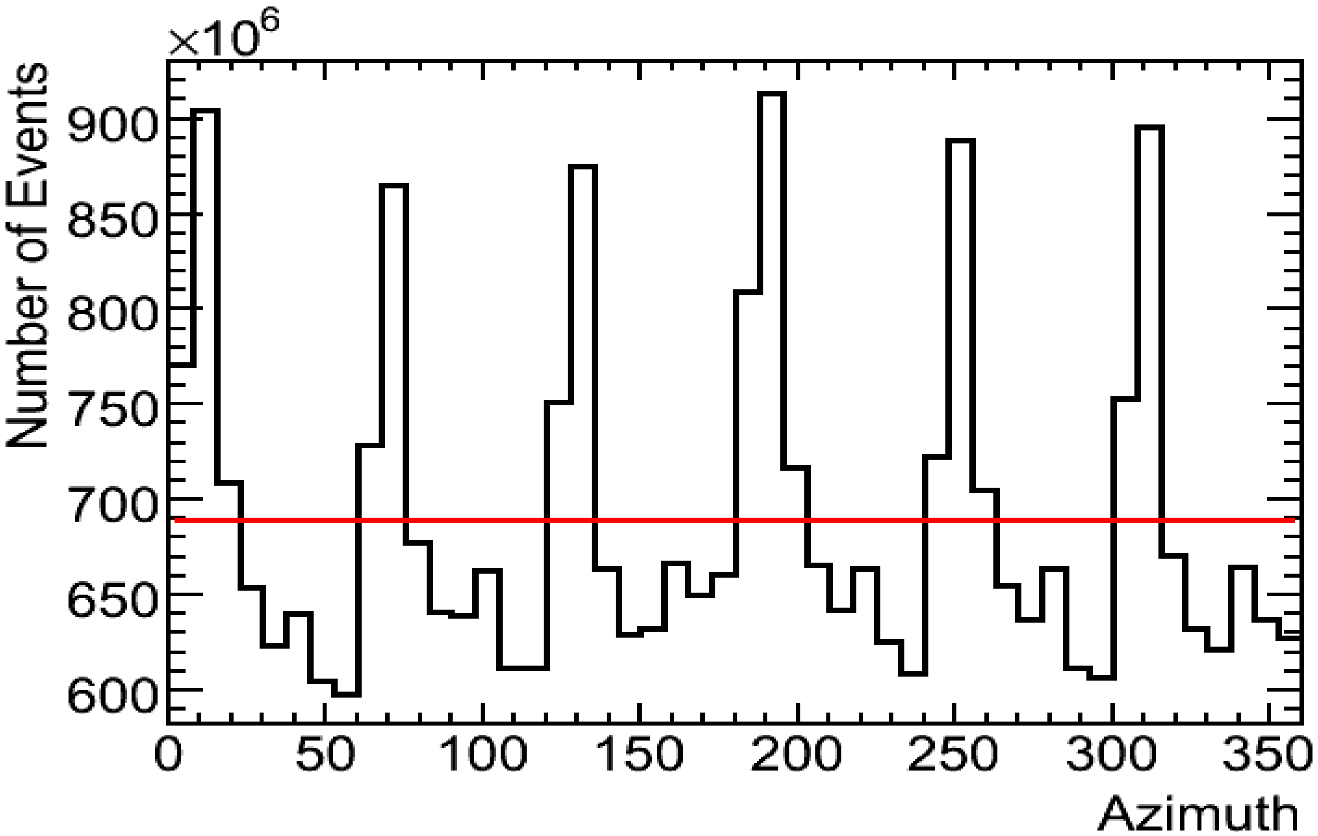

$$w_i(\delta) = \frac{\bar{n}(\delta)}{n_i(\delta)} = \frac{mean\ \#\ events\ in\ \delta}{number\ of\ events\ in\ bin}$$

local azimuth angle distribution stable over time ($<10^{-5}$)

acceptance correction better than 10^{-5}

systematic uncertainties IceCube-59

statistical stability tests + anti-sidereal effect

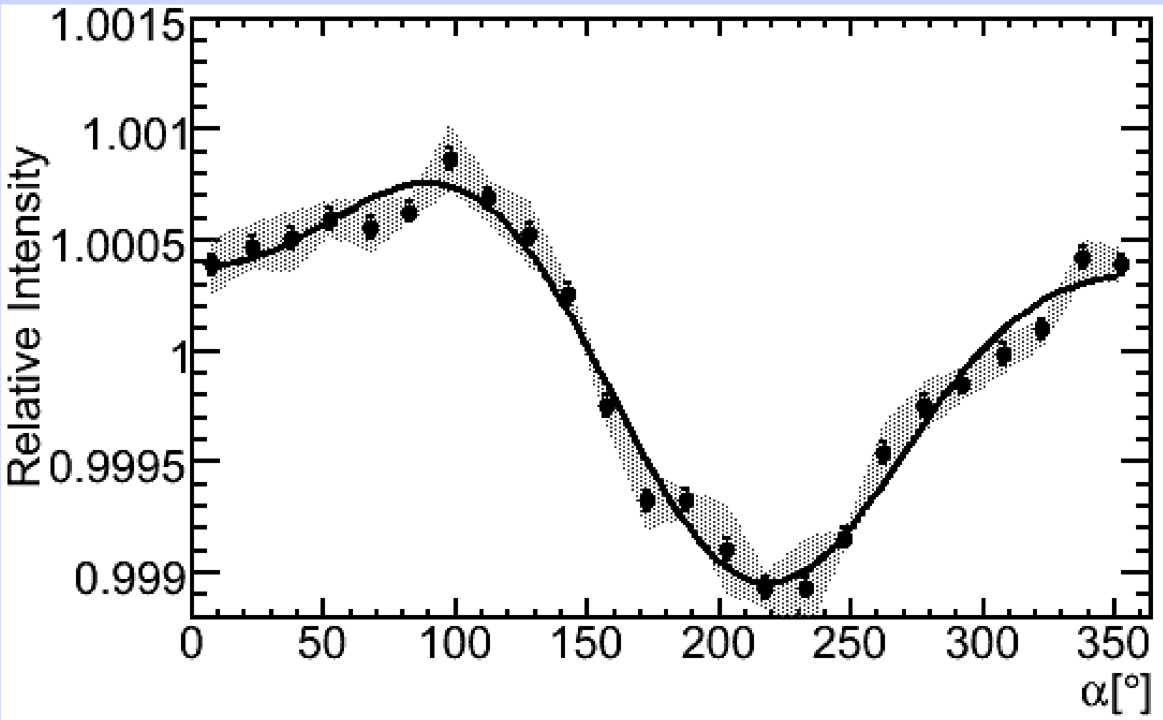

20 TeV

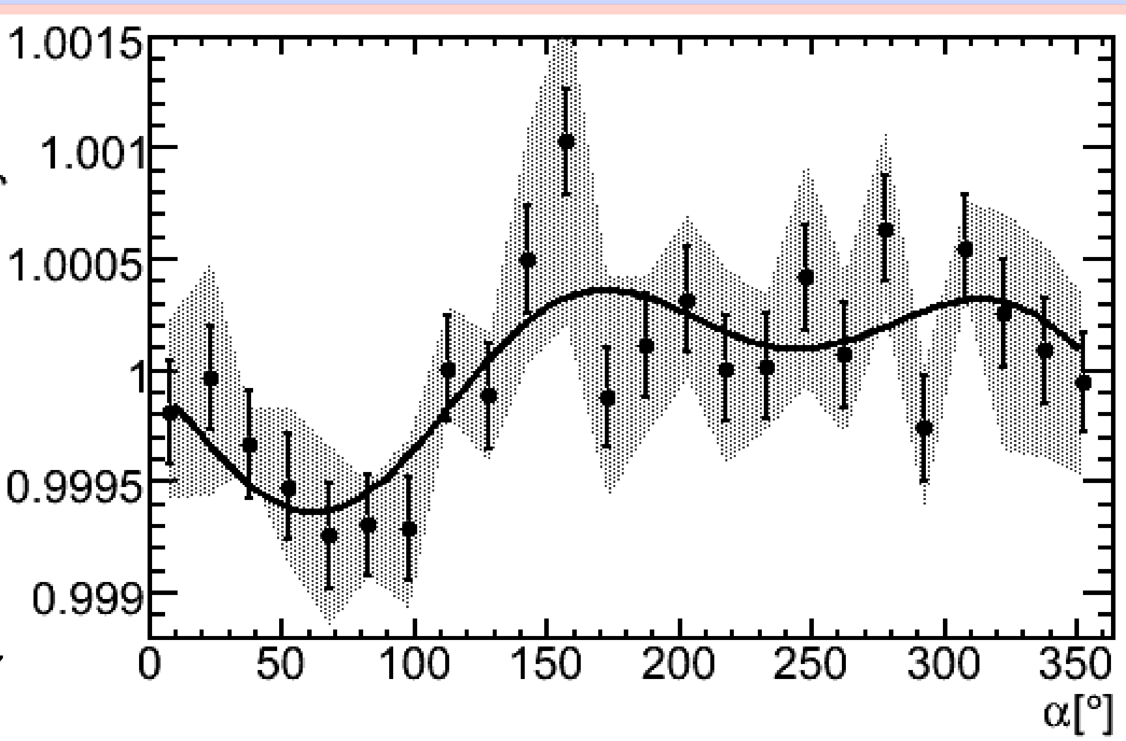

400 TeV

statistical stability tests:

- summer/winter season datasets
- rate ≷ median daily rate
- even/odd sub-runs (2 mins data)
- random sub-run selection
- use ~24 hr full days (214/324 d)

growing IceCube & temperature correlation

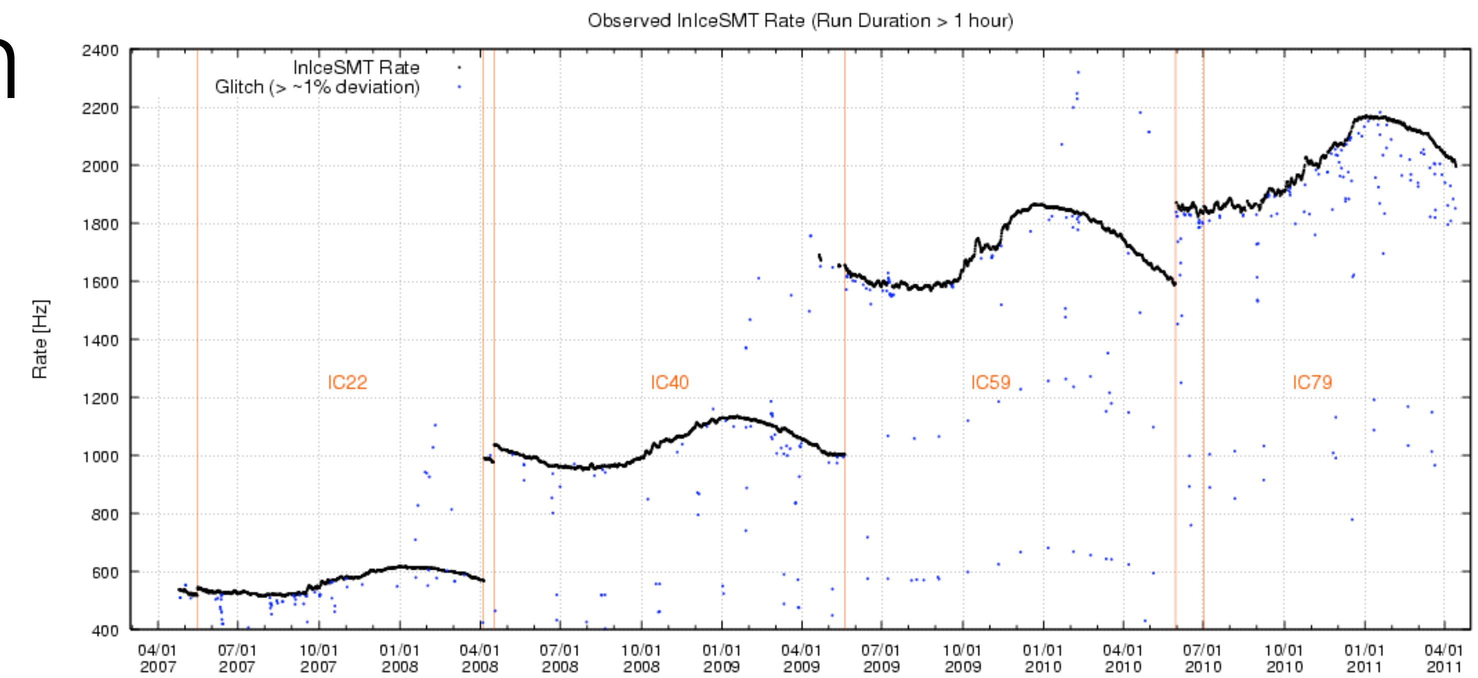

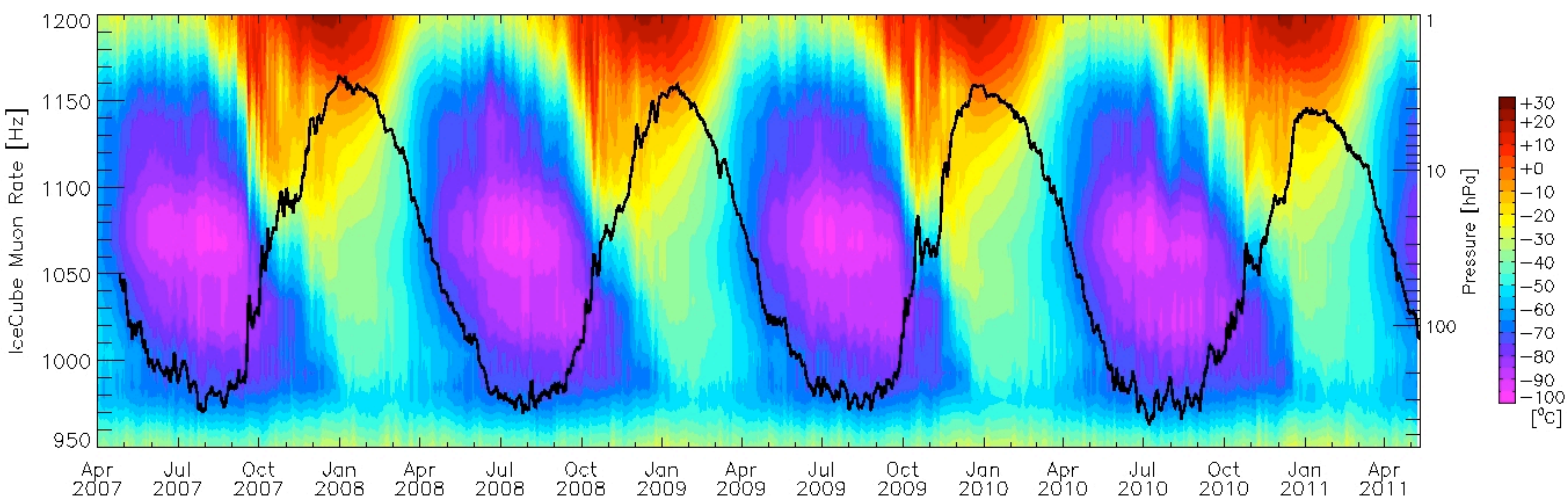

Farley, & Storey, Proc. Phys. Soc., 67, 996, 1954

Nagashima, et al., Nuovo 907 Cimento C, 6, 550, 1983

anti- / extended-sidereal reference frames

A static distribution in **solar** (sidereal) reference frame averages to zero in **sidereal** (solar) frame after one year

An annual modulation of the **solar** (sidereal) distribution does not compensate and produces distortions on the **sidereal** (solar) anisotropies

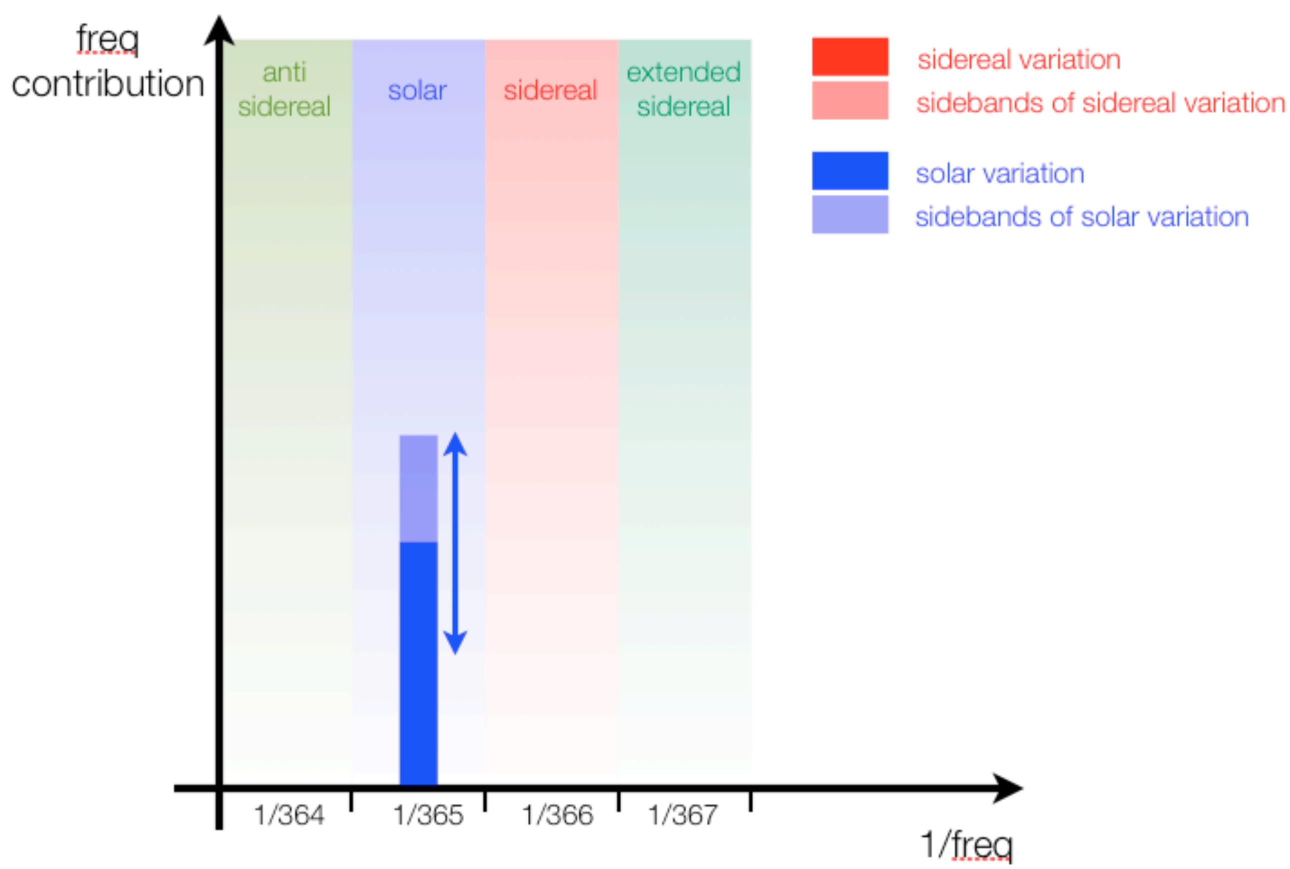

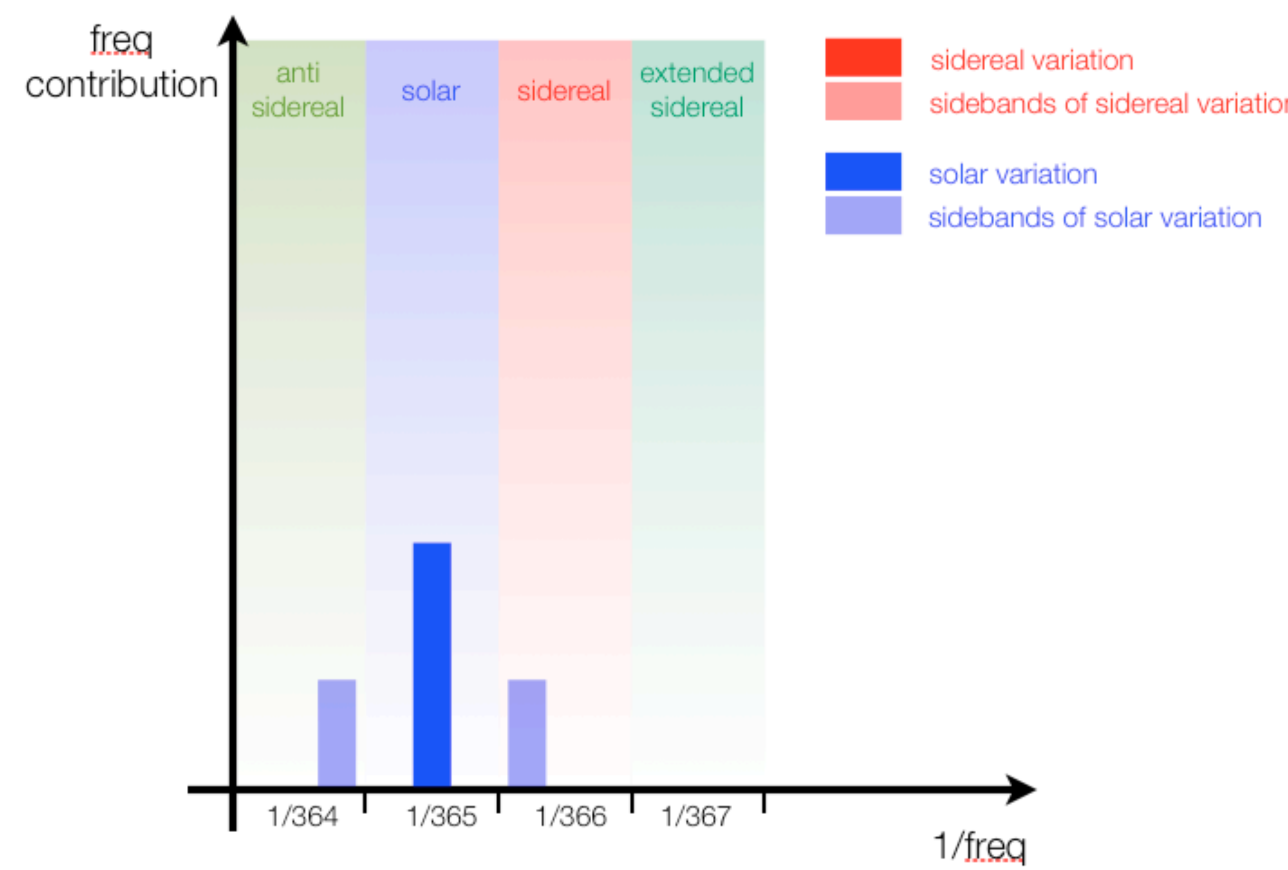

Farley, & Storey, Proc. Phys. Soc., 67, 996, 1954

Nagashima, et al., Nuovo 907 Cimento C, 6, 550, 1983

anti- / extended-sidereal reference frames

A static distribution in solar (**sidereal**) reference frame averages to zero in sidereal (solar) frame after one year

An annual modulation of the solar (**sidereal**) distribution does not compensate and produces distortions on the sidereal (**solar**) anisotropies

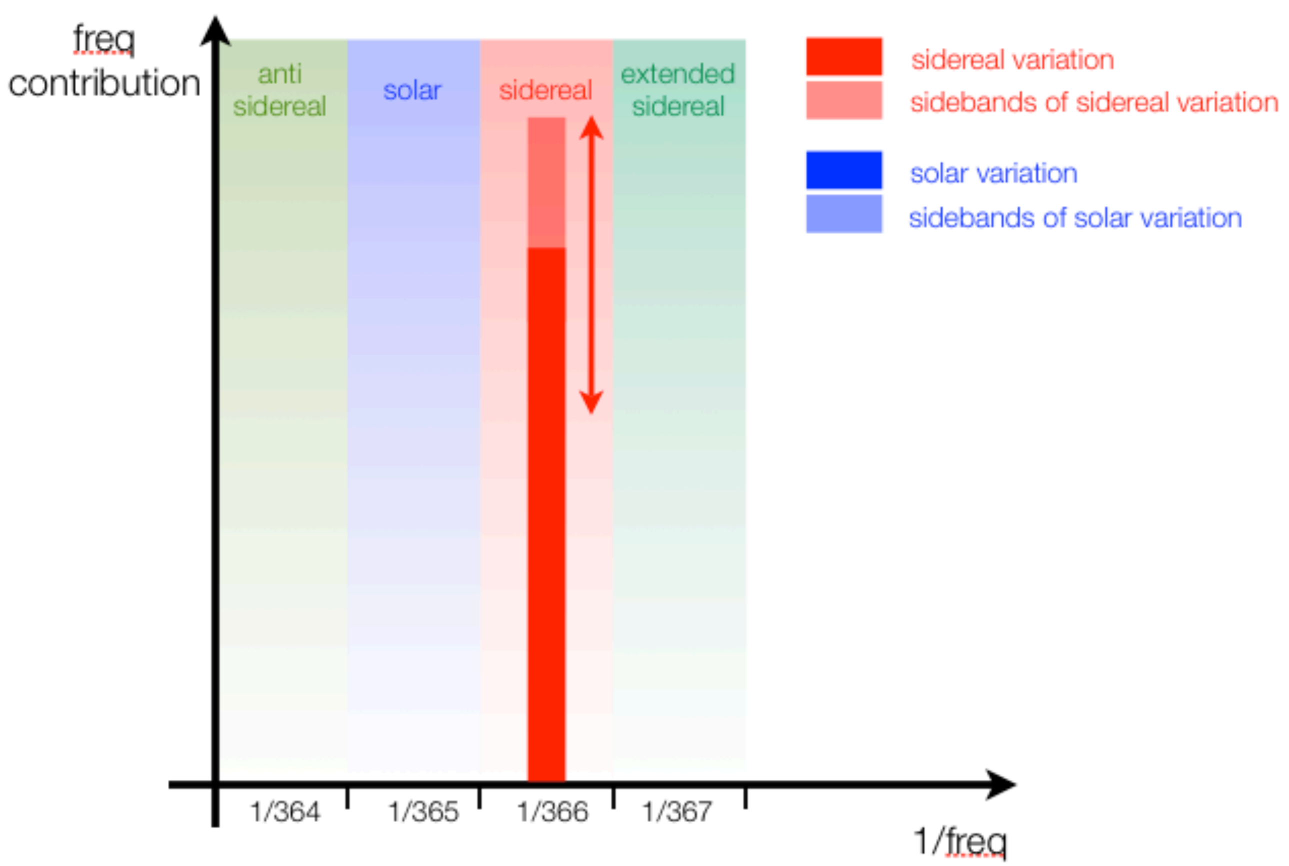

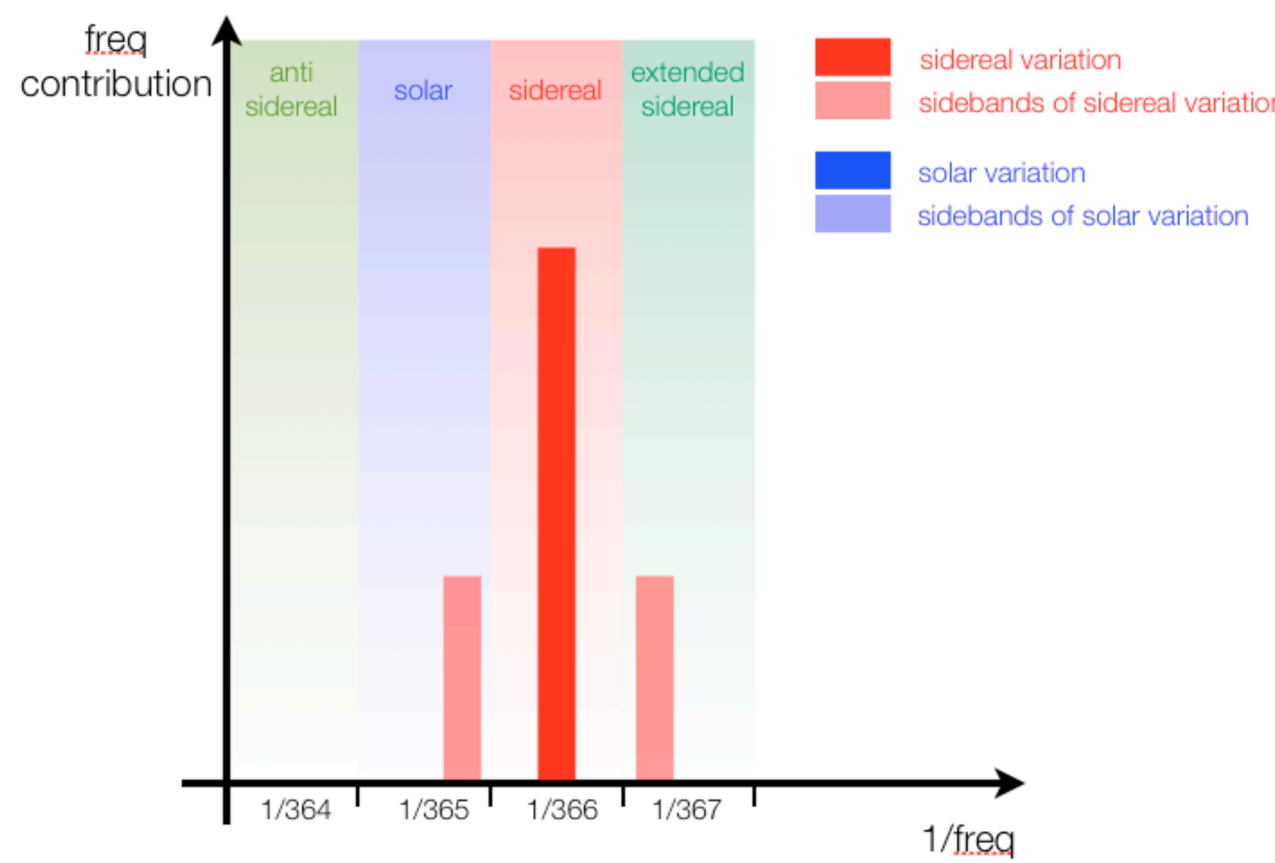

anti- / extended-sidereal reference frames

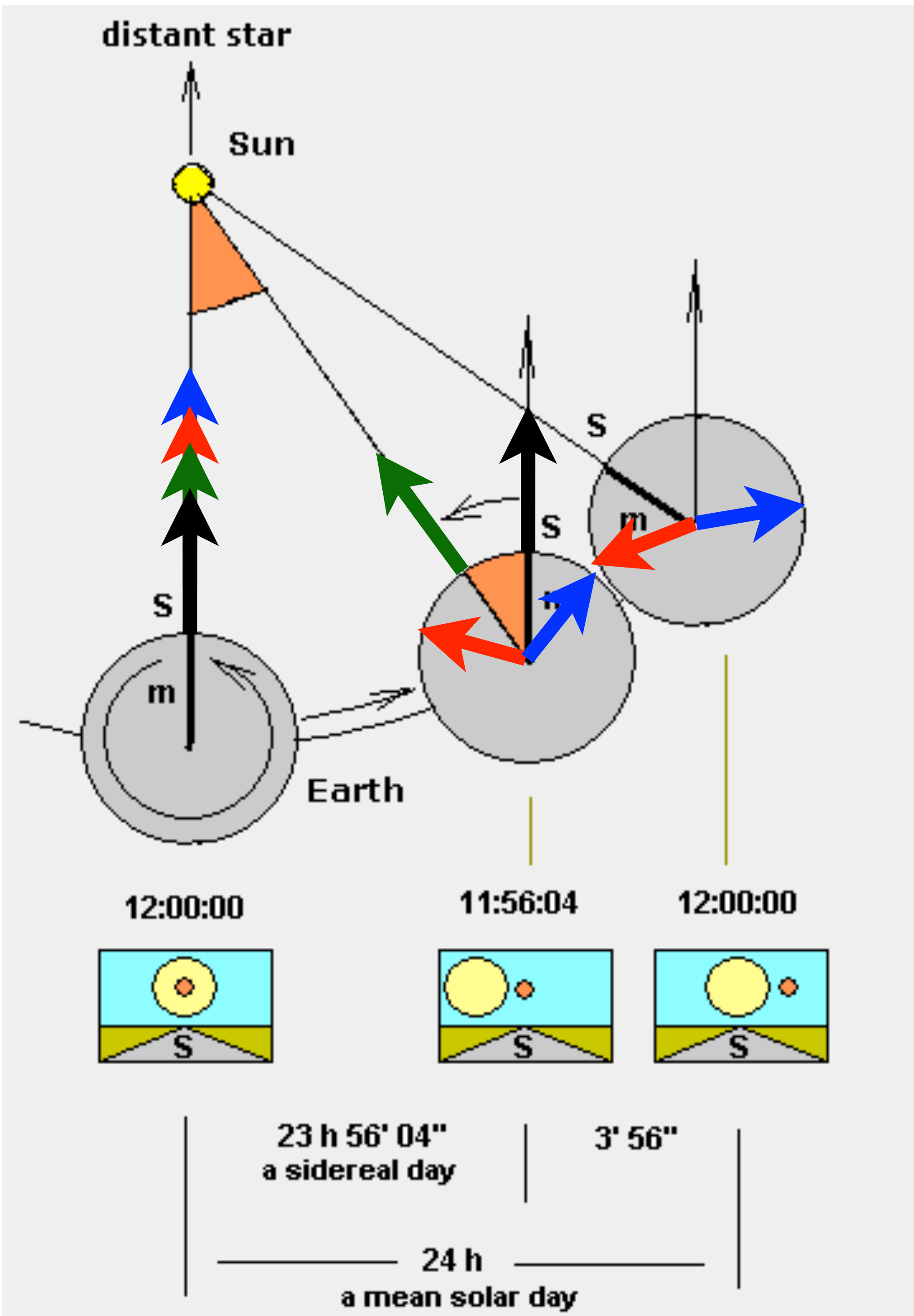

The **anti**- / **extended**-sidereal reference frames are unphysical and no anisotropy is expected

An anisotropy in **anti**-sidereal (**extended**-sidereal) frame is to be associated to the corresponding distortion of the sidereal (solar) arrival distributions

solar time

sidereal time

anti-sidereal time

extended-sidereal time

anisotropy vs energy

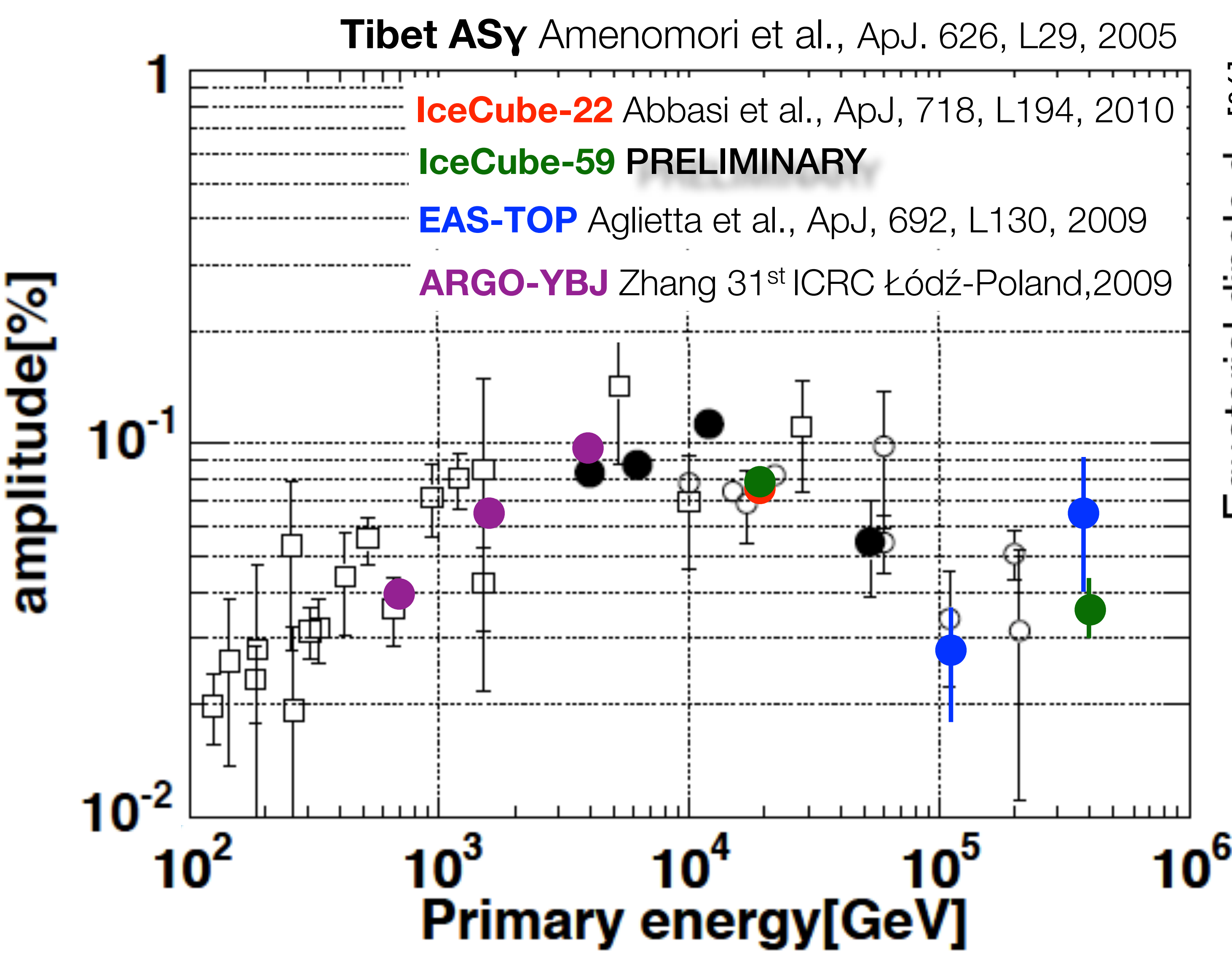

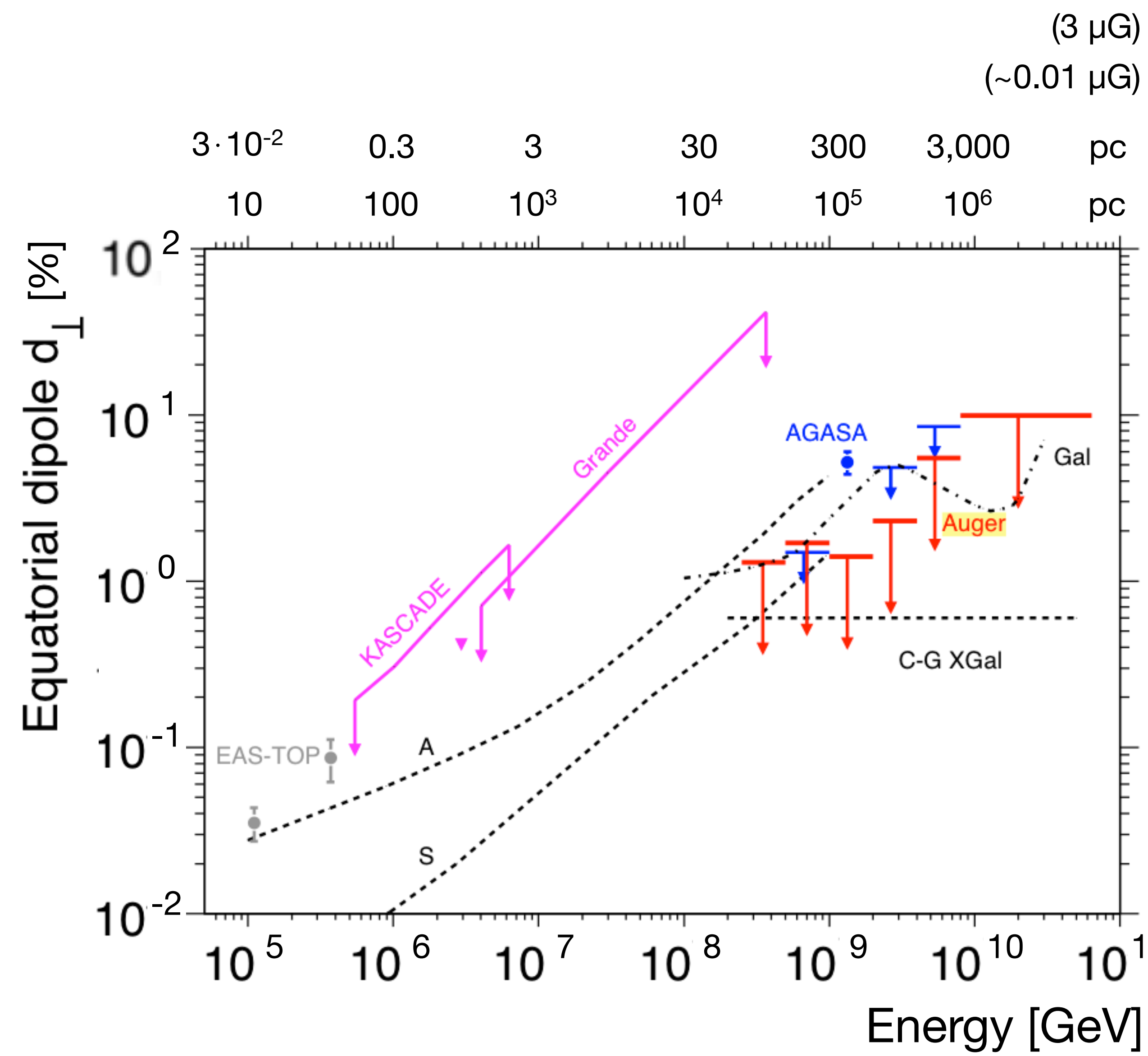

Abreu et al., Astrop. Phys., 34, 627, 2011

(3 µG)

$3\cdot10^{-5}$	$3\cdot10^{-4}$	$3\cdot10^{-3}$	$3\cdot10^{-2}$	0.3	gyro-radius (pc)
7	70	700	7,000	70,000	gyro-radius (AU)

heliospheric influence

galactic influence

the interstellar magnetic field

scale : < 40 pc

visual comparison only

statistical significance

equatorial coordinates

Tibet-III

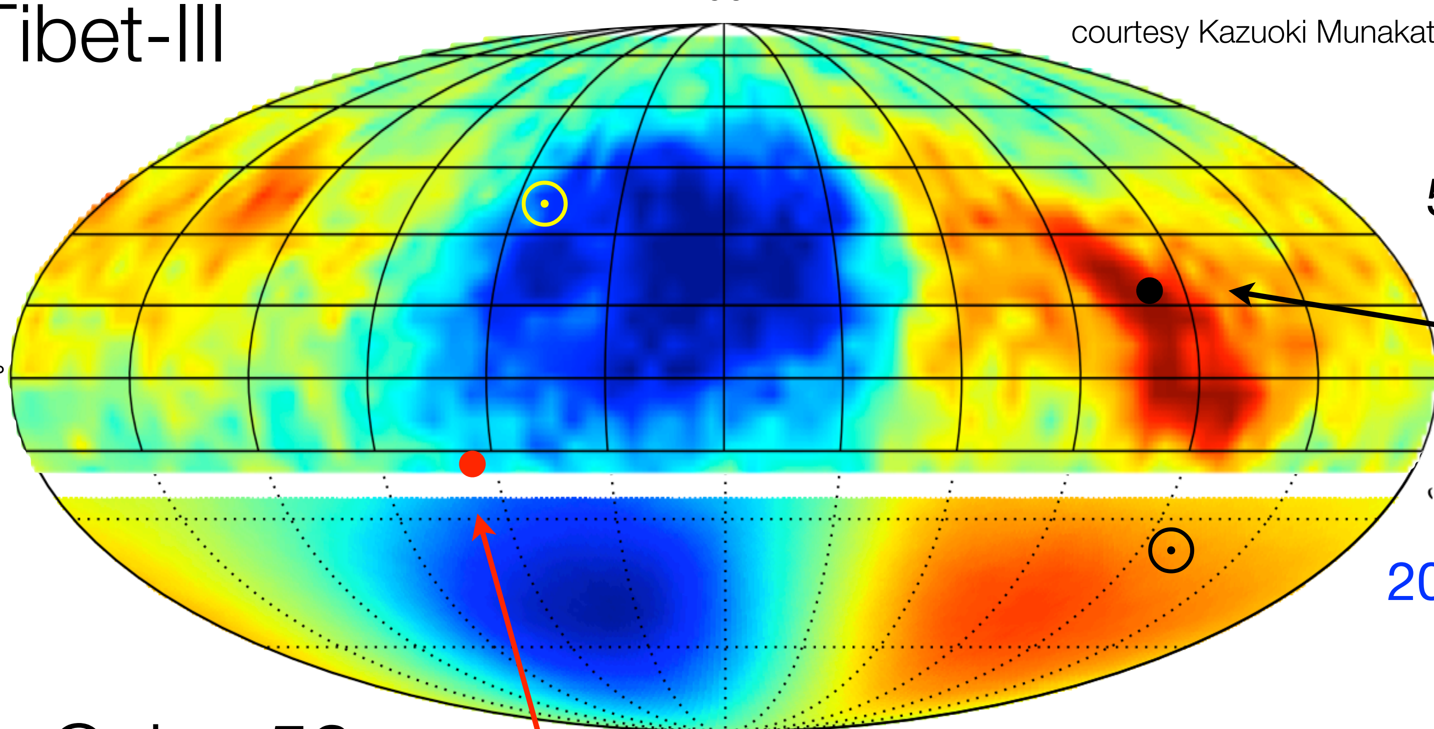

5 TeV

20 TeV

IceCube-59

heliospheric tail

heliospheric nose

Tibet-III

5 TeV

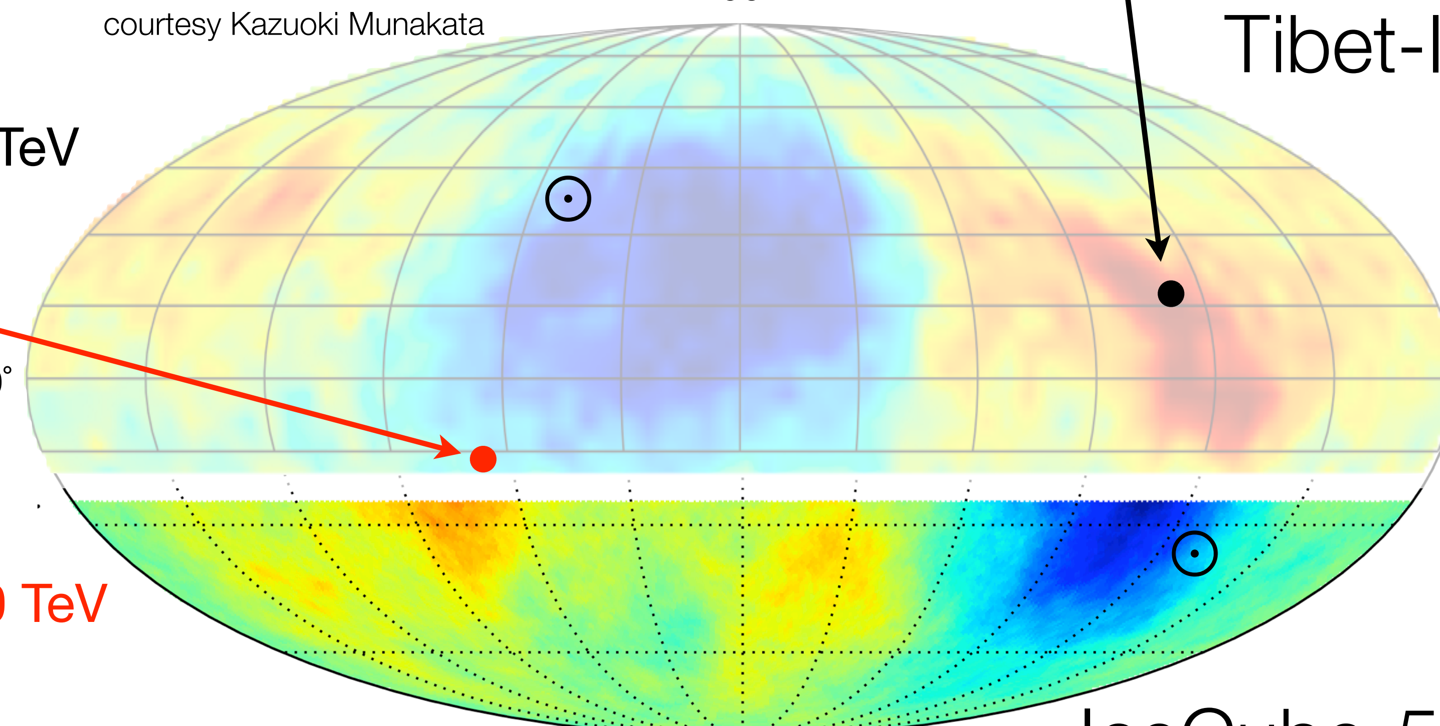

400 TeV

IceCube-59

⊙ local interstellar magnetic field

cosmic ray anisotropy

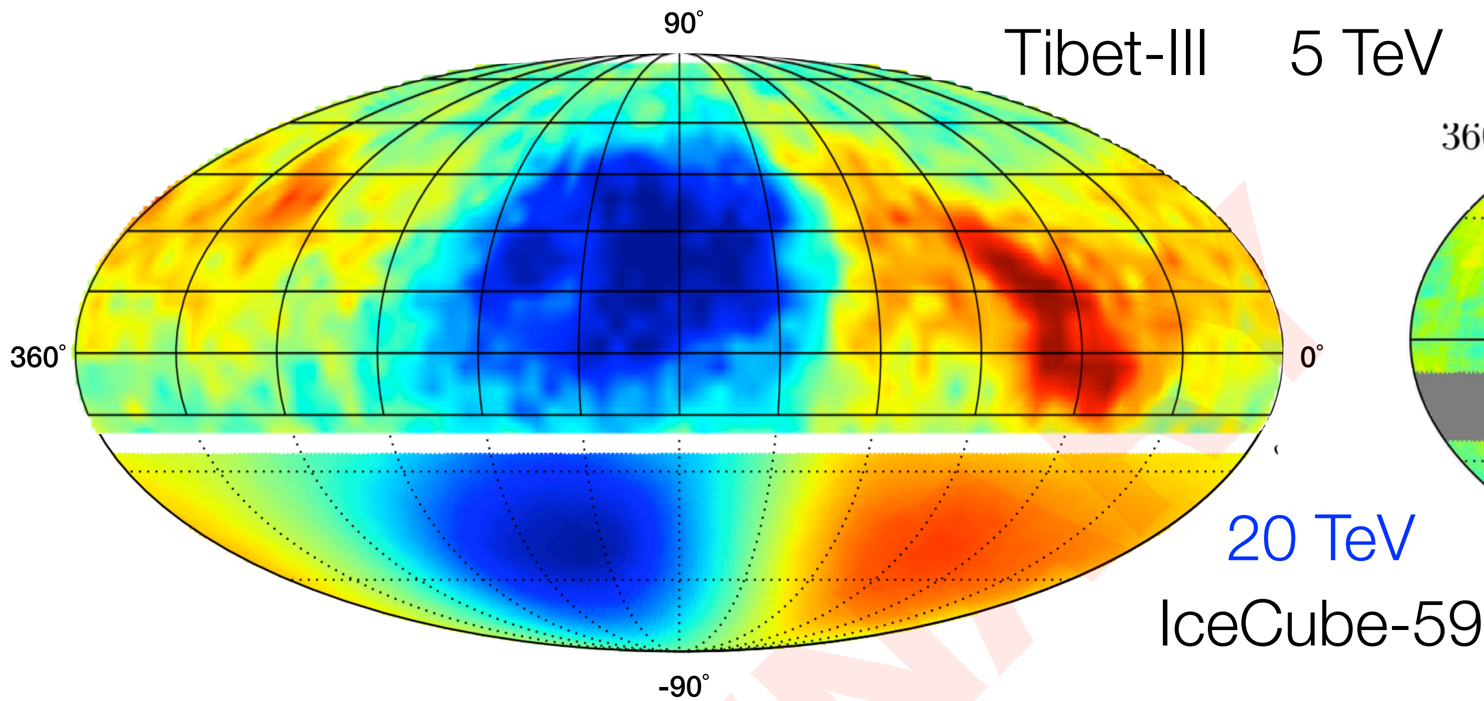

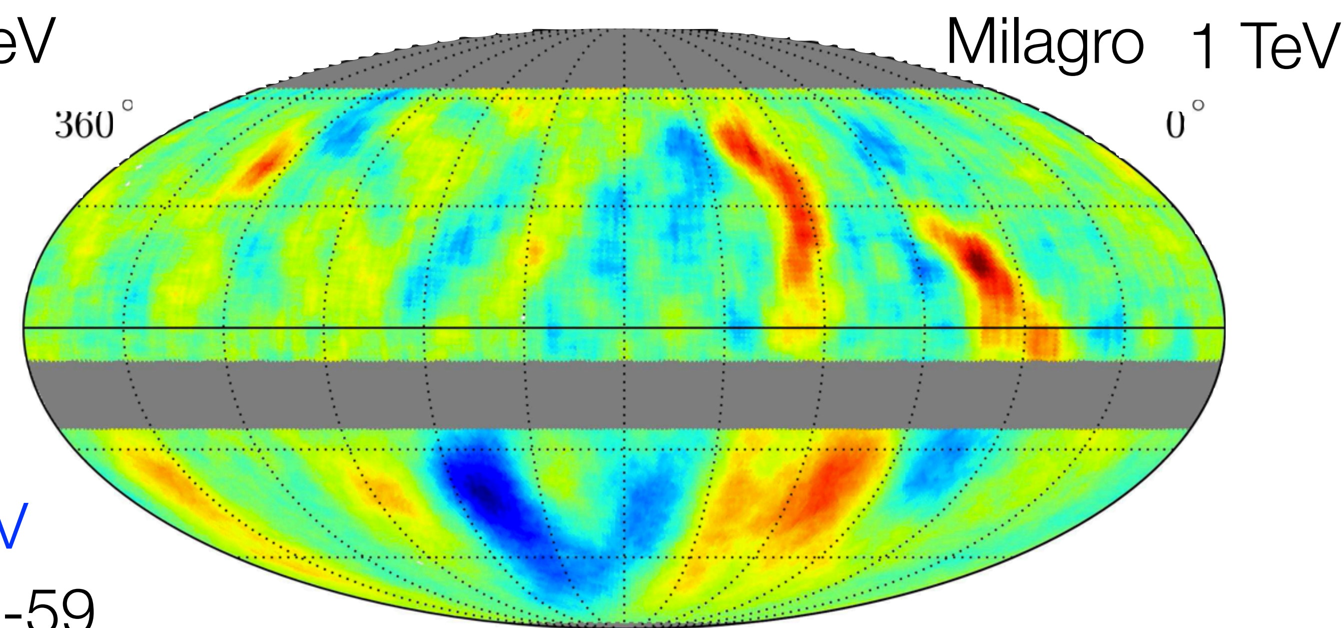

statistical significance

equatorial coordinates

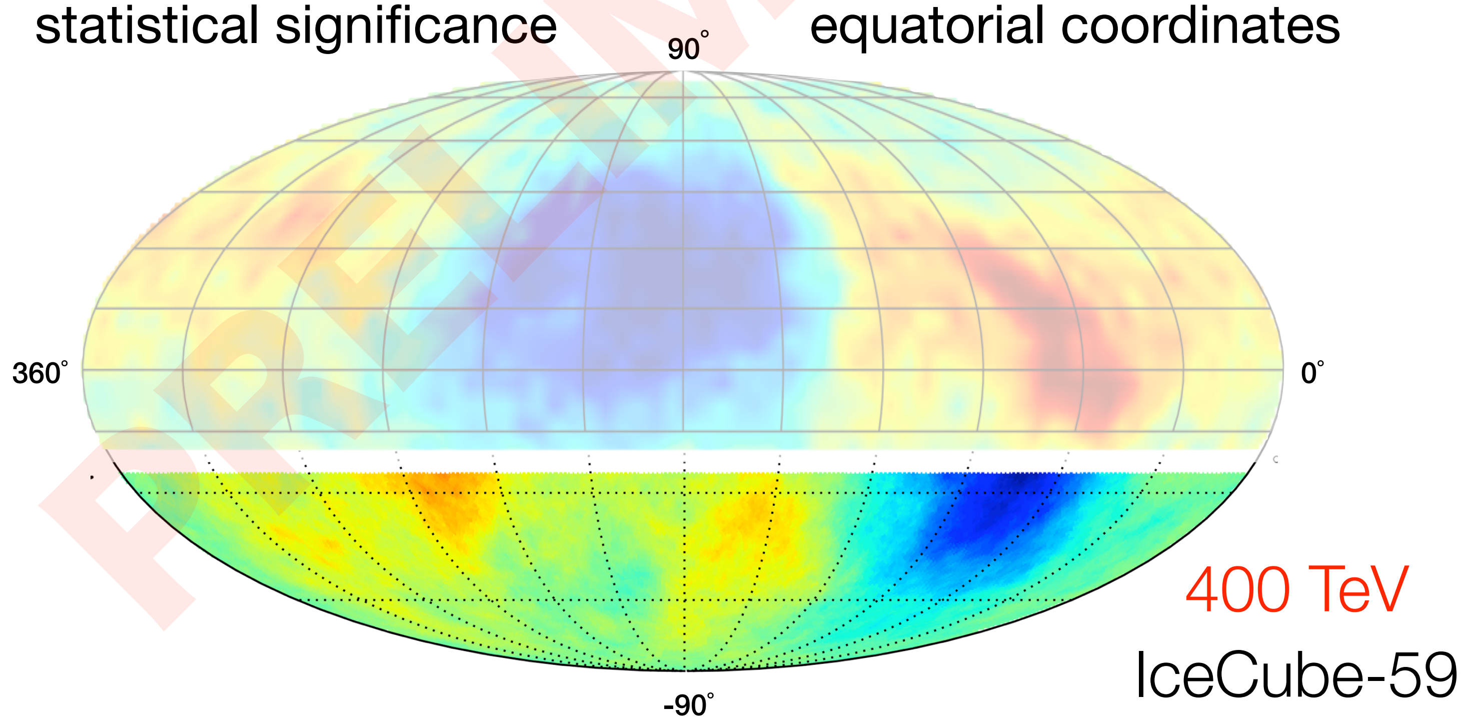

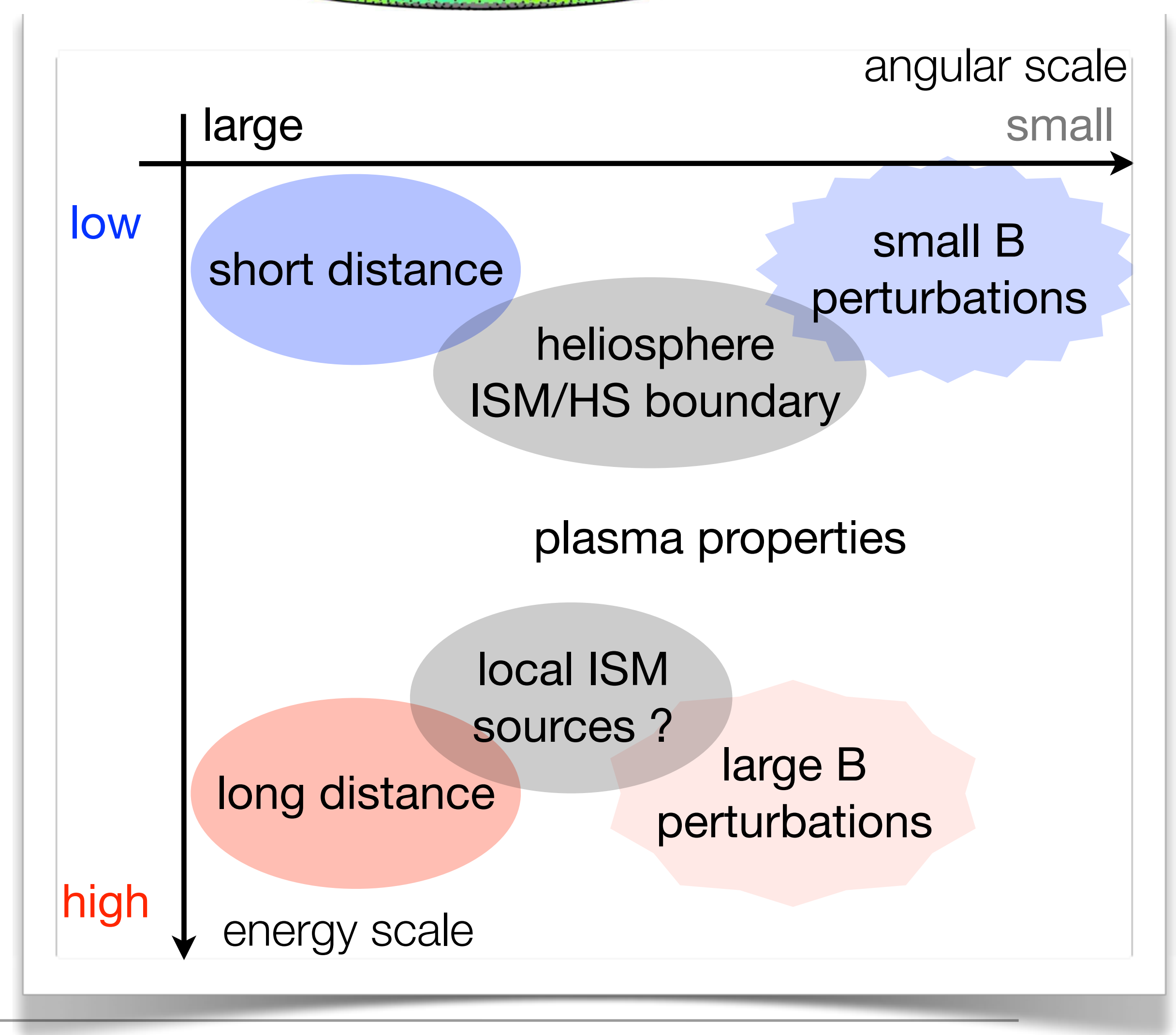

our galactic neighborhood

Amenomori et al., ICRC 2007, Mérida (Mexico)

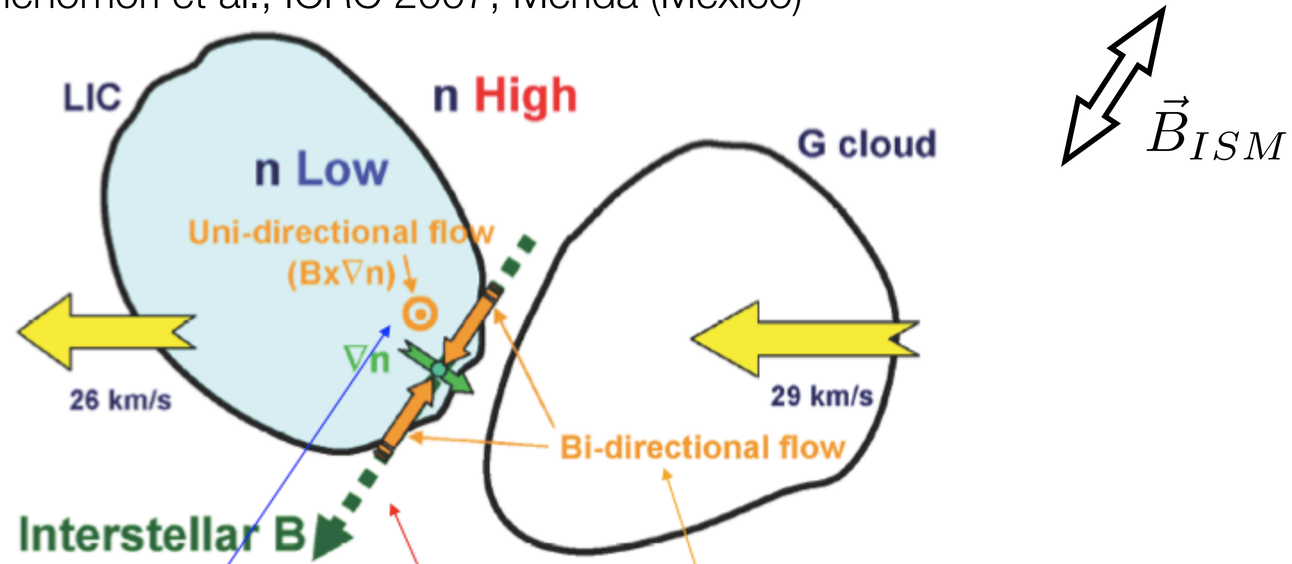

FIGURE 2. A cartoon of the LIC (left) viewed from the galactic north-pole (see [8] for more detail). Another cloud (G cloud) is overtaking the LIC from the Galactic center on the right side. A broken line represents the LISMF line through the heliosphere just inside the LIC boundary. If the GCR density (n) is lower inside the LIC than outside, the BDF is expected from the pitch angle diffusion of GCRs into LIC along the LISMF line. The UDF is also expected from B×G drift anisotropy (see text).

$$I_{n,m} = a_{1\perp}\cos\chi_1(n,m:\alpha_1,\delta_1) + a_{1/\!/}\cos\chi_2(n,m:\alpha_2,\delta_2) + a_2\cos^2\chi_2(n,m:\alpha_2,\delta_2)$$

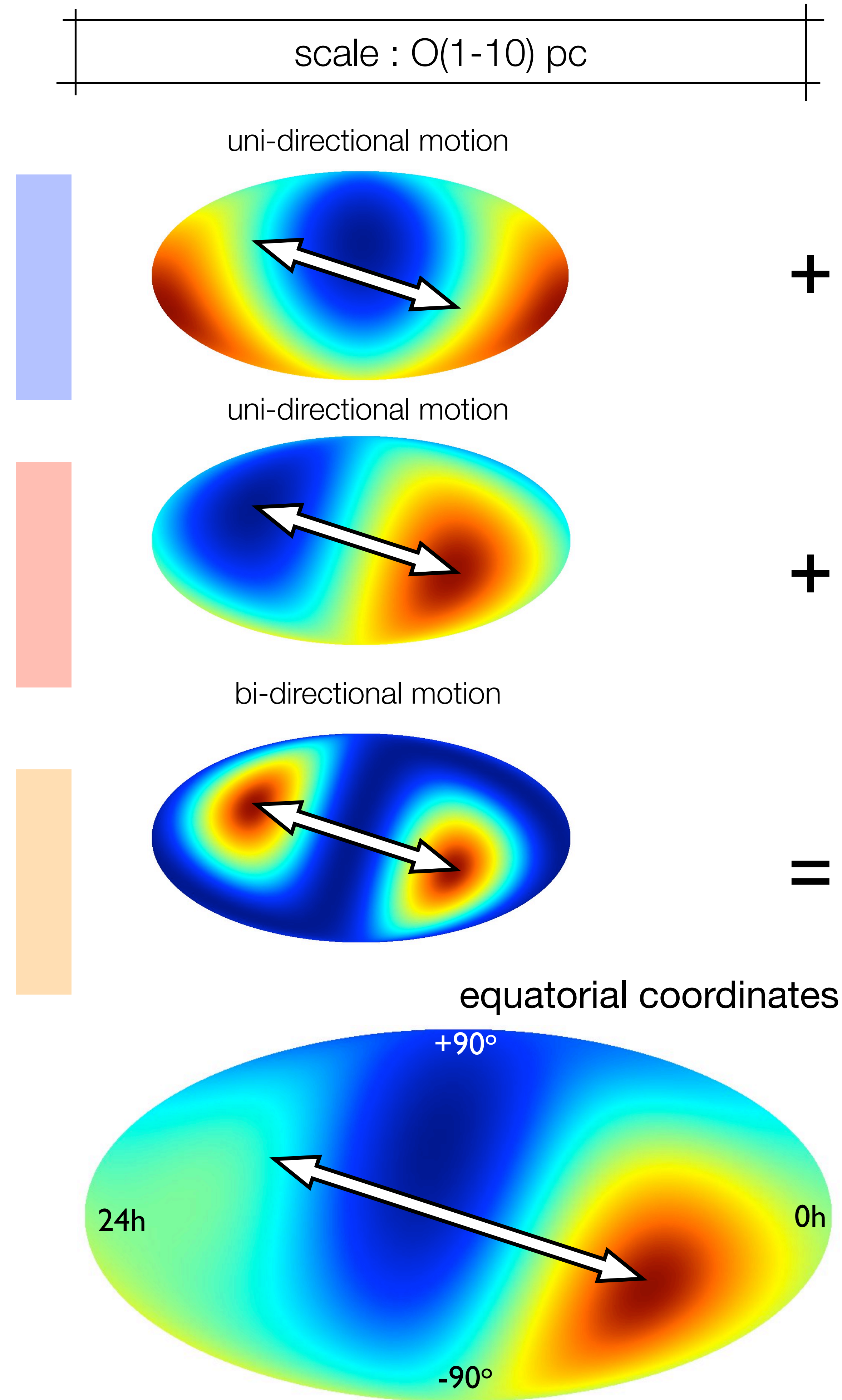

- magnetic field compression between cloudlets
- can produce anisotropy from isotropic flux
- or enhance existing anisotropy

our galactic neighborhood

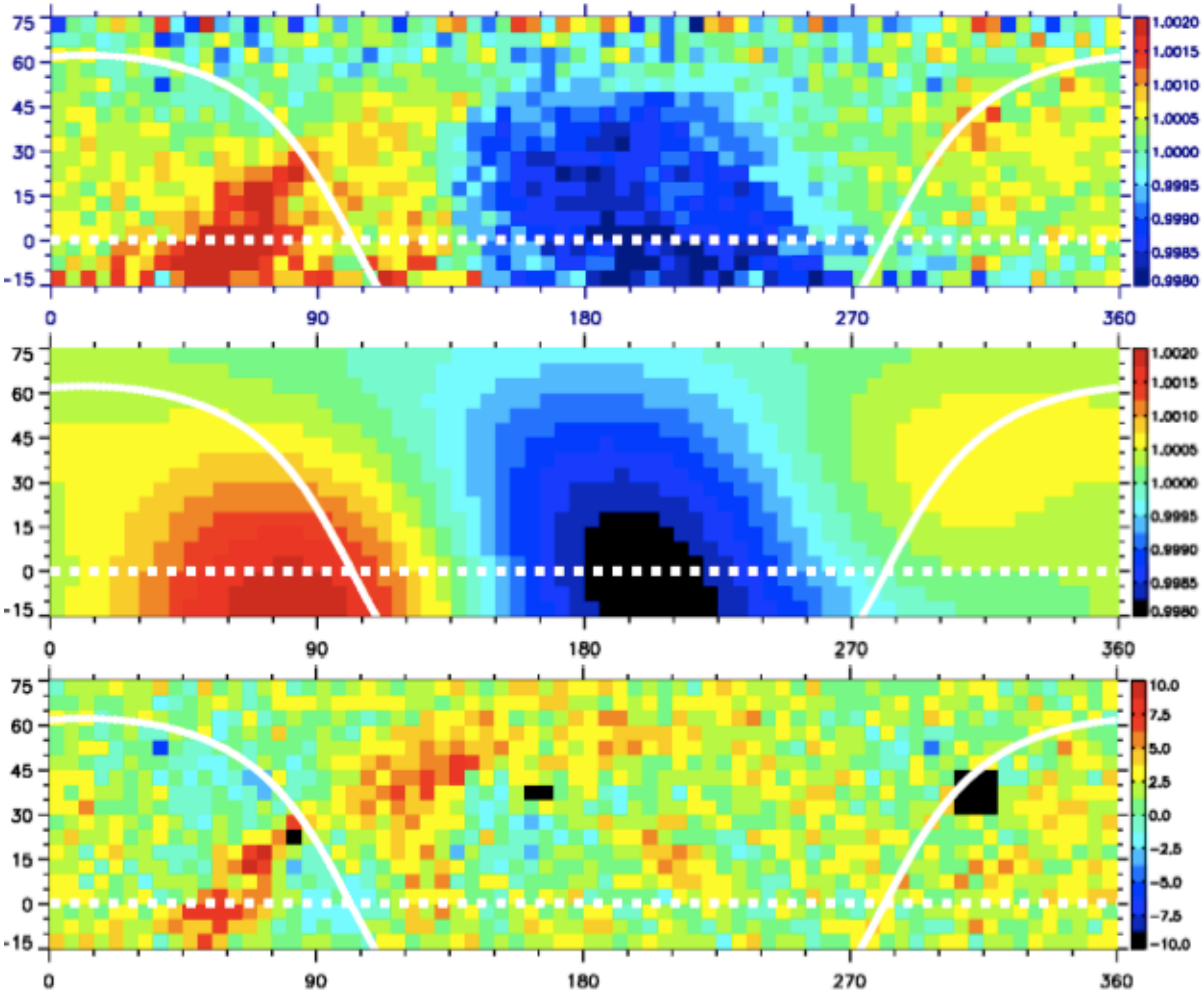

Tibet-III @ 5 TeV

anisotropy almost consistent with

uni-directional flow (dipole)
+
bi-directional flow (quadrupole)

equatorial coordinates

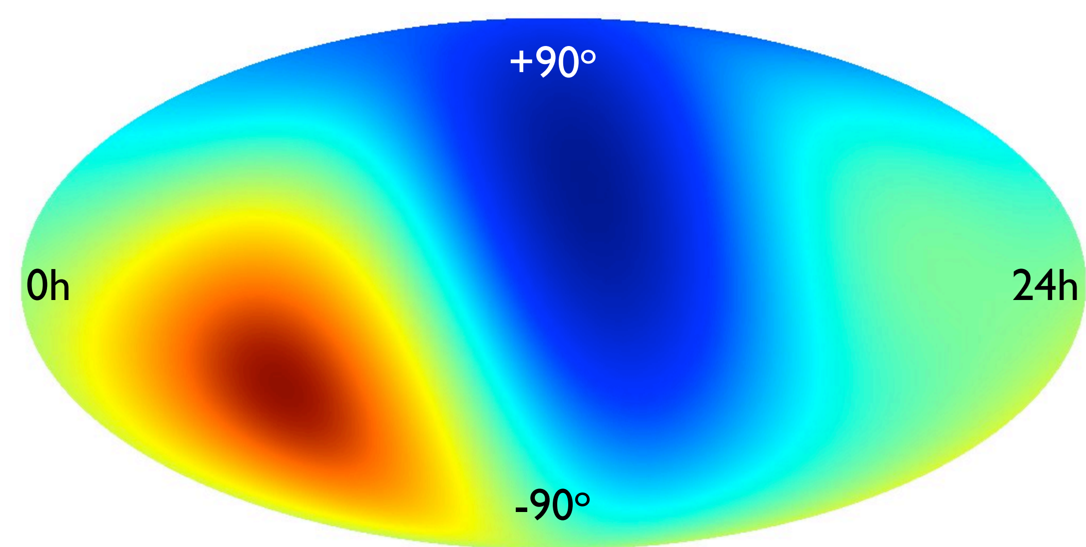

our galactic neighborhood

relative intensity
equatorial coordinates

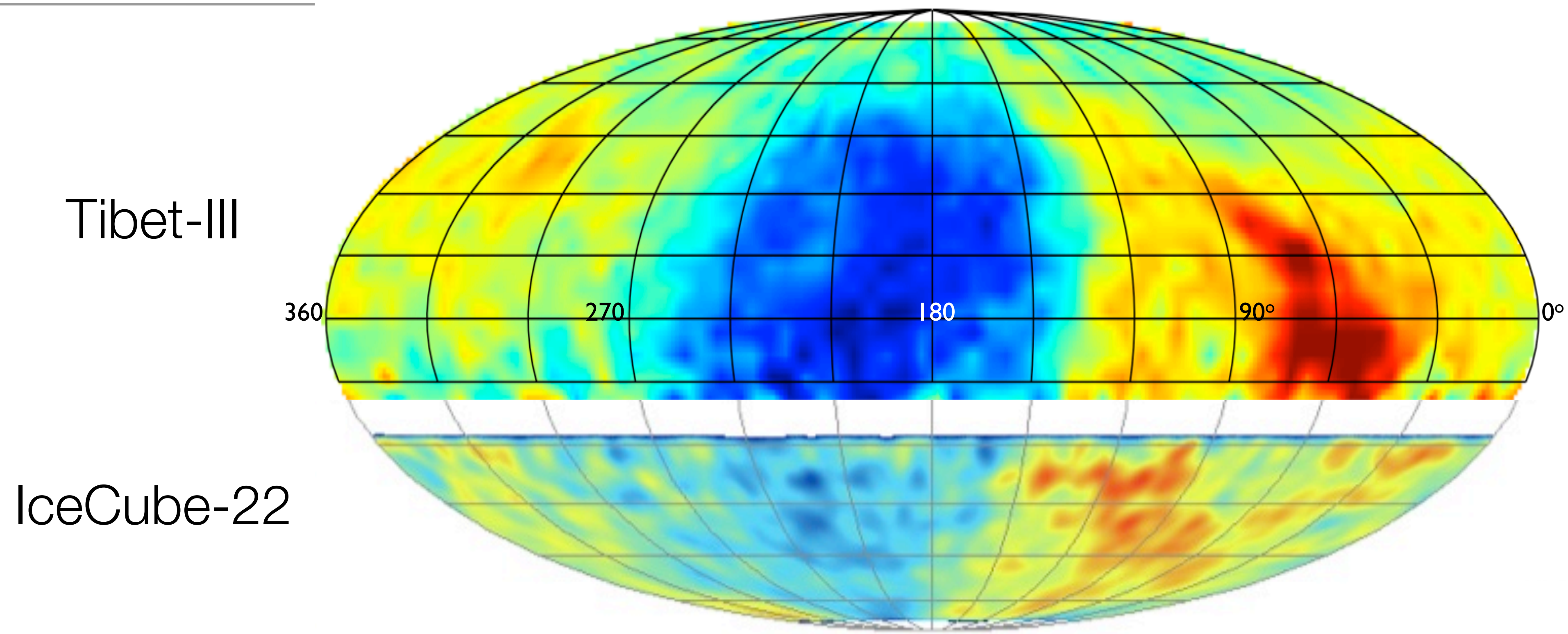

IceCube @ 20 TeV

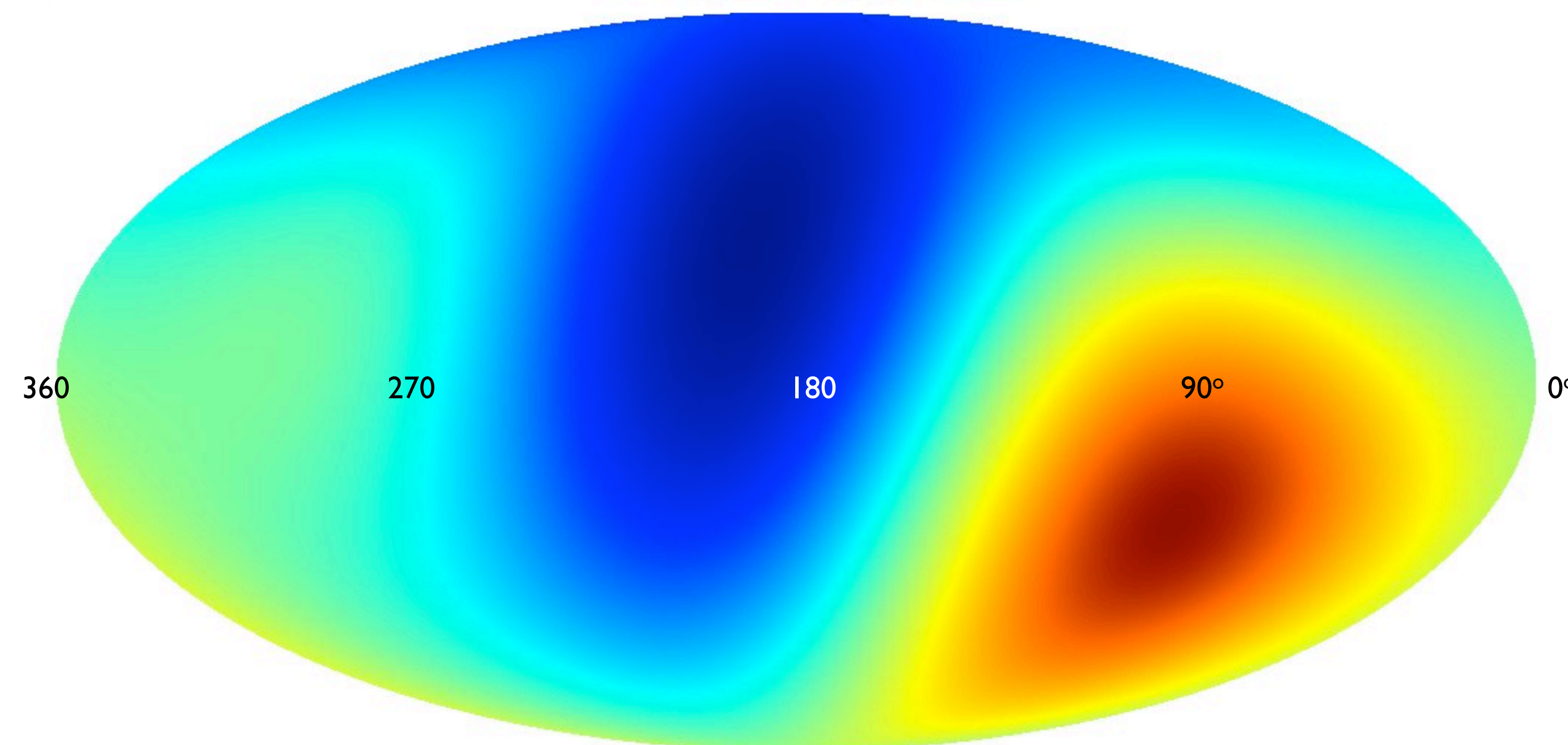

large scale features qualitatively well described by the global fit

it is the smaller angular features that appear to be interesting

low energy cosmic ray anisotropy in arrival direction

Nagashima et al., J. Geophys. Res., Vol 103, No. A8, Pag. 17,429 (1998)

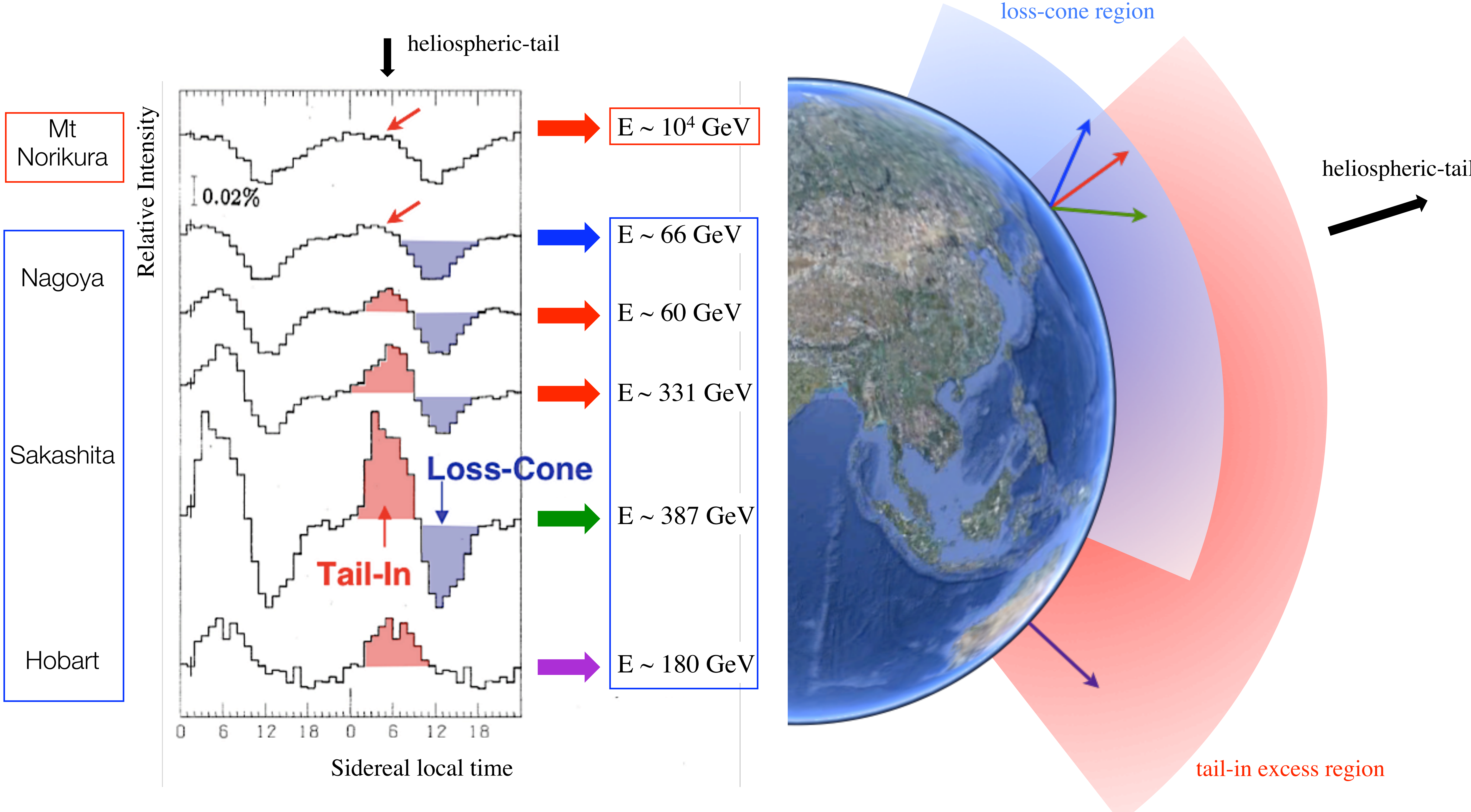

structures in cosmic ray spectrum

PAMELA - Adriani et al., Science, 332, 69, 2011

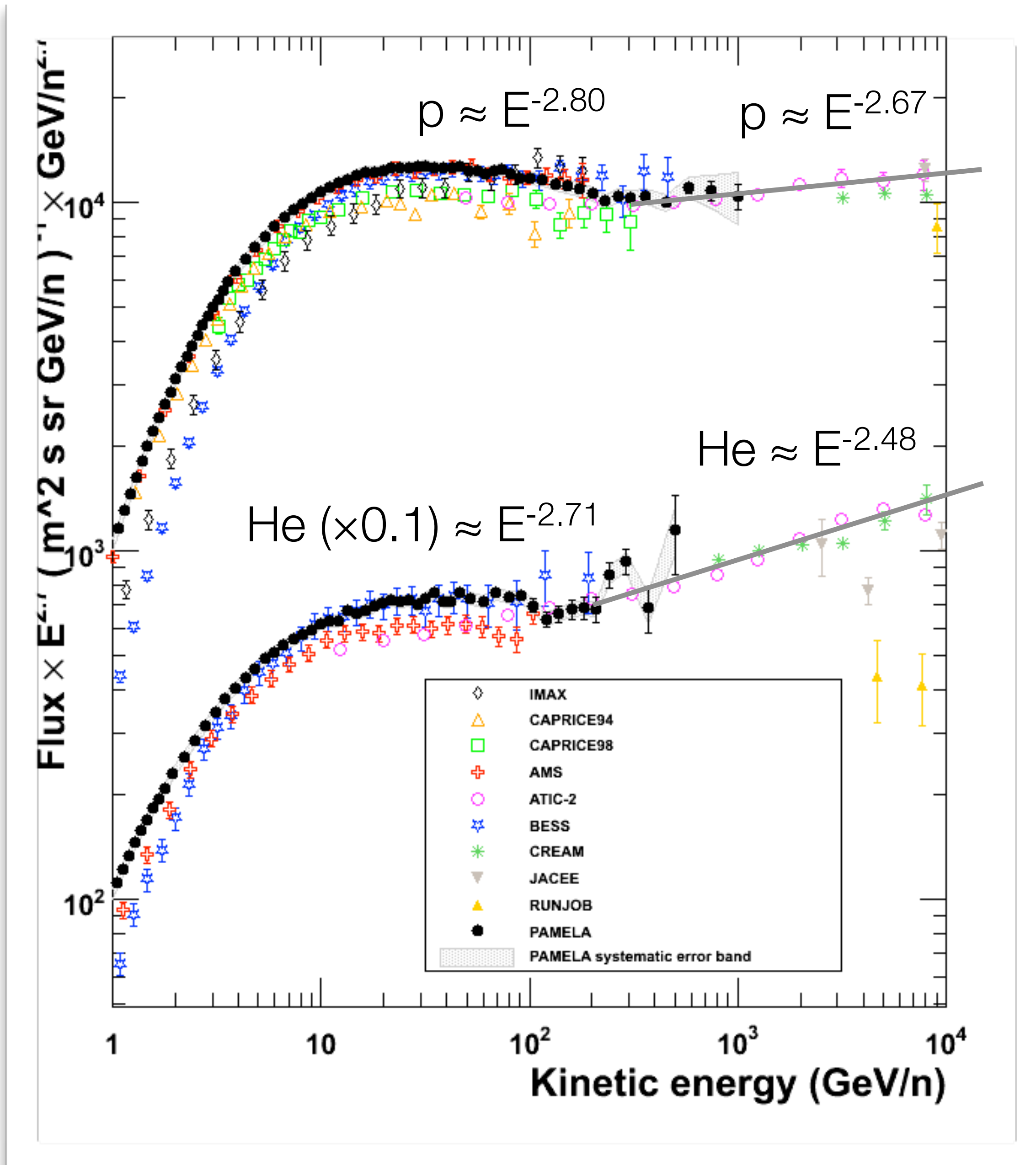

CREAM - Ahn et al., ApJ, 714, L89, 2010

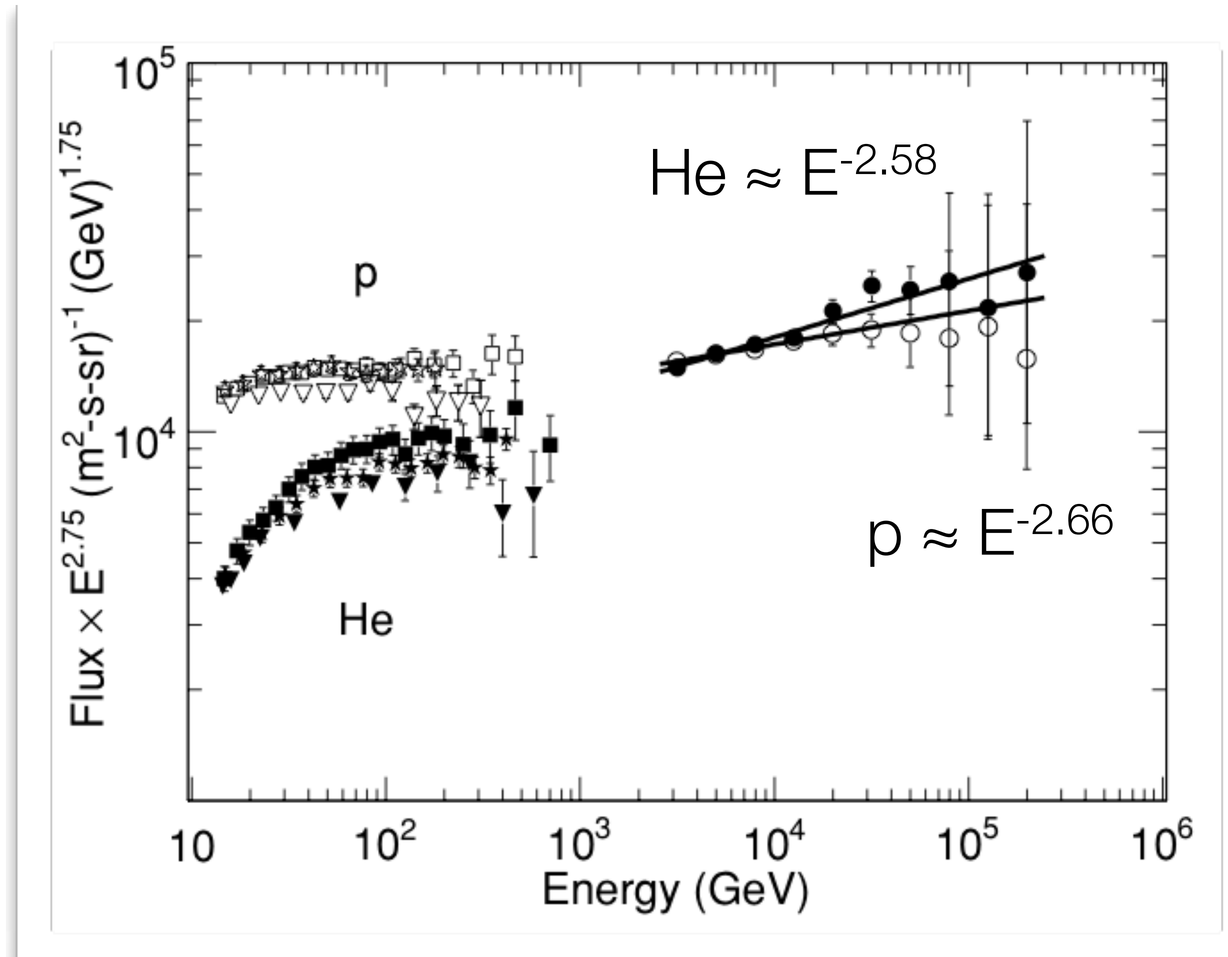

- **spectral concavity** from non-linear acceleration or propagation processes
- **nearby source** of cosmic rays ?

spectral concavity / hardening

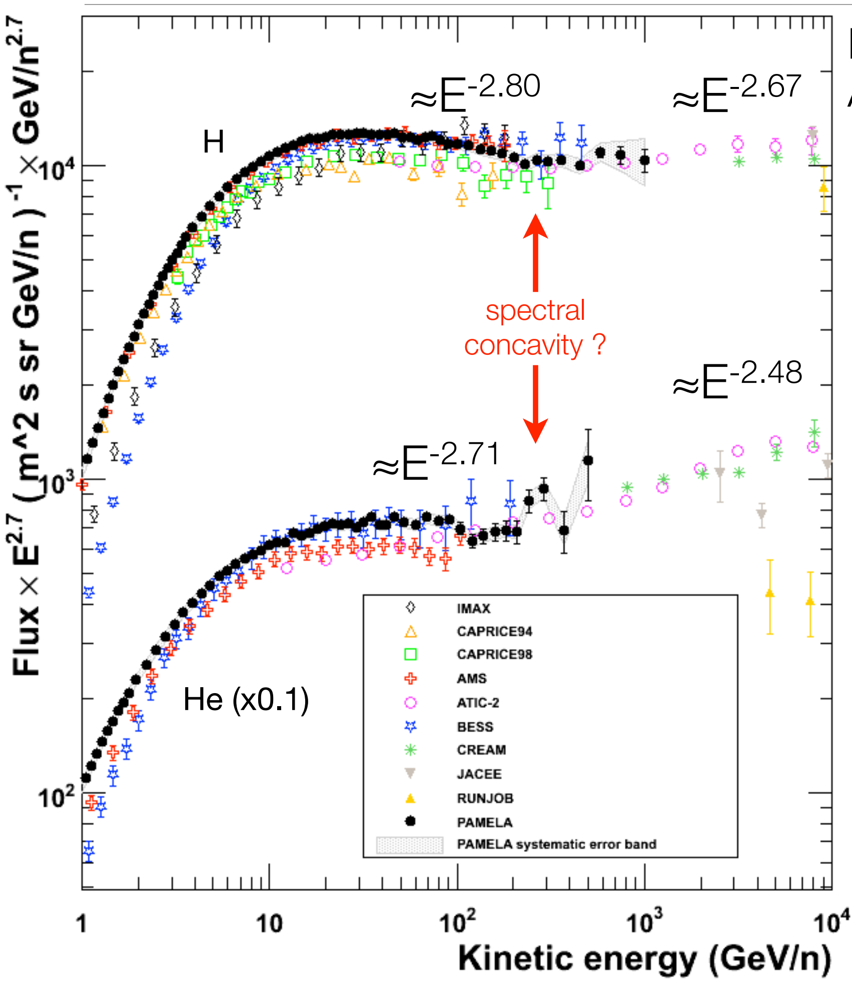

PAMELA
Adriani et al., Science, 332, 69, 2011

KASCADE-Grande
Arteaga-Velázquez et al., arXiv:1009.4716